UNIVERSIDADE DA BEIRA INTERIOR
Ciências da Saúde

Síntese de nano-veículos poliméricos para entrega de fármacos com atividade anti-tumoral

Duarte Miguel de Melo Diogo

Dissertação para obtenção do Grau de Mestre em
Ciências Biomédicas
(2º ciclo de estudos)

Orientador: Professor Doutor Ilídio Joaquim Sobreira Correia
Coorientador: Mestre Vítor Manuel Abreu Gaspar

Covilhã, junho de 2014

“Labor omnia vincit”

-Publius Vergilius Maro (adapted)

Acknowledgments

First, I would like to thank my supervisor, Professor Ilídio Correia, for the opportunity to work with him and his group. I am also grateful for his orientation and his support during my master thesis. I would like to thank my co-supervisor, Vítor Gaspar for the support, criticism and guidance. I also thank him for his enthusiasm that kept me motivated. I am grateful for every skill taught and for always believing in me and in my work. To both, I thank for my growth as researcher but also as a person.

I thank Professor Eugénia Gallardo and David Markl for providing me the UPLC column, the internal standards and all the UPLC support. Without their help this work would not be feasible.

To André Moreira and Elisabete Costa I thank for their friendship and support. I appreciated their company during the execution of the many protocols and in the long lab nights. To them I wish all the best. I show gratitude to my lab partners for their fellowship and for setting-up many memorable moments that I will not forget.

I thank all my family, especially my mother, father, sister and grandparents for their continuous support, comprehension and affection. I thank my girlfriend Diana for her support and unconditional love.

Finally, I thank all my long-time friends.

Abstract

Lung cancer is presently one of the most incident diseases that affects the worldwide population and is also considered one of the most deadly. In Portugal, lung cancer mortality and incidence has also been growing in the last decade. Despite all the efforts towards the development of efficient treatments no cure is yet available for this type of cancer. Chemotherapy is currently the gold standard therapy for lung cancer treatment, however, this strategy has proven to be rather inefficient mostly due to the intrinsic properties of chemotherapeutic drugs. In fact, these type of drugs are known for their poor solubility, low bioavailability and non-specific accumulation, which leads to systemic toxicity and undesired side effects. Moreover, cancer cells promptly adapt to the presence of these therapeutic agents, becoming resistant to their action and promoting their elimination. Such activity is mediated by drug-resistance mechanisms that take advantage of drug efflux through ABC transmembranar transporters. These transporters play a crucial role in the shuttle of drugs to the extracellular medium, thus promoting cancer resistance.

Based on these facts, it is urgent to develop strategies that can overcome these issues, improving chemotherapy efficacy and patient survival rates. In the past two decades, nanotechnology-based solutions have been developed to circumvent these problems. Several specialized vehicles have been developed with the aim to reduce the drawbacks of chemotherapy problems. These drug delivery systems are nanoscale platforms that are capable of encapsulating anti-tumoral drugs and usually accumulate in tumoral tissues due to tumor leaky vasculature. However, strategies that can overcome cancer drug resistance are yet poorly explored since only in the past years this issue has become a major priority.

In the present thesis, a nanocarrier capable of self-assembly and of encapsulating a novel triple drug combination was formulated with amphiphilic polymers to be used in cancer therapy. This nanovehicle was formulated with D-α-tocopherol polyethylene glycol 1000 succinate-poly(lactic acid) (TPGS-PLA) diblock copolymers, which can assemble into nanosized and stable micelles, with a core-shell architecture. When dispersed in aqueous environments these micelles were capable of encapsulating with high efficiency, a novel and untested triple drug combination. This combination has the ability to target different altered pathways in cancer cells and, at the same time, has the potential to act on drug efflux pumps that are linked to cancer drug resistance. This combination comprises an FDA approved drug for NSCLC (Crizotinib), a novel and potent cell cycle arrester that is under clinical trials (Palbociclib) and an ABC efflux transporters inhibitor (Sildenafil). Moreover, the micellar system has TPGS in its composition and so it can also benefit from TPGS MDR1 inherent inhibiting activity.

The novel triple free drug combination revealed to have a synergistic cytotoxic effect in lung cancer cells. On the other hand, the dual drug combination of Crizotinib and Palbociclib reflected an additive effect. These results validate the triple drug combination encapsulation strategy in TPGS-PLA micelles herein employed for lung cancer therapy. Moreover, the uptake studies revealed that micelles were internalized by cancer cells, a crucial parameter to increase the drugs bioavailability and to reduce systemic toxicity associated with chemotherapy. As expected, the triple drug loaded micellar formulations exhibited the highest cytotoxic effect, reflecting the synergy obtained for its free drug combination.

In summary, the novel and versatile drug delivery approach developed herein with two strong chemotherapeutic drugs (Crizotinib and Palbociclib) and two agents with the capacity to target cancer drug resistance mechanisms (Sildenafil and TPGS) demonstrates enormous potential for lung cancer therapy.

Keywords

Cancer treatment, cell resistance, micellar carriers, multidrug therapy, TPGS-PLA.

Resumo Alargado

Na atualidade, o cancro do pulmão surge como o mais fatal em ambos os sexos e também como o mais prevalente. A sua elevada taxa de mortalidade tem sido associada ao seu diagnóstico tardio. O desenvolvimento de cancro do pulmão está constantemente associado a fatores de ordem ambiental e de estilo de vida (consumo de tabaco). Para além disto, as terapias disponíveis para o tratamento deste tipo de cancro não são eficazes, o que contribui para a sua elevada mortalidade. A baixa eficácia dos tratamentos disponíveis está associada a problemas inerentes aos fármacos e ao desenvolvimento de resistência a estes agentes terapêuticos por parte das células cancerígenas. Os agentes quimioterapêuticos têm baixa solubilidade, fraca biodisponibilidade e acumulação não específica, parâmetros que contribuem para a sua citotoxicidade sistémica e graves efeitos secundários. Por outro lado, as células cancerígenas desenvolvem múltiplos mecanismos que lhes conferem resistência à ação dos fármacos quimioterapêuticos, dentro dos quais a sobreexpressão de bombas de efluxo tem sido descrita como um dos principais. Estas bombas transmembranares expelem os fármacos quimioterapêuticos para fora da célula, fazendo assim com que estes não exerçam a sua atividade terapêutica. Estes factos evidenciam a necessidade urgente de desenvolver novas abordagens terapêuticas que permitam melhorar o prognóstico clínico e a qualidade de vida dos pacientes afetados por esta doença tão devastadora.

Os recentes desenvolvimentos na área da Nanotecnologia têm apresentado estratégias capazes de colmatar os problemas gerais inerentes aos fármacos anti-tumorais. Estas estratégias passam pelo desenvolvimento de veículos à escala nanométrica, que são capazes de encapsular compostos bioativos e de os entregar preferencialmente nas células cancerígenas devido ao seu tamanho reduzido. Assim, a biodisponibilidade dos fármacos aumenta e a sua toxicidade sistémica, bem como os efeitos secundários, diminuem. Atualmente, existem vários nanoveículos que já são aplicados na clínica para o tratamento do cancro, contudo são poucos os sistemas que entregam fármacos quimioterapêuticos em simultâneo com agentes capazes de reverter a resistência a estes mediada pela ação de bombas de efluxo.

Tendo em conta as limitações atuais associadas à quimioterapia, na presente tese é apresentado o desenvolvimento de um nanoveículo para a terapia do cancro do pulmão, com estrutura "núcleo-concha". Este sistema foi produzido usando um bloco polimérico de D-α-tocopherol polyethylene glycol 1000 succinate-poly(lactic acid) (TPGS-PLA)TPGS-PLA, que tem uma estrutura anfifílica, permitindo assim formar nanoveículos micelares. Nas micelas o TPGS, como tem uma estrutura predominantemente hidrofílica, forma a concha, enquanto que o PLA forma o núcleo hidrofóbico. O bloco polimérico de TPGS-PLA forma espontaneamente micelas estáveis, quando disperso em ambientes aquosos, com baixa concentração micelar crítica. Com o intuito de desenvolver um nanoveículo para fins terapêuticos e com potencial para reverter

a resistência do cancro, as micelas TPGS-PLA foram também formuladas de modo a encapsular uma combinação de fármacos para a terapia do cancro do pulmão. A combinação de fármacos encapsulados nas micelas de TPGS-PLA incluiu o Crizotinib, Palbociclib e Sildenafil.

O Crizotinib é um potente fármaco anti-tumoral usado no tratamento de cancro do pulmão. Por outro lado, o Palbociclib atua interrompendo a progressão do ciclo celular e encontra-se ainda em ensaios clínicos. No entanto resultados preliminares demonstraram a sua elevada atividade biológica. O Sildenafil é um agente capaz de inibir vários tipos de bombas de efluxo, que são responsáveis por conferir às células cancerígenas resistência contra os fármacos quimioterapêuticos.

Na presente tese, diferentes combinações contendo estes fármacos, na sua forma livre, foram testadas *in vitro*. A combinação que possuía os três fármacos apresentou um efeito citotóxico sinérgico, enquanto que a combinação contendo dois fármacos (Crizotinib/Palbociclib) revelou apenas um efeito aditivo. Estes resultados evidenciam que a combinação que usa os três fármacos em simultâneo é mais vantajosa, pois potencia uma terapia cujo efeito é superior à soma dos efeitos individuais de cada fármaco. Contudo, uma administração destes três fármacos na sua forma livre seria desafiante devido às interações fármaco-fármaco, à alteração dos seus perfis farmacocinéticos e ainda devido a possíveis problemas de citotoxicidade sistémica. Desta forma, neste estudo desenvolveu-se uma formulação terapêutica que consiste na encapsulação simultânea dos três fármacos em micelas de TPGS-PLA. As micelas foram capazes de encapsular os fármacos com grande eficiência, exibindo no final deste processo um tamanho de 158,3 nm e um potencial zeta de -30,3 mV. Esta formulação para além de beneficiar da atividade dos fármacos que encapsula, pode ainda beneficiar da atividade do TPGS, nomeadamente no que diz respeito à inibição das bombas de efluxo. Estes nanoveículos foram capazes de ser internalizados pelas células cancerígenas, um facto importante uma vez que os alvos dos fármacos que transportam são intracelulares. Em termos de atividade, a formulação micelar contendo a combinação dos três fármacos revelou ser, das que foram estudadas, aquela com maior atividade citotóxica.

Em suma, na presente tese foram desenvolvidas micelas de TPGS-PLA para a entrega simultânea de 2 fármacos anti-tumorais (Crizotinib e Palbociclib) e de um fármaco e polímero (Sildenafil e TPGS) com capacidade para reverter um dos principais mecanismos associados à resistência das células cancerígenas à quimioterapia. Esta formulação micelar, que nunca antes tinha sido testada, revelou-se muito eficaz, tendo por isso um grande potencial para ser futuramente usada no tratamento do cancro do pulmão.

Palavras-chave

Resistência celular, terapia multifármaco, TPGS-PLA, transportadores micelares, tratamento do cancro.

List of Publications

Articles in peer reviewed international journals:

Vítor M. Gaspar, Cristine Gonçalves, Duarte de Melo-Diogo, Elisabete C. Costa, João A. Queiroz, Chantal Pichon, Fani Sousa, Ilídio J. Correia, Poly (2-ethyl-2-oxazoline)-PLA-g-PEI Amphiphilic Triblock Micelles for Co-delivery of Minicircle DNA and Chemotherapeutics, Journal of Controlled Release (7.633), 2014, in press.

Duarte de Melo-Diogo, Vítor M. Gaspar, Elisabete C. Costa, André F. Moreira , David Markl, Eugénia Gallardo, Ilídio J. Correia, "Combinatorial delivery of Sildenafil-Crizotinib-Palbociclib by TPGS-PLA micelles for improved cytotoxic effect in lung cancer", European Journal of Pharmaceutics and Biopharmaceutics (3.826), submitted.

André F. Moreira , Vítor M. Gaspar, Elisabete C. Costa, Duarte de Melo-Diogo, Paulo Machado, Catarina M. Paquete, Ilídio J. Correia, "Preparation of end-capped pH-sensitive mesoporous silica nanocarriers for on-demand drug delivery", European Journal of Pharmaceutics and Biopharmaceutics (3.826), submitted.

Poster communications:

David Oppolzer, João F.G. Marques, Duarte de Melo-Diogo, Vítor M. Gaspar, Eugénia Gallardo, Ilídio J. Correia, "Simultaneos Determination of Sildenafil and Crizotinib using HPLC-DAD", 8º Encontro Nacional de Cromatografia, 2nd of December 2013, Covilhã, Portugal.

André F. Moreira, Vítor M. Gaspar, Elisabete C. Costa, Duarte de Melo-Diogo, Paulo Machado, Catarina M. Paquete and Ilídio J. Correia, "Synthesis and characterization of MCM-41 type sílica nanoparticles by a Stöber modified method", Encontro Bienal das Divisões Técnicas da Sociedade Portuguesa de Materiais (SMP), 4th of May, Covilhã, Portugal.

Elisabete C. Costa, Vítor M. Gaspar, Duarte de Melo-Diogo, André F. Moreira, João F.G. Marques, Paula Coutinho and Ilídio J. Correia, "Evaluation of nanoparticles uptake in breast cancer co-cultures", Encontro Bienal das Divisões Técnicas da Sociedade Portuguesa de Materiais (SMP), 4th of May, Covilhã, Portugal.

Index

Figure Index

Table Index

Abbreviations

A549	non-small human lung adenocarcinoma epithelial cell line
ABC	ATP-binding cassette
ABCG2; BCRP	breast cancer resistance protein
ALK	anaplastic lymphoma kinase
ATP	adenosine triphosphate
BcL-2	B-cell lymphoma 2
CAFs	cancer associated fibroblasts
$CDCl_3$	chloroform
CDK	cyclin-dependent kinase
cGMP	cyclic guanosine monophosphate
CI	combination index
CLSM	confocal laser scanning microscopy
C-M	crizotinib loaded TPGS-PLA micelles
CMC	critical micellar concentration
c-Met	hepatocyte growth factor receptor
CP-M	crizotinib and palbociclib loaded TPGS-PLA micelles
CPS-M	crizotinib, palbociclib and sildenafil loaded TPGS-PLA micelles
Crizotinib/Palbociclib	dual drug combination
Crizotinib/Palbociclib/Sildenafil	triple drug combination
DACHPt	dichloro-(1, 2-diaminocyclohexane) platinum(II)
DCM	dichloromethane
DGS	direção-geral da saúde
DIC	differential interference contrast
DL	drug loading content
DLS	dynamic light scattering
DMEM-F12	dulbecco's modified eagle medium: nutrient mixture F-12
DNA	deoxyribonucleic acid
DOX	doxorubicin
DP	degree of polymerization
ECM	extracellular matrix
EE	encapsulation efficiency
EGF	epidermal growth factor
EGFR	epidermal growth factor receptor
EMEM	eagle's minimum essential medium
EPR	enhanced permeability and retention

FBS	fetal bovine serum
FDA	food and drug administration
FTIR	fourier transform infrared spectroscopy
HPLC	high performance liquid chromatography
IC50	half maximal inhibitory concentration
IFP	interstitial fluid pressure
I.V.	intravenous administration
L-LA; LA	l-lactide
MDR	multidrug resistance
MDR1	multidrug resistance protein 1
MetOH	methanol
MMPs	matrix metalloproteinases
Mn	number average molecular weight
mPEG	methoxy-PEG
MRC-5	human fetal lung fibroblast cell line
MRP1	multidrug resistance-associated protein 1
MRP4, ABCC4	multidrug resistance protein 4
MRP5, ABCC5	multidrug resistance protein 5
MTS	3-(4,5-dimethylthiazol-2-yl)-5-(3-carboxymethoxyphenyl)-2-(4-sulfophenyl)-2H-tetrazolium
NMR	nuclear magnetic resonance
NSCLC	non-small cell lung cancer
P(Asp)	poly(aspartic acid)
P(Glu)	poly(glutamic acid)
p53	tumor supressor p53
PBS	phosphate buffer saline
PCL	poly(caprolactone)
PDE5	phosphodiesterase type 5
PDI	polydispersity
PDLLA	poly(D,L-lactide)
PEG	poly(ethylene glycol)
PEGMA	poly(ethylene glycol) monomethyl ether methacylate
PEO	poly(ethylene oxide)
PEO-PPO-PEO	pluronic
P-gp	p-glycoprotein
PHEMA	poly(2-hydroxyethyl methacrylate)
PLA	poly(lactide acid)
PLGA	poly(lactic-co-glycolic acid)
PMS	phenazine methosulfate
PPO	poly(propylene oxide)

pRb	retinoblastoma protein
PVA	poly(vinyl alcohol)
RES	reticuloendothelial system clearance
RITC	rhodamine B isothiocianate
ROP	ring-opening polymerization
ROS	reactive oxygen species
RT	room temperature
SCLC	small cell lung cancer
SEM	scanning electron microscopy
siRNA	small interfering ribonucleic acid
Sn(Oct)2	tin(II) bis(2-ethylhexanoate)
SN-38	7-ethyl-10-hydroxy-camptothecin
TAMs	tumor associated macrophages
TEA	triethylamine
TGF	transforming growth factor
TMS	tetramethylsilane
TOS	D-α-tocopherol succinate
TPGS	D-α-tocopherol polyethylene glycol succinate
UPLC	ultra performance liquid chromatography
UV-VIS	ultraviolet-visible
VEGF	vascular endothelial growth factor
WHO	world health organization
XRD	x-ray powder diffraction

Chapter 1

Introduction

1. Introduction

1.1. Cancer

1.1.1. Cancer: a pathology in constant evolution

Cancer is a rapidly evolving disease, being presently a major cause of dead worldwide (Lozano et al., 2012). According to the World Health Organization (WHO) reports, in 2012 more than 8 million people died from cancer and 14.1 million new cases have been diagnosed. Nevertheless, the annually published reports elaborated by Siegel and co-workers estimates that 1.7 million people will be diagnosed with cancer and that 586 thousand deaths, will be attributed to this disease, in the United States in 2014 (Siegel et al., 2014). In Portugal, the *Direcção-Geral de Saúde* (DGS) estimates that in 2015 more than 45 thousand people will have cancer diagnosed. This incidence will be growing reaching almost the 60 thousand mark in 2030.

Several risk factors are associated with cancer development and these include: i.) genetic predisposition, ii.) environmental cues (pollution and ultraviolet light exposure), and iii.) lifestyle (food, tobacco and alcohol consumption) (Jemal et al., 2011). Some of these risk factors are family related while others can be preventable. In general, most cancers share associated risk factors, although particular cancers may have associated specific risk factors (Jemal et al., 2011). These factors, contribute for the transformation of a healthy cell into a tumoral cell by a process named carcinogenesis - **Figure 1**.

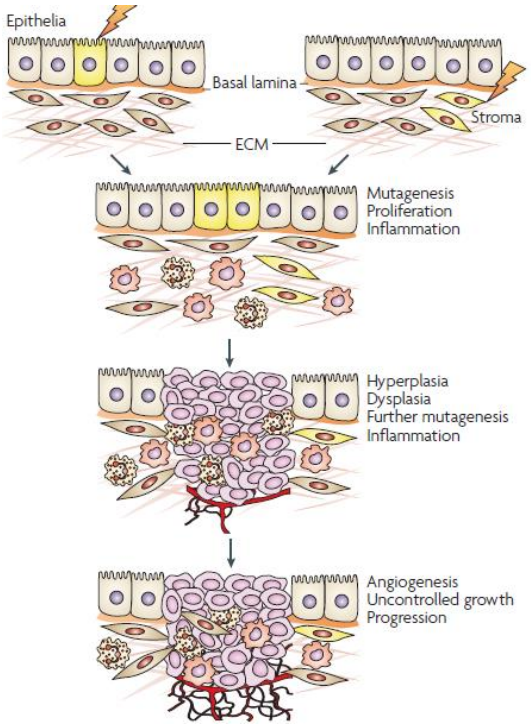

Figure 1 - Representation of the carcinogenesis process. ECM represents extracellular matrix (Adapted from Albini and Sporn, 2007).

Carcinogenesis is a highly complex and uncontrolled process, where both stromal and epithelial cells experience genetic and epigenetic modifications (Albini and Sporn, 2007). These changes provide cancer cells with unique features that make them hard to treat and allow them to rapidly evolve. These newly acquired features were thoroughly described by Hanahan and Weinberg and were termed "Cancer Hallmarks" (Hanahan and Weinberg, 2011). Sustainable proliferative signaling and unlimited replication capacity, mainly through production of mitogenic grow factors and through the presence of high telomerase levels, are cancer hallmarks (Hanahan and Weinberg, 2000). Cancer cells can also evade growth suppressors like tumor suppressor p53 (p53) and retinoblastoma protein (pRb). Moreover, cancer cells can acquire anti-apoptotic mechanisms, for example by overexpressing B-cell lymphoma 2 (BcL-2), thus rendering them resistant to cell death (Hanahan and Weinberg, 2011).

Cancer cells also stimulate immune system cells to secrete pro-inflammatory cytokines that promote cancer growth. Moreover, the formation of new blood vessels (neovascularization) supplies nutrients and soluble growth factors to the tumor, supporting its hyperplastic and dysplastic development, resulting in additional modifications that might endow cancer cells with the capacity to metastasize and invade other organs. The capacity of cancer cells to induce angiogenesis and to metastasize are also cancer hallmarks. Recently, the capacity of cancer cells to avoid immune system destruction and the capacity to change the metabolic pathways were reviewed as additional cancer hallmarks (Hanahan and Weinberg, 2011).

Apart from these main characteristics an emerging body of evidence indicate that cancer cells interact with their surrounding environment and recruit various cells types to sustain their progression (Hanahan and Coussens, 2012). Moreover, the extracellular matrix (ECM), soluble factors and signaling molecules are also impactful in cancer progression (Swartz et al., 2012). These surrounding non-cellular elements and the various types of cells surrounding the tumor constitute the tumor microenvironment - **Figure 2** (Hanahan and Weinberg, 2011). The important role of the tumor microenvironment is changing the concept that cancer is not only comprised by a mass of malignant cells in uncontrolled proliferation, but instead as cells with a malignant phenotype that interact and are supported by their surrounding environment.

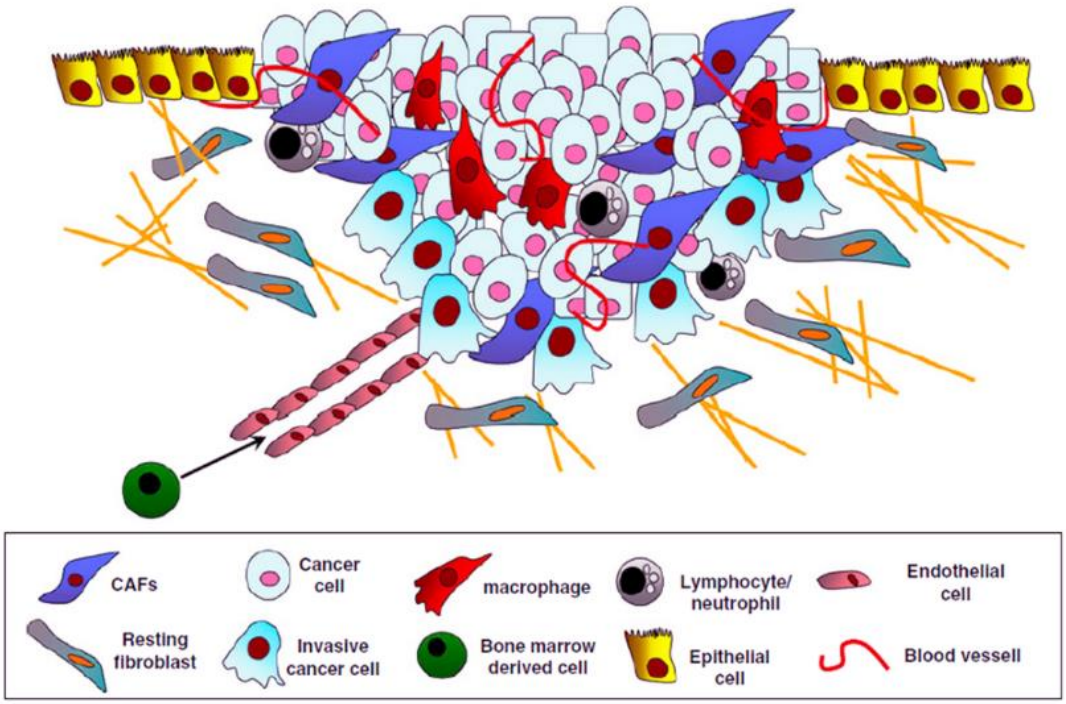

Figure 2 - Illustration of the tumor microenvironment and its major cellular constituents (Adapted from Cirri and Chiarugi, 2012).

The tumor microenvironment is populated with different cells that further sustain various cancer hallmarks or even make them more evident (Hanahan and Coussens, 2012). In this process several stromal cells such as cancer associated fibroblast (CAFs), infiltrating immune system cells, endothelial cells and pericytes participate and support specific cancer hallmarks as illustrated in **Figure 3**. For example, CAFs role is crucial since they secrete growth factors and cytokines that can support tumor growth (Xing et al., 2010). Moreover, CAFs and cancer cells interactions can alter the ECM and basement membrane, promoting cancer cell invasion (Xing et al., 2010). Matrix metalloproteinases (MMPs) secreted by CAFs can also help in ECM remodeling thus contributing to cancer invasion, metastization and also support angiogenesis through vascular endothelial growth factor (VEGF) secretion (Egeblad and Werb, 2002; Xing et al., 2010). CAFs also secrete pro-inflammatory cytokines that attract immune system cells (Xing et al., 2010).

Immune system cells also populate the tumor microenvironment, where tumor associated macrophages (TAMs) play a crucial role in tumorigenesis (Quail and Joyce, 2013). TAMs promote tumor growth, and angiogenesis through VEGF secretion (Mantovani et al., 2006). They also promote cancer cells invasion through epidermal growth factor (EGF) and MMP secretions (Quail and Joyce, 2013). Moreover, TAMs are also capable of suppressing immune system responses (Quail and Joyce, 2013). Despite CAFs and TAMs, there are other types of cells that also contribute for cancer hallmarks and their functions are summarized in **Figure 3** (Hanahan and Coussens, 2012).

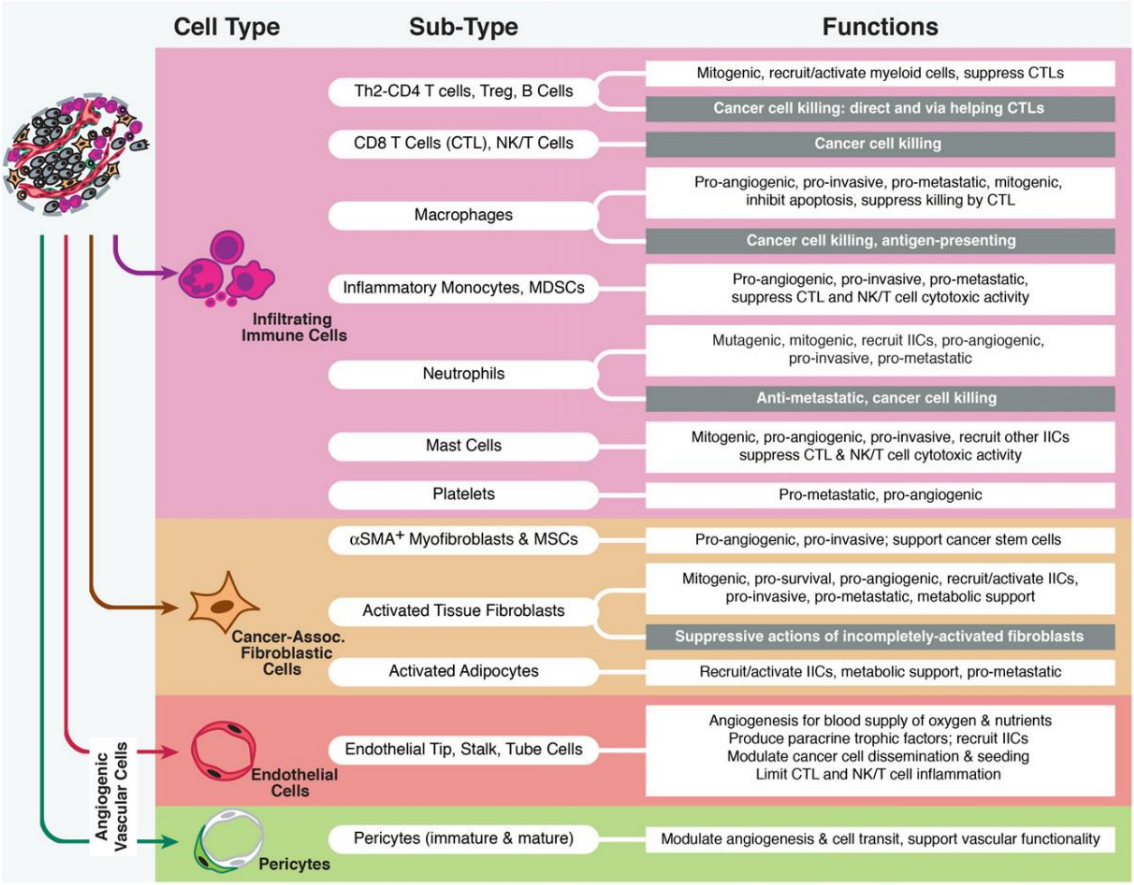

Figure 3 - Contribution of tumor microenvironment populated cells to the major cancer hallmarks. The different stromal cells and their subtypes have distinct contributions to cancer hallmarks. However, contributions against the hallmarks maintenance are also reported (highlighted in gray) (Adapted from Hanahan and Coussens, 2012).

1.1.2. Lung cancer

Among all known types of cancers, lung cancer is one of the most deadly worldwide. Just for 2014 in US, 224 thousand new lung cancer cases and 159 thousand deaths are expected (Siegel et al., 2014). According to the latest report from DGS, lung cancer mortality and incidence has also been growing in Portugal. The high mortality and morbidity associated with lung cancer is often correlated with its late diagnosis (Kadara et al., 2012). Several risk factors are associated with lung cancer. The familiar history and alterations in tumor suppressor proteins such as p53 or pRb are lung cancer associated risk factors (Herbst et al., 2008). Moreover, lifestyle factors such tobacco exposure/consumption and environmental factors such long term air pollution exposure are also risk factors associated with this disease (Herbst et al., 2008; Raaschou-Nielsen et al., 2013).

Lung cancer commonly develops in the central airway in smoking individuals and generally in the peripheral airways in non-smoking or passive smokers - **Figure 4** (Herbst et al., 2008). The lung carcinogenesis process begins with alterations in cellular pathways and functions, due to

genetic and epigenetic changes. These modifications produce hyperplastic and dysplastic cells that can invade the surrounding tissues and in later phases metastasize to other organs.

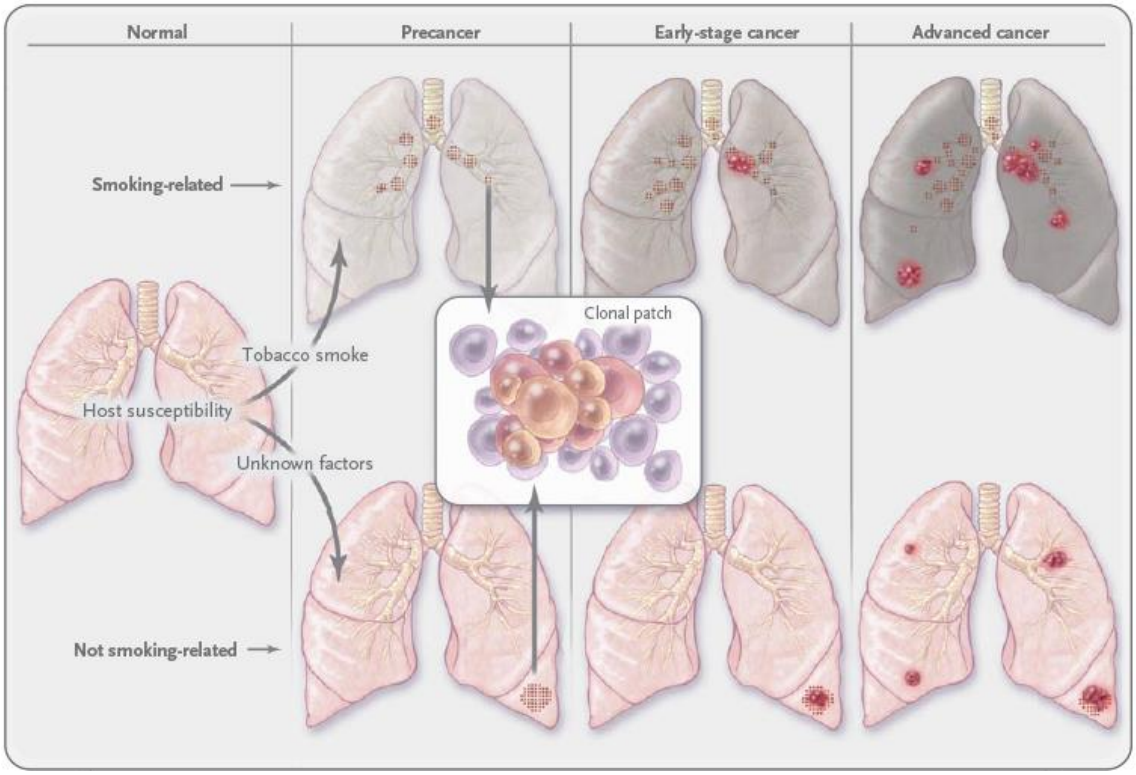

Figure 4 - Lung cancer carcinogenesis. The carcinogenesis process starts with genetic or epigenetic changes that affect cells integrity (pre-cancer). Later, the tumor develops, new vessels are formed (angiogenesis) and cancer cells invade the surrounding tissues (early stage). Metastasis occurs in latter stages (advanced cancer) (Adapted from Herbst et al., 2008).

Lung cancer is currently classified in two major types: small cell lung cancer (SCLC) and non-small cell lung cancer (NSCLC). This classification is based on the size of lung cancer cells observed under the microscope, i.e., SCLC are small when visualized using a microscope whereas NSCLC are larger. SCLC accounts for 15% of lung cancer cases (Kadara et al., 2012). In this lung cancer subtype, treatment options include Platinum based drugs such as Cisplatin and Carboplatin (van Meerbeeck et al., 2011). Combinatorial therapy of Cisplatin and Etoposide is a common therapy for late stages (Kalemkerian et al., 2011). Other drugs such as Paclitaxel, Docetaxel or Gemcitabine constitute the single-drug therapy administered after cancer relapse (Kalemkerian et al., 2011). Thoracic and brain (commonly affected by metastasis) radiation are also considered in SCLC treatment (Kalemkerian et al., 2011). Concerning surgical resection, it should only be performed in SCLC earlier stages, since in late stages cancer is often metastasized to inaccessible organs (Kalemkerian et al., 2011).

In what concerns NSCLC, epidermal growth factor receptor (EGFR) and anaplastic lymphoma kinase (ALK) mutations are very frequent in patients with this type of malignancy (Ettinger et

al., 2012). Chemotherapy that specifically targets these altered pathways is particularly valuable to achieve a higher therapeutic efficacy and improve patient survival rate (Ettinger et al., 2012). For example, Erlotinib is currently administered in EGFR mutated tumors and Ceritinib recently had Food and Drug Administration (FDA) approval for ALK positive NSCLC (Ettinger et al., 2012; Shaw et al., 2014). Combinatorial chemotherapy is also used in NSCLC and has shown slight improves in patient survival (Ettinger et al., 2012). Whenever NSCLC metastasize (like SCLC), tumor resection is not performed and instead, systemic therapy is applied (Ettinger et al., 2012). In this later NSCLC stage, radiation therapy can also be applied to target specific metastasized sites like the brain (Ettinger et al., 2012).

In both subtypes of lung cancer, the 5 year survival rate is dependent on the cancers development stage. Due to lung cancer late diagnosis, it is often treated in later stages, where the 5 year survival rates are below 15% for NSCLC and below 9% for SCLC, as reported by the US National Cancer Institute. In these later stages cancer cells metastasize and chemotherapy is the main treatment option. However, after multiple administrations cancer cells generally acquire resistance to chemotherapy (Shanker et al., 2010). The comprehension of cancer resistance mechanisms and the development of strategies to overcome them is essential to improve the therapeutic outcomes.

1.1.3. Cancer drug resistance - mechanisms and strategies

Cell resistance to chemotherapeutics is currently one of the main reasons for inefficacy of cancer treatments. Cancer cells can acquire multidrug resistance (MDR) through: i.) increased activity of growth factor receptors, ii.) constitutive activation of deoxyribonucleic acid (DNA) repair mechanisms, iii.) inhibition of apoptosis via modulation of various signaling pathways, iv.) increased drug metabolism, v.) mutations in drug intracellular targets, vi.) decreased dug influx and vii.) increased drug efflux - **Figure 5** (Gottesman, 2002; Gottesman et al., 2002; Holohan et al., 2013).

Cancer cells can develop resistance to inhibitors of growth factors receptors. For example they acquire resistance to EGFR inhibitors through mutations and modifications in the signaling cascade precursors (Sartore-Bianchi et al., 2009; Sos et al., 2009). Also, DNA repair mechanism are often upregulated in cancer cells, thus rendering them resistant to DNA targeted drugs, such as Cisplatin or Carboplatin (Bouwman and Jonkers, 2012). Resistance to chemotherapy is also developed by promoting modifications in key regulators of apoptosis, such as the BcL-2 family (Holohan et al., 2013). Chemotherapeutic agents are often substrates of cytochrome P450 enzyme and thus susceptible to be metabolized reducing their plasma levels and consequently their therapeutic potential (Gottesman, 2002). Moreover, modifications in the drug targets can also confer drug resistance. For instance, cancer cells can acquire resistance to Crizotinib through secondary mutations that affect the ALK tyrosine kinase domain and by reprograming their proliferation pathways (KIT and EGFR pathways) (Katayama et al., 2012).

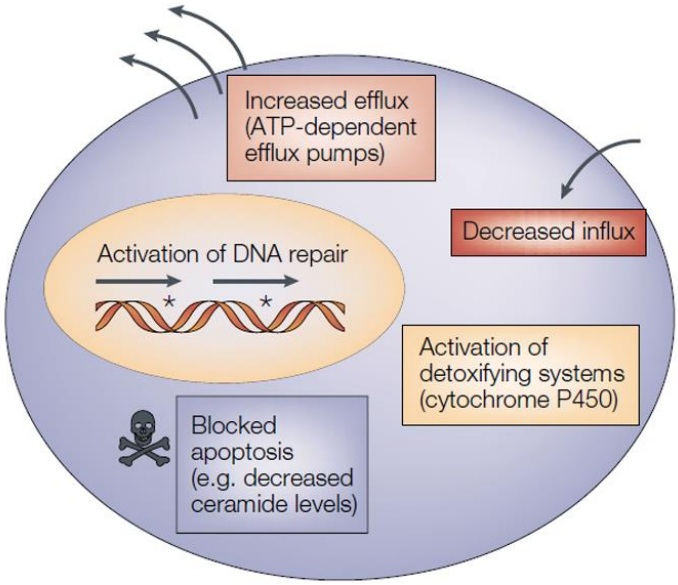

Figure 5 - Representation of major cancer drug resistance mechanisms. Cancer drug resistance can be mediated through changes in drug influx and efflux, metabolism of chemotherapeutic drugs, resistance to apoptosis and upregulation of DNA repair mechanisms. Additionally, modifications in drugs targets and in growth factor receptors also contribute to cancer drug resistance (not represented) (Adapted from Gottesman et al., 2002).

The efflux of chemotherapeutic drugs, i.e., the shuttle of drugs to the extracellular medium is an important cancer drug resistance mechanism and is mainly mediated by adenosine triphosphate (ATP)-binding cassette (ABC) transporters (Holohan et al., 2013). Among all types of ABC transporters, three have been particularly investigated regarding cancer resistance: i.) multidrug resistance protein 1 (MDR1 also known as P-glycoprotein (P-gp)), ii.) multidrug resistance-associated protein 1 (MRP1) and iii.) breast cancer resistance protein (BCRP or ABCG2) (Holohan et al., 2013).

These efflux transporters are generally overexpressed in cancer cells as a response to chemotherapeutics and play a crucial role in mediating cells resistance to commonly administered drugs (Doublier et al., 2012; Stordal et al., 2012). For example Doxorubicin (DOX) is a substrate to both MDR1, MRP1 and BCRP (Gottesman et al., 2002). Paclitaxel and Etoposide are MDR1 and MRP1 substrates (Ozben, 2006). Other chemotherapeutic drugs are also substrates of drug efflux transporters (Gottesman et al., 2002; Ozben, 2006).

Despite the identification of ABC transporters as a main cause for the inefficiency of chemotherapeutics, the clinical trials using drugs capable of inhibiting these efflux pumps have not yet been successful (Falasca and Linton, 2012; Fletcher et al., 2010). Besides drug based ABC transporter inhibition, other technologies such as small interfering ribonucleic acid (siRNA) are also capable of inhibiting drug efflux pumps by silencing the pumps expression. However, in addition to non-specific accumulation concerns, siRNA based therapies are limited to the

inhibition of a single type of drug efflux pump and only have a therapeutic effect in a limited time-frame (Shim and Kwon, 2010).

In this context, combinatorial therapies composed of multiple chemotherapeutic drugs and agents capable of reversing MDR are an attractive strategy that can improve chemotherapy efficacy and ultimately increase the patients survival rate (Falasca and Linton, 2012).

1.1.4. Combinatorial therapy

Cancer cells intracellular machinery promptly adapts to the presence of chemotherapeutics, thus rendering the cells resistant to chemotherapy and contributing to its inefficacy.

Combinatorial chemotherapy is a treatment modality that may introduce some improvements in cancer treatment. This concept is based on the targeting of various altered pathways simultaneously, through the use of different chemotherapeutics, and can also include agents capable of MDR reversal, to improve the therapeutic outcome.

In this context, investigating novel drug mixtures could be a valuable approach to discover particularly effective combinations for cancer therapy. The combination of Crizotinib, a known lung cancer chemotherapeutic drug, Palbociclib, a novel and potent cell cycle arrester and Sildenafil, a drug capable of inhibiting several types of ABC transporters, is a promising combination for lung cancer therapy since major cancer hallmarks are targeted at once.

Crizotinib is an FDA approved drug for non-small cell lung cancer therapy. This drug is a potent inhibitor of hepatocyte growth factor receptor (c-Met) and ALK tyrosine kinases. Met signaling has shown to have impact in carcinogenesis, contributing to tumor growth, survival, invasion and metastization (Gherardi et al., 2012; Peters and Adjei, 2012). It is important to emphasize that ALK aberrant signaling also contributes to cell resistance to apoptosis (Hallberg and Palmer, 2013). Moreover, Crizotinib is also capable to induce apoptosis via the Caspase-3 signaling pathway and of inhibiting P-gp activity (Okamoto et al., 2012; Zhou et al., 2012). The latter is particularly interesting since Crizotinib can inherently inactivate one of the major efflux transporters (P-gp) (O'Bryant et al., 2013).

Palbociclib is a novel drug with cell cycle arresting properties that soon will be used in phase III of clinical trials for breast cancer therapy (Rocca et al., 2014). Palbociclib is a bioactive and highly selective cyclin-dependent kinase (CDK) 4 and 6 inhibitor, that acts by binding to CDK4/6 ATP site (Rocca et al., 2014). It prevents pRB phosphorylation resulting in G1 cell cycle arrest and it can lead to tumor regression through its cell cycle arresting capacity (Fry et al., 2004). Palbociclib combination with different drugs for cancer therapy has been investigated and both synergistic and antagonistic effects were observed (Rocca et al., 2014). In fact, the combination of Palbociclib with chemotherapeutic drugs such as Paclitaxel, Carboplatin or DOX has shown antagonist effects (the overall effect of the combination is inferior to the sum of the drugs

individual effects) (Dean et al., 2012; Roberts et al., 2012). However, the currently available data shows that Palbociclib combination with endocrine agents, such Tamoxifen and Trastuzumab is advantageous (Rocca et al., 2014).

Sildenafil or Viagra® (commercial designation) is a known drug used to treat male erectile dysfunction (Boolell et al., 1996). It inhibits cyclic guanosine monophosphate (cGMP)-specific phosphodiesterase type 5 (PDE5), resulting in increased cGMP intracellular levels that are linked to increased vasodilatation (Boolell et al., 1996). In addition to this activity, Sildenafil is an inhibitor of P-gp, BCRP, multidrug resistance protein 4 (ABCC4; MRP4) and multidrug resistance protein 5 (ABCC5; MRP5) (Shi et al., 2011a; Shi et al., 2011b). Sildenafil capacity to inhibit several types of efflux transporters confer it a MDR inhibiting potential. However, it is important to point out that non-specific ABC transporters inhibition could also promote drug accumulation in healthy cells and thereby increase the systemic toxicity (Fletcher et al., 2010). In fact, the free drug administration of Sildenafil combined with therapeutic drugs may cause undesired accumulation of these drugs cocktails in healthy tissues and increase organ-specific cytotoxicity (Lin et al., 2013). Nevertheless, its combination with DOX and Paclitaxel has been proved to be advantageous *in vivo*, since its inclusion promoted significant reductions in the tumor weight (Chen et al., 2014; Das et al., 2010).

The combinatorial therapy approach for cancer treatment is under extensive investigation. In fact, currently a search with the terms “combination cancer” in clinicaltrials.gov lists around 3000 trials recruiting for this modality. However, this therapy is challenging due to unknown drug-drug interactions in the plasma and also tissue partitioning. Moreover, since the combination of multiple bioactives can lead to antagonistic results and systemic cytotoxicity, these combinations need to be carefully investigated (Roberts et al., 2012; Sandler et al., 2006). In this context, the current developments attained in Nanomaterials science may contribute for improving combinatorial therapies by increasing the bioavailability of chemotherapeutics in target cells, whilst, decreasing systemic exposure.

1.2. Nanotechnology in cancer treatment

1.2.1. Nanomedicines - potential and application

In the past years, a great effort has been done to develop nanotechnologies capable of improving cancer treatment (Zamboni et al., 2012). Nanomedicine based strategies aim to i.) improve chemotherapeutic drugs efficacy, ii.) increase the therapeutic window and iii.) lower the undesired side effects (Zamboni et al., 2012). Nanoparticles can be produced with organic or inorganic compounds, and have a size that ranges from 1 to 1000 nm (Schroeder et al., 2012). Nanoparticles tend to accumulate preferentially in tumor tissues (Jain and Stylianopoulos, 2010; Parveen et al., 2012). Thereby they can increase drugs bioavailability, reduce the drug dose necessary to attain a therapeutic effect and, more importantly, reduce non-specific toxicity, diminishing chemotherapeutics undesired side effects (Parveen et al., 2012).

For nanoparticles to achieve optimal anti-tumoral activity, they must possess precise features that endow them with the capacity to be stable in the complex biological environment (Ernsting et al., 2013). Moreover, these characteristics have to be precisely designed to achieve an optimal therapeutic efficacy. Therefore, nanoparticles have to be formulated with a focus on application-oriented design. In fact, during the nanoparticle production process the final characteristics of the nanodevice ultimately affect its pharmacokinetic/pharmacodynamic profile, i.e., the nanodevice characteristics will influence its absorption, distribution, metabolism and excretion (pharmacokinetic profile) and also influence their therapeutic effect (pharmacodynamic profile).

1.2.2. Nanoparticles rationale design - factors affecting nanoparticles therapeutic efficacy

Nanoparticles administration routes include i.) ocular, ii.) nasal, iii.) oral, iv.) pulmonary, v.) transdermal and vi.) parenteral (Park, 2014). During their circulation in the human body, there are several nanoparticle features that will dictate their biological fate, namely their organ accumulation or excretion, interaction with blood components or diverse cell types, that account for the overall success of the systems for cancer treatment (Ernsting et al., 2013).

The route of administration largely influences the biological fate of the nanocarriers since they will encounter different barriers until they reach the target site. This section will mainly be focused on the biological processing of nanodevices after intravenous administration (i.v.) since this route is currently the most commonly applied (Etheridge et al., 2013). In fact, all FDA approved drug-loaded nanovehicles are administered intravenously - **Table 1** (Etheridge et al., 2013). Despite this, it should be emphasized that recently other administration routes such as the oral route is receiving an ever growing attention (Mei et al., 2013).

Table 1 - FDA approved nanovehicles to deliver chemotherapeutic drugs in cancer treatment (Adapted from Etheridge et al., 2013 and Prabhakar et al., 2013).

Commercial Name	Nanovehicle description	Therapeutic drug	Administration Route	Type of tumor approved for
Abraxane	Albumin-drug conjugate nanoparticle	Paclitaxel	Intravenous	Metastatic breast cancer
DaunoXome	Liposome	Daunorubicin Citrate	Intravenous	HIV-related Kaposi's sarcoma
Doxil	PEGylated Liposome	DOX	Intravenous	HIV-related Kaposi's sarcoma Metastatic ovarian cancer Metastatic breast cancer

Regardless of the type of nanocarrier, generally following i.v., nanoparticles have to be stable in circulation to increase their likelihood of being extravasated to diseased tissues. Also a premature drug release from the nanocarrier will lead to hepatic first-pass metabolism and cytotoxicity. Following i.v., nanoparticles have to avoid renal clearance and avoid reticuloendothelial system clearance (RES). Then nanoparticles still have to extravasate into the tumor microenvironment and penetrate in the tumor. Finally nanoparticles have to be internalized by cancer cells and release their content inside cancer cells - **Figure 6** (Ernsting et al., 2013).

Immediately after intravenous injection, nanoparticles must remain stable in the plasma, avoid renal filtration and RES clearance by circulating monocytes, macrophages of the liver (Kupffer cells) and splenocytes. Nanoparticles characteristics such as size, surface decoration and charge are crucial for assuring the success of this initial phase.

Nanoparticles size should not be lower than 5.5 nm or otherwise the nanocarriers will be rapidly cleared by renal filtration (Choi et al., 2007). Liver fenestrations size (50-100 nm) also have an influence in pharmacokinetics and particles should not have a size lower than 50 nm or they will extravasate through liver fenestrations and interact with hepatocytes and Kupffer cells (Ernsting et al., 2013). Generally it is accepted that particles size should not exceed the 200 nm, or they will undergo spleen filtration, however, this upper size limit tends also to be affected by other aspects like nanoparticles deformability and shape (Ernsting et al., 2013).

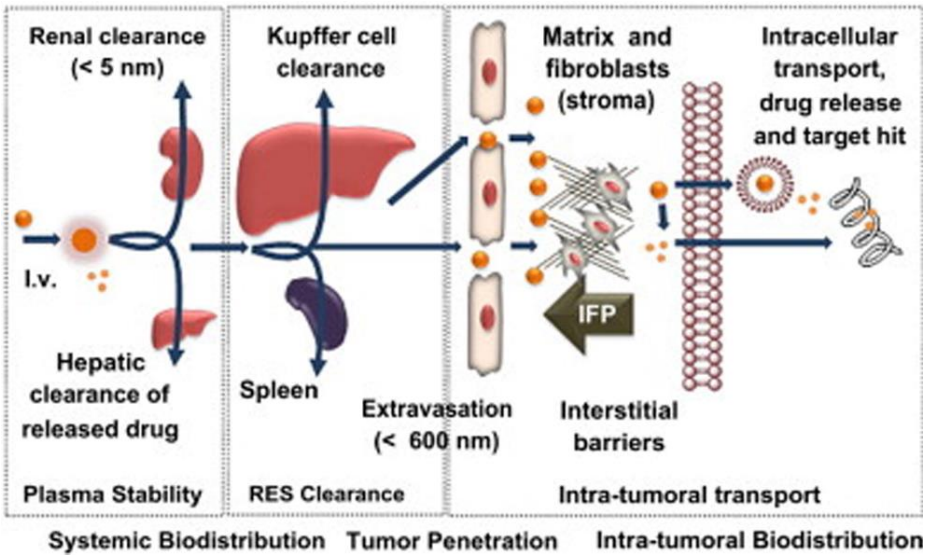

Figure 6 - Factors affecting nanoparticles pharmacokinetics, biodistribution and intratumoral penetration following intravenous injection. IFP represents interstitial fluid pressure (Adapted from Ernsting et al., 2013).

The nanocarriers surface decoration is a key factor that mediates RES interactions since it affects nanoparticles protein aggregation, phagocytosis and macrophage uptake (Ernsting et al., 2013). Decorating nanoparticles surface with poly(ethylene glycol)(PEG) is a common strategy that confers "stealth" properties to nanoparticles, in such a way that it reduces opsonization and RES clearance (Jokerst et al., 2011). However PEGylation mechanism are not so linear and its efficacy is dependent on factors such as PEG density, size of the polymer chain and spatial orientation (Walkey et al., 2012; Yang et al., 2014).

Particles surface charge also affects the pharmacokinetic profile of the nanoparticles. In the literature it is generally reported that particles of zeta potential (ζ) lower than -10mV will have strong RES uptake and particles of zeta higher than +10 mV will exhibit high protein absorption, thus rendering the so called neutral particles ($-10 \leq \zeta \leq +10$ mV) the most appropriate for therapy since they have both low RES uptake and low protein absorption (Ernsting et al., 2013).

After avoiding renal filtration and RES clearance, nanoparticles must accumulate near the tumor site. To achieve this, particles extravasate through the abnormal and leaky tumor vasculature that has fenestrations of 400 to 600 nm (Yuan et al., 1995). This phenomenon is called Enhanced Permeability and Retention (EPR) effect, and particles of size 20-200nm are considerate to be optimal for accumulating by the EPR effect, being capable to extravasate and accumulate in the interstitial space - **Figure 7** (Danhier et al., 2010). However, in nanoparticles design, not only the size parameters for the EPR effect should be taken into consideration, but also, the previously mentioned size restrictions that impact on renal and RES clearance. Moreover, following extravasation, particles residence in the tumoral interstitial space is promoted by poor lymphatic drainage (Danhier et al., 2010).

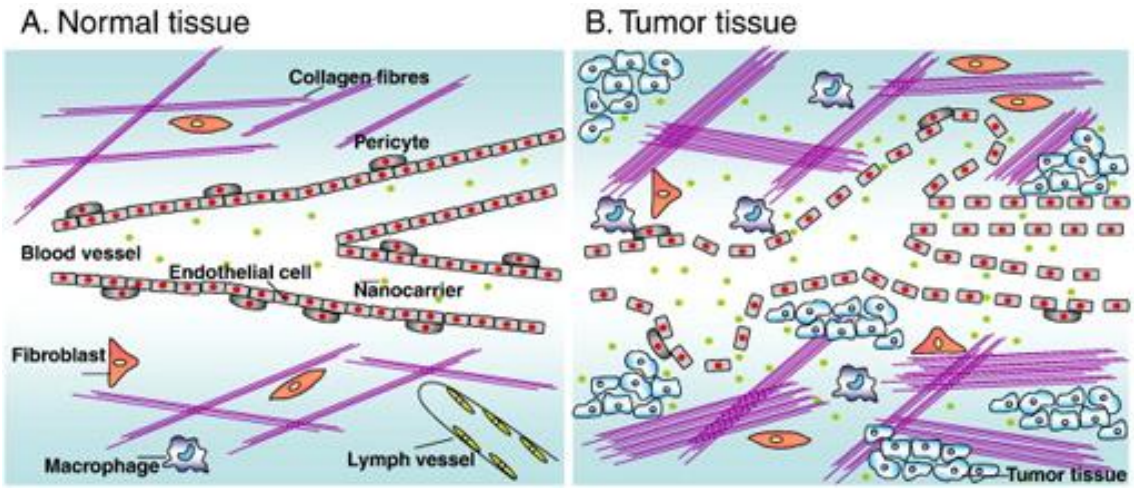

Figure 7 - Comparison between normal tissue organization and tumoral tissue organization. A) Normal tissue has regular blood vessels, lymphatic drainage and regular populations of fibroblasts and macrophages. B) Tumoral tissue vasculature is leaky and has abnormal lymphatic drainage. Moreover, the fibroblast and macrophages populations are bigger, with CAFs and TAMs present. The collagen fibers are also in higher quantity (Adapted from Danhier et al., 2010).

Following retention in tumor interstitial tissue, nanoparticles still have to penetrate into the tumor, be internalized and release their cargo inside cancer cells in order to promote a therapeutic effect. Several tumor-related factors influence this process including the tumor vasculature, interstitial fluid pressure (IFP), the presence of stromal cells and TAMs. The remaining factors such as size, shape, zeta potential, composition and targeting ligands are nanoparticle-related characteristics (Ernsting et al., 2013).

Tumor has an heterogeneous vasculature, and as consequence its periphery is highly perfused whereas its core is poor on blood supply, resulting in an heterogeneous nanoparticle distribution inside the tumor (Lee et al., 2010). The abnormal tumor vasculature and the absence or poor lymphatic drainage, produces high interstitial fluid pressure, a characteristic associated to the majority of known solid tumors, thus resulting in inefficient tumoral uptake nanoparticles - **Figure 7** (Heldin et al., 2004). The cells that populate the tumor microenvironment, also influence nanoparticles tumor penetration. Namely, fibroblasts contractile forces and their secreted collagen also impair nanoparticles tumor penetration (Danhier et al., 2010). TAMs can sequester nanoparticles, thus reducing their availability for tumor penetration, affecting the overall therapeutic outcome (Ernsting et al., 2013).

Regarding nanoparticle-related characteristics affecting the carriers uptake by cancer cells, once again size is an important feature. Nanoparticle size affects their internalization by cancer cells and each delivery system seems to have an optimal nanoparticle size that favors its internalization (Chithrani et al., 2006; Gratton et al., 2008). Shape also plays an important role in nanoparticles uptake, however, regarding this parameter various studies report that the spherical shape is optimal, while others demonstrate that a rod-like shape is more advantageous

(Ernsting et al., 2013). Generally, positively charged particles tend to have a greater uptake in cancer by electrostatic interactions with cancers cells negatively charged membrane proteoglycans (Ernsting et al., 2013). On the other hand, electrostatic interactions between nanoparticles and ECM components can have a negative impact in their tumor penetrating capacity. For instance, positively charged nanoparticles tend to interact with hyaluronan (negatively charged) whereas negatively charged nanoparticles will interact with collagen (positively charged), resulting in reduced tumor penetration (Ernsting et al., 2013). The nanoparticles intrinsic composition, coating or emulsifying agents have also contributions in nanoparticles cellular uptake (Zhang and Feng, 2006a). Moreover, nanoparticles can possess targeting moieties, resulting in nanoparticles specific uptake mediated by endocytosis in cells expressing the receptor for the targeting ligand. Still for an optimal therapeutic outcome, the previous factors that influence nanoparticles pharmacokinetics and biodistribution should be taken into consideration in the rationale design process.

1.2.3. Nanoparticles for cancer therapy: a diversified pool of opportunities

Presently, a myriad of nanocarriers from diverse materials have been developed for therapeutic applications. Generally, nanovehicles can be divided in organic and inorganic **- Figure 8** (Nazir et al., 2014). Organic nanoparticles include liposomes and polymerosomes. These nanodevices have an aqueous core and are particularly useful to deliver both water and non-water soluble biopharmaceuticals. Dendrimers are another class of nanodevices composed by a repeated hyperbranched structures and are capable of delivering covalently and non-covalently bound drugs. Polymeric nanospheres are particles with a polymeric hydrophobic core surrounded by hydrophilic shell. They can be formulated with hydrophobic polymers, hydrophobic plus hydrophilic polymer mixtures and amphiphilic polymers**.** Polymeric micelles are composed of amphiphilic polymers that self-assemble in water into nanosized core-shell structures. Polymer-drug conjugates can also self-assemble and form nanodevices, an example of known application is the drug-PEGylation.

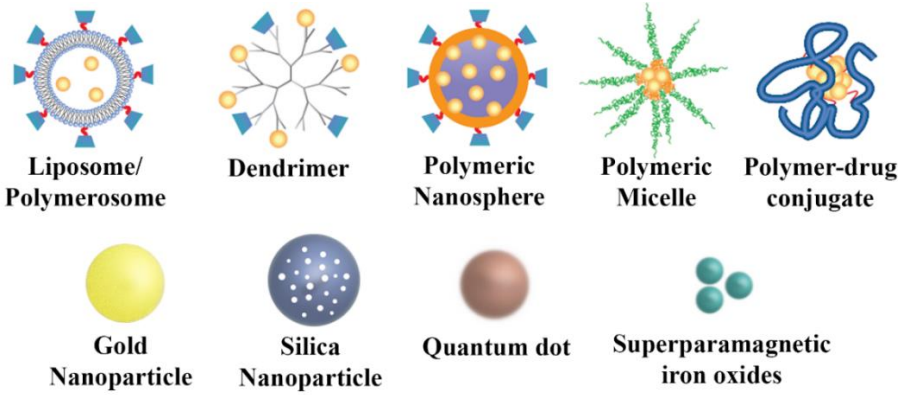

Figure 8 - Schematic representation of the different types of organic (upper row) and inorganic (lower row) nanovehicles (Adapted from Peer et al., 2007 and Yezhelyev et al., 2009).

Regarding inorganic nanoparticles, gold nanoparticles have a broad spectrum of application from therapy, to cancer detection and diagnosis (theranostics). Silica nanoparticles are porous and can encapsulate therapeutic agents on their pores. Quantum dots are useful for imaging applications due to their near infrared fluorescence. Superparamagnetic iron oxides are most useful in imaging applications and as thermal therapy agents.

There are different nanovehicles and each one has an optimal set of applications. Polymeric micelles are a promising nanodelivery system for cancer therapy and their features will be highlighted in the next section.

1.3. Polymeric nanovehicles in cancer treatment

1.3.1. Polymeric micelles

Polymeric micelles are one of the most appealing nanovehicles for cancer treatment. Polymeric micelles are made of amphiphilic polymers or block copolymers with amphiphilic properties, that self-assemble in water forming nanosized carriers (Owen et al., 2012). The hydrophobic segment of the amphiphilic polymer forms the micelles core and the hydrophilic segment the shell - **Figure 9**. The polymer assembly into nanosized particles only takes place when the polymer concentration is above a concentration, termed critical micellar concentration (CMC).

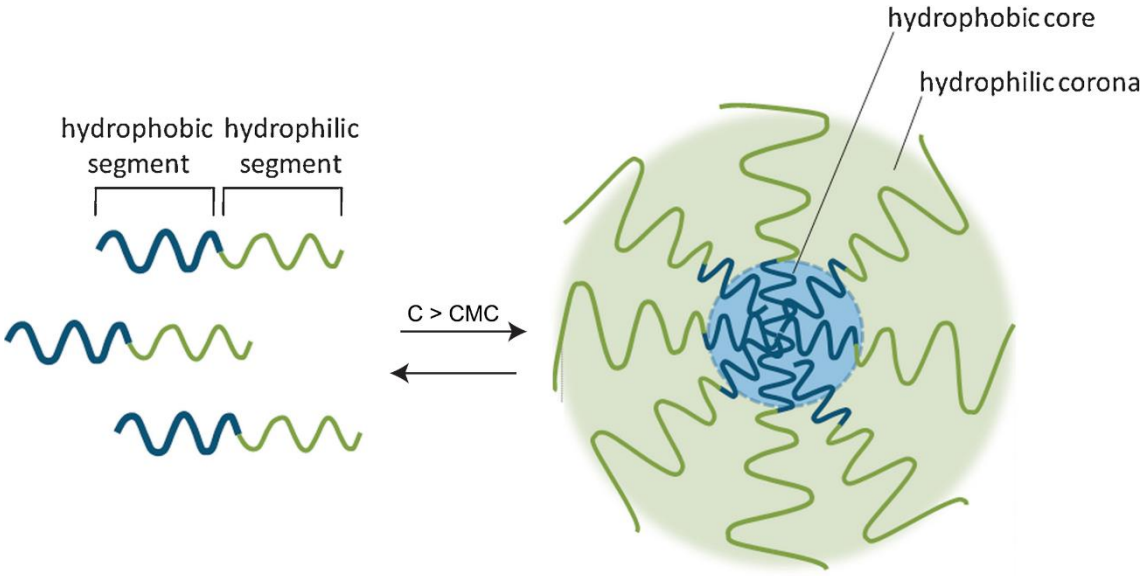

Figure 9 - Micelles self-assembling at concentrations above CMC. C represents the amphiphilic polymer concentration and CMC represents critical micellar concentration (Adapted from Owen et al., 2012).

Polymeric micelles have good properties that renders them exceptional carriers for drug delivery purposes. Their formulation is very straightforward since they self-assemble in aqueous environments. The polymeric micelles entrap hydrophobic drugs in their core, during the self-assembling process and have high loading capacity (Gong et al., 2012). The drug entrapment is promoted by drug-polymer and drug-drug hydrophobic interactions in the micelles hydrophobic core. Besides this, micelles are biocompatible and are often formulated with biodegradable polymers (Deng et al., 2012). Most of the times, polymeric micelles have EPR effect suitable characteristics such as long circulation time and adequate size, thus being capable of improving chemotherapeutic drugs bioavailability (Gong et al., 2012).

The applicability of polymeric micelles in cancer treatment is reflected by the number of formulations under clinical evaluation (Etheridge et al., 2013). Polymeric micelles based on PEG, poly(aspartic acid) (P(Asp)), poly(glutamic acid) (P(Glu)) or poly(D,L-lactide) (PDLLA) to

deliver drugs such as Paclitaxel, Cisplatin or DOX are some examples - **Table 2** (Gong et al., 2012).

Table 2 - Polymeric micelles formulations under clinical evaluation (Adapted from Gong et al., 2012).

Name	Polymer	Hydrophilic Segment	Hydrophobic Segment	Drug	Type of Cancer
Genexol®-PM	mPEG-PDLLA	mPEG	PDLLA	Paclitaxel	Solid Tumors
NK105	PEG-P(Asp) derivative	PEG	P(Asp) derivatives	Paclitaxel	Stomach Cancer
NC-6004	PEG-P(Glu)(Cisplatin)	PEG	P(Glu) bounded to Cisplatin	Cisplatin	NSCLC
NC-4016	PEG-P(Glu) (DACHPt)	PEG	P(Glu) bounded to DACHPt	DACHPt	Solid Tumors
NK012	PEG-P(Glu)(SN-38)	PEG	P(Glu) conjugated to SN-38	SN-38	Solid Tumors
NK911	PEG-P(Asp)(DOX)	PEG	P(Asp) conjugated to DOX	DOX	Solid Tumors
SP1049C	Pluronic L61, F127	PEO-PPO-PEO		DOX	Solid Tumors

DACHPt: dichloro-(1, 2-diaminocyclohexane) platinum(II); SN-38: 7-ethyl-10-hydroxy-camptothecin; methoxy-PEG (mPEG); Pluronic: PEO-PPO-PEO (PEO: Poly(ethylene oxide); PPO: poly(propylene oxide)).

In pre-clinical studies other block copolymers have shown promising characteristics for cancer therapy. They are commonly comprised by poly(caprolactone) (PCL), poly(lactide acid) (PLA) or poly(lactic-co-glycolic acid) (PLGA). Moreover, polymers capable of modulating micelles release have been dragging some attention since they can promote the micelles cargo release in the presence of an external stimuli.

1.3.2. Materials of amphiphilic nature in polymeric micelles design

Polymeric micelles can be engineered using different amphiphilic polymers. The micelles shell usually is a PEG- derivative as mPEG or poly(ethylene glycol) monomethyl ether methacylate (PEGMA).

Using PEG as the hydrophilic polymer offers some advantages such as easy end-group functionalization, lower interaction with blood components, prevention of opsonization and prolonged circulation times (Knop et al., 2010). PEG is also biocompatible and can protect drugs from enzymatic degradation (Elsabahy and Wooley, 2012). PEG can be removed by renal filtration if its weight does not exceed 40-60 kDa (Knop et al., 2010).

The hydrophilic polymer has to be conjugated with a polymer of hydrophobic nature in order to allow micelles formation. Regarding hydrophobic polymers, two of the most commonly employed are PLA and PLGA (Panyam and Labhasetwar, 2003). These polyesters are biocompatible and biodegradable in the human organism (Kumari et al., 2010). These polymers are hydrolyzed into their monomers, glycolic and/or lactic acids, and will serve as metabolic precursors in Krebs cycle (Panyam and Labhasetwar, 2003). The polymer biodegradability is influenced by factors such molecular weight and crystallinity, and the degradation rate of the hydrophobic chain allows the release of the entrapped drugs with a sustained profile (Anderson and Shive, 2012; Madhavan Nampoothiri et al., 2010).

Several combinations of PEG with lactide-based hydrophobic polymers are reported in the literature and those are very versatile nanodelivery systems. Nasongkla and co-workers formulated targeted PEG-PLA micelles containing DOX and superparamagnetic iron oxides for multimodality cancer treatment (Nasongkla et al., 2006). PCL is also often polymerized in PEG derivatives for nanodelivery purposes. Gou *et al.* prepared Curcumin loaded mPEG-PCL micelles for colon cancer therapy that demonstrated good anticancer activity both *in vitro* and *in vivo* (Gou et al., 2011). Other hydrophilic polymers such as poly(2-hydroxyethyl methacrylate) (PHEMA) or D-α-tocopherol polyethylene glycol succinate (TPGS) have also been conjugated with lactide based polymers for drug delivery purposes (Wu et al., 2013; Zhang and Feng, 2006a).

1.3.3. Ring-opening polymerization

The formulation of diblock copolymers containing hydroxyl terminated hydrophilic polymers and PLA, PCL or PLGA can be performed by ring-opening polymerization (ROP) of the lactide, caprolactone or lactide and glycolide monomers, respectively. The ROP is the most efficient method to polymerize poly(esters) and produces products with well controlled molecular weight (Thomas, 2010). Among all ROP catalysts, tin(II) bis(2-ethylhexanoate) ($Sn(Oct)_2$) is FDA approved and is the most used in industrial and biomedical applications (Dijkstra et al., 2011). The mechanism of polymerization of lactones using this catalyst is through the so-termed

coordination-insertion mechanism - **Figure 10** (Thomas, 2010). In the initiation step, $Sn(Oct)_2$ will react with the initiator, generating Tin(II) alkoxides, the true initiator - **Figure 10 A** (Dijkstra et al., 2011). Then, the monomer (polymer precursor) coordinates with the $Sn(Oct)_2$ metal center, through its carbonyl oxygen, and the alkoxide end chain will attack the carbonyl carbon of the monomer, resulting in the ring opening - **Figure 10 B** (Stanford and Dove, 2010). An extended chain will be formed and the polymerization propagates, with the coordination of another monomer with the newly formed alkoxide (Thomas, 2010). ROP is widely applied in the literature to polymerize hydrophobic segments on PEG and Vitamin E derivatives, for example, mPEG-PLA, TPGS-PLA or TPGS-PLGA diblock copolymers synthesis.

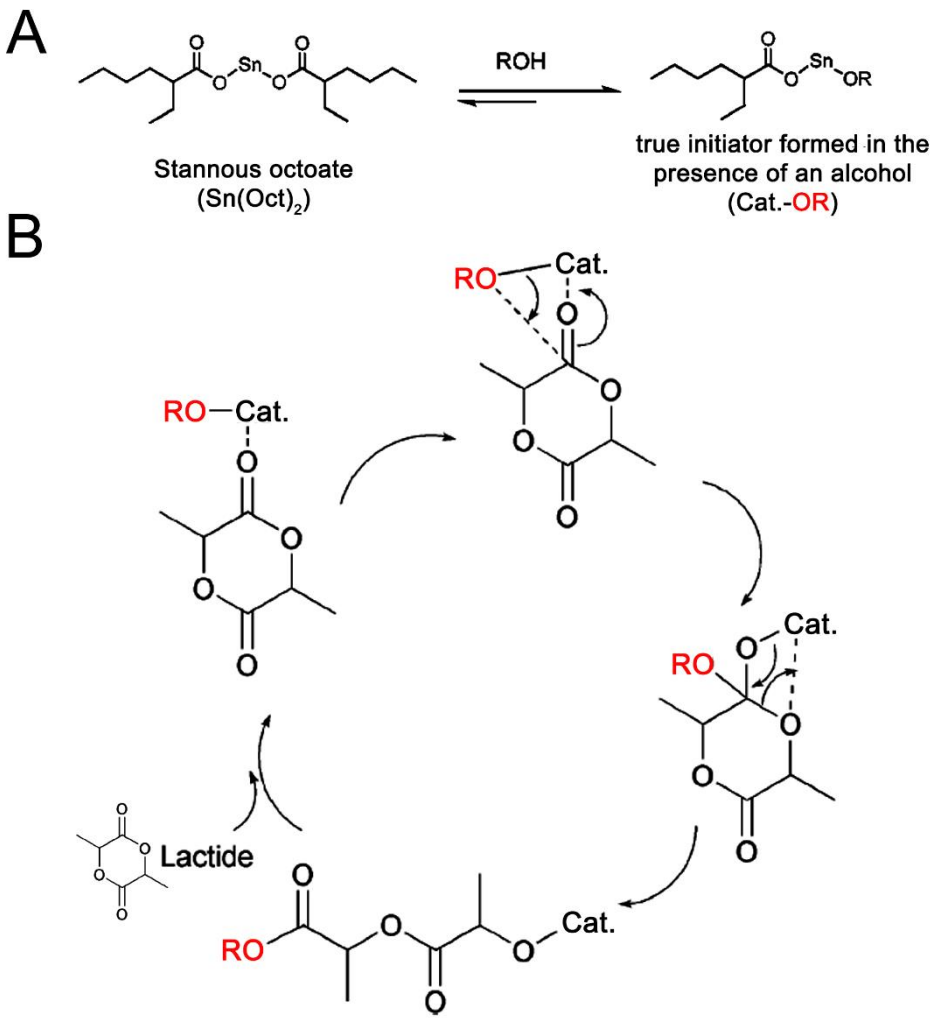

Figure 10 - Coordination-insertion mechanism for lactide polymerization. A) Synthesis of the true initiator. B) coordination-insertion of lactide in a polymer with OH-. Cat. represents $Sn(Oct)_2$ and -OR can represent several polymers with hydroxyl groups such as mPEG or TPGS (Adapted from Dijkstra et al., 2011 and Williams, 2007).

1.3.4. Vitamin-E based nanomedicines

The Vitamin E family is constituted by tocopherols and tocotrienols, either in alpha (α), beta (β), gamma (γ), and delta (δ) form, having a total of 8 isomers - **Figure 11** (Wong and Radhakrishnan, 2012). Vitamin E has several roles in different cell functions (Duhem et al., 2014).

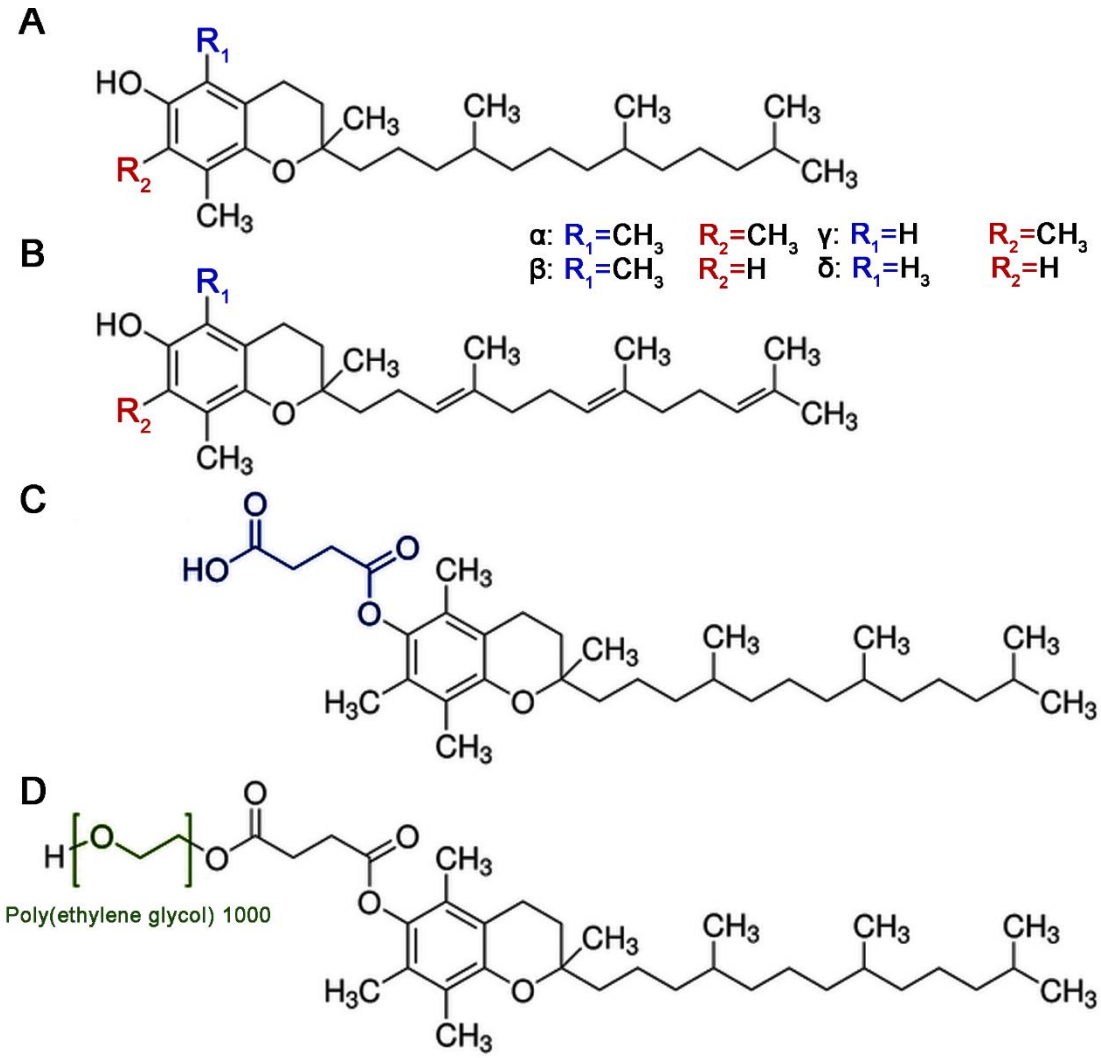

Figure 11 - Vitamin E family members and derivatives. A) Structure of tocopherols. B) Structure of tocotrienols. C) TOS and D) TPGS. (Adapted from Wong and Radhakrishnan, 2012).

D-α-Tocopherol succinate (TOS) is a vitamin E ester and has shown anticancer activity in several cancer cell lines, however, the half maximal inhibitory concentration (IC50) is high compared to common therapeutic drugs (Dong et al., 2011). The anti-tumoral mechanisms of TOS were recently reviewed in the literature by Duhem and co-workers (Duhem et al., 2014). In brief, TOS can inhibit tumor cell proliferation (either by affecting DNA synthesis or cell cycle) and can induce extrinsic (Fas and transforming growth factor (TGF) pathways) and mostly intrinsic (reactive oxygen species (ROS) mediated) mediated apoptosis of tumor cell (Duhem et al.,

2014). TOS can also inhibit angiogenesis (inhibition of VEGF and other factors) and tumor metastization (inhibition MMP-9) (Duhem et al., 2014).

TGPS is a PEGylated Vitamin E derivatives that also has applications in cancer treatment. This compound has shown to be more potent than TOS in inducing apoptosis and ROS generation (Youk et al., 2005). TPGS also has intrinsic P-gp inhibition activity and among all tested PEG chains lengths, the TPGS with a PEG chain of 1000 Da has shown the best efflux pumps inhibition (Collnot et al., 2006). The TPGS mechanism of action on P-gp is through inhibition of P-gp ATPase (Collnot et al., 2007).

Recently, a breakthrough study revealed the anti-tumoral mechanisms of TPGS in breast cancer cells (Neophytou et al., 2014). It was unveiled that TPGS can induce apoptosis by inhibiting AKT phosphorylation, thus resulting in downregulation of Survivin and BcL-2. This downregulation induces the activation of pro-apoptotic caspases (caspases -3 and -7) and cell death mediated by caspase-independent mechanisms was also observed. G1/S cell cycle arrest was observed and linked to Survivin downregulation.

The TPGS anti-tumoral activity, MDR1 inhibiting capacity and its capacity to solubilize poorly-soluble drugs, due to its amphiphilic nature, make it a versatile agent in drug delivery formulations. In fact, in the past decade, TPGS application in nanodelivery systems has grown and it has been widely used in different types of nanovehicles (Zhang et al., 2012). Win *et al*. formulated paclitaxel-loaded PLGA nanoparticles emulsified with TPGS (Win and Feng, 2006). In this study the TPGS emulsified nanoparticles showed a greater anticancer activity compared to poly(vinyl alcohol) (PVA) emulsified or non-emulsified nanoparticles. TPGS coated nanoparticles have also increased cellular uptake compared to non-coated particles (Kulkarni and Feng, 2013). TPGS-PLA nanoparticles, where TPGS is chemically linked to PLA, have further revealed an increased cancer cellular uptake, compared to the TPGS and PVA coated PLGA nanoparticles (Zhang and Feng, 2006a). Shieh and co-workers prepared TPGS coated nanoparticles that were capable of increasing DOX cytotoxicity in DOX resistant cancer cells (Shieh et al., 2011).

The TPGS intrinsic advantages and the superior effects of the nanoformulations containing it leave no doubt that its applicability in cancer therapy either as excipient or block for nanodevices assembly is advantageous.

1.3.5.Co-delivery of multiple drugs by nanovehicles

Nanovehicles are capable of encapsulating multidrugs simultaneously. The nanodelivery of multiple biopharmaceuticals can avoid the issues of free multidrug administration, such as unexpected drug interactions, modification in drug pharmacokinetics and cytotoxicity. Through the nanovehicles-mediated co-delivery of multiple drugs that are delivered inside the tumoral cells, the non-specific toxicity and drug interactions in plasma are greatly diminished.

Moreover, it can target simultaneously multiple aberrant pathways, resulting in synergistic drug effects that are more potent, and at the same time resulting in toxicity reduction since lower doses are needed to achieve the same anti-tumoral effect - **Figure 12** (Parhi et al., 2012). Furthermore, the multidrug delivery can contain agents capable of MDR reversal that can target ABC transporters, thus resulting in a decreased drug efflux and thus leading to increased drug accumulation and anticancer activity.

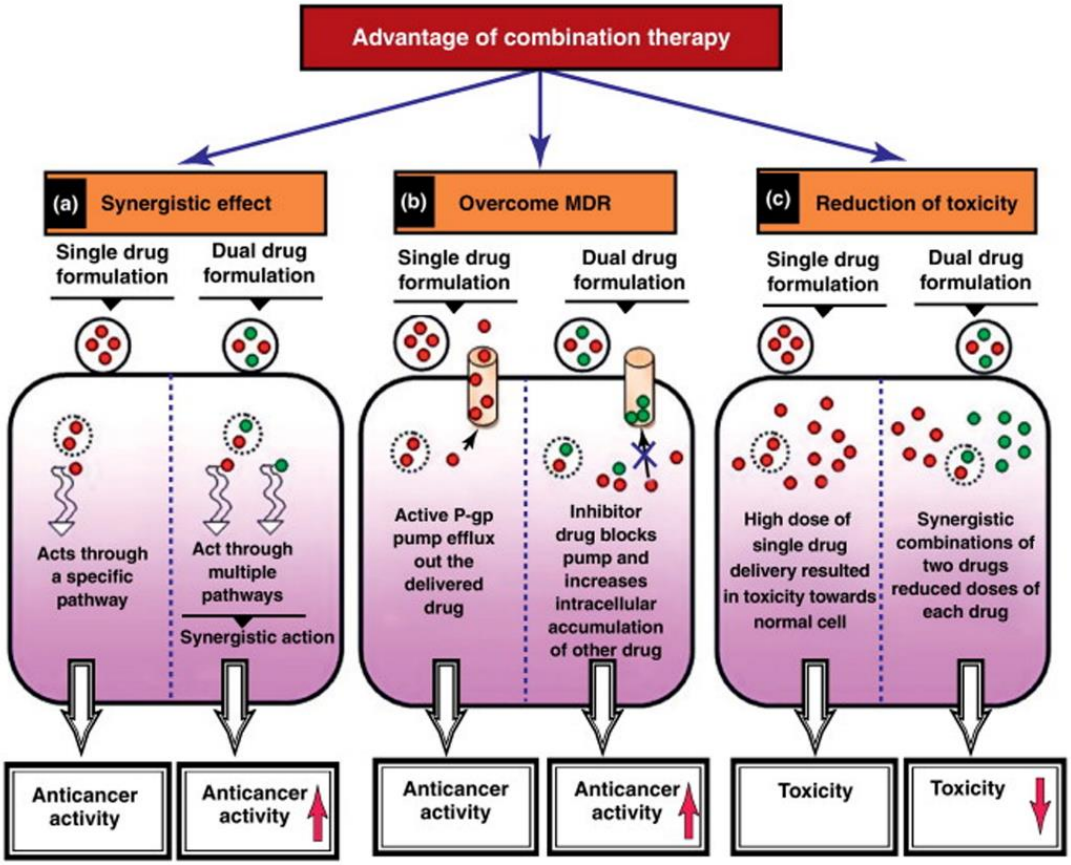

Figure 12 - Advantages of nanoparticle mediated co-delivery in cancer therapy. Co-delivery of multiple pharmaceuticals can result in synergistic effects, thus reducing the amount of drug necessary to attain a therapeutic effect. The reduction of drug dosage can reduce non-specific toxicity. The co-delivery approach might also include agents capable of overcoming multidrug resistance, thus increasing the anticancer activity of the formulation (Adapted from Parhi et al., 2012).

Wang and co-workers formulated micelles that co-encapsulated DOX and Curcumin and this formulation showed superior results compared to those of single drug, both *in vitro* and *in vivo* (Wang et al., 2013). Xiong *et al*. formulated DOX and P-gp siRNA loaded micelles where the P-gp siRNA incorporation increased the anti-tumoral activity of the DOX formulations (Xiong and Lavasanifar, 2011).

Nanodelivery systems to overcome drug-efflux mediated resistance without using siRNA are also under extensive investigation. In this approach, the co-delivery of pharmaceuticals with

Cyclosporin A or TPGS (all having MDR-1 inhibitory activity) have shown promising results. Soma and co-workers formulated nanoparticles encapsulating both DOX and Cyclosporin A, and the addition of the P-gp inhibitor increased the nanoformulation toxicity in drug resistant cancer cells (Soma et al., 2000). Tan *et al.*, formulated TPGS-PLA nanoparticles for co-encapsulation of Docetaxel and Tamoxifen (Tan et al., 2014). The co-delivery of those drugs in the nanoformulation decreased the antagonistic effect observed when they were administered as free drugs. Zhu and co-workers formulated porous PLGA nanoparticles, co-encapsulating Docetaxel and TPGS (Zhu et al., 2014). The inclusion of TPGS in the nanoformulation resulted in an increased anticancer activity both *in vitro* and *in vivo*, increased *in vitro* cell toxicity in cancer cells overexpressing P-gp and decreased P-gp mediated efflux.

Nanocarrier mediated co-delivery of multiple drugs by nanovehicles is an exciting field with promising possibilities. The advantageous of such treatment modality that consists in delivering multiple drugs or to deliver them with agents capable of inhibiting drug efflux was emphasized by these previous studies. However, the drug efflux agents used in the nanovehicles are often limited to the inhibition of one type of drug efflux transporter (commonly P-gp) and nanoformulations with agents capable of inhibiting a broad type of drug efflux pumps should be explored given their advantages in cancer therapy (Marques et al., 2014b). In this context, the co-delivery of multipharmaceuticals such as Crizotinib, Palbociclib and Sildenafil by TPGS-PLA micelles looks a promising strategy for lung cancer therapy. In this thesis, a nanoformulation with bioactive chemotherapeutic drugs such Crizotinib and Palbociclib, and two agents capable of inhibiting a broad type of drug efflux pumps, TPGS and Sildenafil, was produced and its therapeutic efficacy evaluated for lung cancer therapy.

Aims

The global objective of this thesis was to develop a micellar nanovehicle capable of co-deliver chemotherapeutic drugs that target cancer hallmarks and agents capable of reversing cancer multidrug resistance, for lung cancer therapy. The specific aims of this thesis include:

- Synthesis and characterization of TPGS-PLA amphiphilic diblock copolymer;
- Physicochemical characterization of TPGS-PLA micelles;
- Optimization and evaluation of the multidrug loading in the micellar carriers and investigation of its release profile;
- Investigation of micelles internalization by lung cancer cells;
- Study of the cytotoxic effect of the different free drug combinations and determination of the nature of its combinatorial effect;
- Evaluation of the cytotoxic activity of the different micellar formulations.

Chapter 2

Materials and Methods

2. Materials and Methods

2.1. Materials

Human fetal lung fibroblast cell line (MRC-5; ATCC® CCL-171™) and non-small human lung adenocarcinoma epithelial cell line (A549; ATCC® CCL-185™) were obtained from ATCC (Middlesex, UK). Fetal bovine serum (FBS) was acquired from Biochrom AG (Berlin, Germany). Cell imaging plates were acquired from Ibidi GmbH (Munich, Germany). Cell culture T-flasks were purchased from Orange Scientific (Braine-l'Alleud, Belgium). L-Lactide (L-LA) monomer and Triethylamine (TEA) were acquired from Tokyo Chemical Industry (Tokyo, Japan). 3-(4,5-dimethylthiazol-2-yl)-5-(3-carboxymethoxyphenyl)-2-(4-sulfophenyl)-2H-tetrazolium (MTS) and phenazine methosulfate (PMS) were obtained from Promega (Madison, WI, USA). Hoechst 33342® and CellLight 2.0® BacMam-GFP were provided by Invitrogen (Carlsbad, CA, USA). $Sn(Oct)_2$ was purchased from Cymit Química (Barcelona, Spain). Dulbecco's Modified Eagle Medium: Nutrient Mixture F-12 (DMEM-F12), Eagle's Minimum Essential Medium Eagle (EMEM), Minimum Essential Medium Non-essential Amino Acid Solution, Pyrene, Resazurin, Rhodamine B isothiocianate (RITC), TPGS and trypsin were purchased from Sigma–Aldrich (Sintra, Portugal). Palbociclib isethionate (PD 0332991) was purchased from Tocris Bioscience (Ellisville, MO, USA). Crizotinib and Sildenafil citrate were a kind gift from Pfizer Inc. Acetone, Dichloromethane (DCM), Methanol (MetOH) and Toluene were purchased from VWR International (Carnaxide, Portugal). All the glassware was borosilicate 3.3 supplied by Labox.

2.2. Methods

2.2.1. Synthesis of TPGS-PLA copolymer

The TPGS-PLA copolymer was synthesized by ROP of LA monomer with TPGS as initiator and $Sn(Oct)_2$ as catalyst, according to previous described methods with slight modifications (Ha et al., 2010; Zhang and Feng, 2006b; Zhao and Feng, 2014).

Initially, a weight ratio of 2:1 of L-LA and TPGS were added to a round bottom flask. The reaction system was then purged with N_2 and sealed. Toluene and $Sn(Oct)_2$ 0.5% were added and the reaction was left to react at 120 ºC for 4 h.

After the reaction time, the solvent was evaporated (Rotavap® R-215, Büchi, Switzerland). The resulting product was recovered by precipitation in MetOH followed by dialysis in acetone and mili-Q water (double deionized and filtered water) during 5 days. Finally, the product was freeze dried (ScanvacCoolSafeTM, ScanLaf A/S, Denmark) and a white powder was obtained.

2.2.2. Nuclear magnetic resonance

The TPGS-PLA block copolymer was characterized through ^{1}H Nuclear Magnetic Resonance (NMR). Prior to spectra acquisition, the polymer samples were dissolved in Deuterated Chloroform ($CDCl_3$) containing tetramethylsilane (TMS) and transferred into 5 mm NMR glass tubes. NMR data was acquired in a Brüker Advance III 400 MHz spectrometer (Brüker Scientific Inc, USA) at a constant temperature of 298 K using a 1D pulse program (zg, Brüker Scientific Inc). The data was recorded with a spectral width of 8 ppm. Data processing was performed in the TOPSPIN 3.1 software (Brüker Scientific Inc).

Peak assignment was performed according to previous reports available in the literature (Yu et al., 2013; Zhang and Feng, 2006b). The number average molecular weight (Mn) of diblock copolymer PLA chain and TPGS-PLA were determined by using the NMR characteristic peaks of TPGS (δ=3.6 ppm; $P_{3.6}$) and PLA (δ=5.2 ppm; $P_{5.2}$) according the following equations (Zhang and Feng, 2006a):

$$M_{n\ PLA} = \frac{4 \times 23 \times 72 \times P_{5.2}}{P_{3.6}} \quad (1)$$

$$M_{n\ TPGS\text{-}PLA} = M_{n\ PLA} + M_{n\ TPGS} \quad (2)$$

The degree of polymerization (DP) was calculated as the follows:

$$DP_{PLA} = \frac{Mn\ PLA}{Mw\ LA} \quad (3)$$

2.2.3. Fourier transform infrared spectroscopy

Fourier transform infrared spectroscopy (FTIR) was performed to confirm the TPGS-PLA block copolymer polymerization. For each sample 256 scans were acquired in a Nicolet iS10 spectrometer (Thermo Scientific Inc., USA). The data was recorded with a spectral width ranging from 4000 cm^{-1} to 600 cm^{-1}, at a resolution of 4 cm^{-1}. OMNIC Spectra software (Thermo Scientific) was used for data analysis.

2.2.4. X-ray powder diffraction

The synthetized TPGS-PLA copolymer was also characterized by X-ray Powder Diffraction (XRD). Prior to acquisition all samples were mounted in silica supports by using a double sided adhesive tape. Samples were acquired in a Rigaku Geigger Flex D-max III/c diffractometer (Rigaku Americas Corporations, USA)equipped with a copper ray tube operated at voltage of 30 kV and a current 20 mA. The data was acquired between 5 and 90°, with a scan step of 1°/min.

2.2.5. Determination of critical micellar concentration

CMC was determined by using Pyrene as a model fluorescent probe (Marques et al., 2014b). Pyrene is a hydrophobic probe that tends to move to micelles core during the micelization process, resulting in an increase in the intensity ratio of $I_{\lambda ex=335}/I_{\lambda ex=333}$ (Owen et al., 2012).

For CMC determination, different TPGS-PLA copolymer solutions with concentrations ranging from 0.001 to 2000 µg/mL were prepared by serial dilutions. Then pyrene was added to the previous solutions. The mixture was subjected to ultrasonication (Branson 5510E-DTH, 135 W, 42 KHz). Finally, the pyrene fluorescence peak ratio was monitored on a Spectramax Gemini XS spectrofluorometer (Molecular Devices LLC, USA) (λ_{ex}= 333 nm and λ_{ex}= 335 nm; λ_{em}= 390 nm).

2.2.6. Formulation of TPGS-PLA micelles

Different TPGS-PLA micelle formulations were prepared by the solvent displacement method (Marques et al., 2014b). To prepare TPGS-PLA micelles without any encapsulated drugs (blank TPGS-PLA micelles), TPGS-PLA diblock copolymer was dissolved in a DCM/MetOH (1:1 v/v) solution. Thereafter, the solvent was evaporated (Rotavap® R-215, Büchi, Switzerland) and the remaining film was hydrated, sonicated, centrifuged and freeze-dried.

To prepare the drug loaded micelles, the process was the same as described above but with the addition of the respective drugs prior to solvent evaporation. For preparation of Crizotinib, Palbociclib and Sildenafil loaded TPGS-PLA micelles (CPS-M), 30 µg of each drug/mg of polymer were added to the dissolved TPGS-PLA copolymer in DCM/MetOH (1:1 v/v). Thereafter, the solvent was evaporated (Rotavap® R-215, Büchi, Switzerland) and the remaining film was hydrated, sonicated, centrifuged. Prior to addition into the polymer-drug mixture, Sildenafil citrate was vortexed in the presence of TEA to form Sildenafil base. To prepare Crizotinib (C-M) or Crizotinib and Palbociclib (CP-M) loaded micelles, the process was the same as described above, but only with the addition of Crizotinib or Crizotinib and Palbociclib respectively.

2.2.7. Characterization of TPGS-PLA size and zeta potential

The TPGS-PLA micelles size distribution and the zeta potential were characterized by dynamic light scattering (DLS) in a Zetasizer Nano ZS instrument (Malvern Instruments, Worcestershire, UK) equipped with a He-Ne 633 nm laser, at a detection angle of 173°. Prior to the analysis the micelles were resuspended in mili-Q water and sonicated. The samples were analyzed using a disposable folded capillary cell, at 25 °C.

Micelles size was determined by Stokes-Einstein equation:

$$D_H = \frac{K_B T}{3 \pi \eta D_T} \quad (4)$$

where D_H is Hydrodynamic Diameter, K_B is Boltzmann's constant, T is Thermodynamic temperature, η is Dynamic viscosity, D_T is Translational diffusion coefficient.

Micelles zeta potential was determined using the Smoluchowski model (*f*(Ka)=1.5):

$$\zeta = \frac{U_E 3\eta}{2\,\varepsilon\, f(ka)} \quad (5)$$

where ζ is Zeta potential, U_E is Electrophoretic mobility, ε is Dielectric constant, f(Ka) is Henry's equation.

2.2.8. Characterization of TPGS-PLA micelles morphology

Micelles morphology was evaluated by Scanning Electron Microscopy (SEM). For SEM analysis the micelle samples were hydrated, dispersed in a cover glass and left to dry overnight. Prior to acquisition, samples were mounted on aluminum stubs and sputter coated with gold with an Emitech K550 sputter coater (Emitech Ltd, UK). Micelles samples were then analyzed on a Hitachi S-2700 and S-3400N (Tokyo, Japan) electron microscope by using an accelerating voltage of 20 kV and different magnifications.

2.2.9. Drug encapsulation efficiency

The drug loading content was determined by ultra performance liquid chromatography (UPLC, Agilent 1200). For these assays an Agilent ZORBAX Eclipse C18 Rapid Resolution column (Agilent Technologies, CA, USA) was used. The encapsulation efficiency (EE) and the drug loading content (DL) were calculated by the following equations:

$$\text{EE (\%)} = \frac{\text{Weight of a single drug in micelles}}{\text{Weight of the single drug fed initially}} \times 100 \quad (6)$$

$$\text{DL (\%)} = \frac{\text{Total drug weight in micelles}}{\text{Weight of micelles}} \times 100 \quad (7)$$

For the simultaneous quantification of all drugs (Crizotinib, Palbociclib and Sildenafil) a mobile phase comprised by Acetonitrile/Na_2HPO_4 (0.015 M, pH 7.4) with 0.01 % (v/v) TEA (28:72) was used. Sample analysis was performed at 24 °C, at constant flow rate of 1 mL/min in 40 min chromatographic runs. Crizotinib, Palbociclib and Sildenafil were detected at 265, 220, and 230 nm, respectively. Protriptyline (294 nm) was used as internal standard for the drug encapsulation efficiency determination, in both water and MetOH.

2.2.10. Drug release profile

Cumulative drug release from TPGS-PLA micellar carriers was evaluated by dispersing CPS-M in release medium (phosphate buffer saline (PBS) solution 0.1 M at pH 7.4) and placed in a shaking water bath at 37 °C. At given intervals the samples were collected, centrifuged and the supernatant analyzed by the above described UPLC method. Meloxican (362 nm) was used as internal standard for UPLC drug release quantification in PBS.

2.2.11. Cell culture maintenance

Cells were cultured in 75 cm^2 T-flasks, at 37 °C and with a humidified atmosphere containing 5 % CO_2. A549 cells were maintained in Hams-F12 medium supplemented with 10 % FBS and 1% streptomycin and gentamycin. MRC-5 lung fibroblast cells were cultured in EMEM medium supplemented with 10 % FBS, 1 % non-essential amino acids and 1% streptomycin and gentamycin. Whenever confluence was achieved, cells were harvested by using 0.18% trypsin. The culture medium was changed every 2 days before all experiments.

2.2.12. Characterization of the cytotoxicity of blank micelles

Micelles biocompatibility was evaluated by the Resazurin assay (Marques et al., 2014a). Resazurin (blue compound) is a non-fluorescent molecule that is reduced by viable cells to resorufin (pink), a fluorescent substrate that can be quantified using the excitation/emission wavelength of 560/590 nm (Sittampalam et al., 2013). The resazurin reduction is mostly due to activity of mitochondrial enzymes such as flavin mononucleotide dehydrogenase, flavin adenine dinucleotide dehydrogenase and nicotinamide adenine dehydrogenase (Czekanska, 2011). This method is non-toxic, highly sensitive and does not require the use of electron acceptors (Sittampalam et al., 2013). In brief, A549 or MRC-5 cells were seeded at a density of 10 x 10^3 cells/well in 96-well plates. After 24 h, the medium was removed and cells were incubated with medium containing blank micelles at different concentrations ranging between 50 and 1000 µg/mL, for 24 and 48 h. Finally, the culture medium was replaced with medium containing 10 % (v/v) Resazurin for 4 h, at 37 °C and 5 % CO_2, in the dark. Resorufin fluorescence was quantified in a plate reader spectrofluorometer (Spectramax Gemini XS, Molecular Devices LLC, USA) at an excitation/emission wavelength of 560/590 nm, respectively. Non-incubated cells were used as negative controls (K-) and ethanol treated cells as positive controls (K+).

2.2.13. *In vitro* cellular uptake of micelles

In vitro micelle cellular uptake was characterized by confocal laser scanning microscopy (CLSM). Prior to analysis, the different micellar formulations loaded with RITC (model hydrophobic fluorescent probe) were prepared by using the previous described solvent evaporation/film hydration method. Cell labeling was performed as previous reported by Costa and co-workers (Costa et al., 2013). Briefly, A549 cells were seeded in a 6 well culture plate and after 24 h they were transfected with the Backman Cell Light 2.0®Actin-GFP probe. Cells were then harvested and seeded in µ-Slide 8 well Ibidi imaging at a density of 20 x 10^3 cells/well. In the following day the cells were incubated with micelles for 4 h, fixed in 4 % paraformaldehyde (15 min, room temperature (RT)) and washed with 1 % PBS. Then, the cells nucleus were labeled with Hoechst 33342® (2 µM, 10 min, RT) and cells were extensively rinsed with PBS. Imaging experiments were performed in a Zeiss LSM 710 confocal microscope (Carl Zeiss SMT Inc., USA) equipped with a Plan Apochromat 63x/1.4 Oil Differential Interference Contrast (DIC) objective. During image acquisition consecutive z-stacks in the cell volume were

acquired. 3D reconstruction of the multiple z-stacks and image analysis were then performed in Zeiss Zen 2010 software.

2.2.14. IC50 determination and evaluation of the synergistic effect of the drugs

To determine the cytotoxicity of Crizotinib, Palbociclib and Sildenafil, A549 cells were seeded in 96-well plates at a density of 8 x 10^3 cells/well. After 24 h the cells were incubated with medium containing different concentrations of Crizotinib, Palbociclib or Sildenafil for 48 h. Cell viability was then measured through the previous described Resazurin assay.

The IC50 determination for dual drug (Crizotinib/Palbociclib) and triple drug combinations (Crizotinib/Palbociclib/Sildenafil) were addressed by MTS assay (Gaspar et al., 2013). MTS is used in combination with an intermediate electron acceptor (PMS), and the latter is reduced in viable cells cytoplasm (Sittampalam et al., 2013). Then the electron acceptor can reduce MTS (yellow dye) to a soluble formazan salt (brown dye), in cell culture medium. Briefly, A549 cells were seeded at a density of 8 x 10^3 cells/well in 96-well plates. 24 h later, the medium was exchanged and the cells incubated with different drug concentrations for 48 h. Subsequently, culture medium was exchanged and a mixture of MTS/PMS was incubated in each well for 4 h, at 37 °C, with 5 % CO_2 atmosphere in the dark. Absorbance measurements were performed in a microplate reader (Anthos 2020, Biochrom, UK) at 492 nm.

In all assays, positive control cells were incubated with absolute ethanol prior to Resazurin or MTS/PMS incubation. Untreated cells were used as negative controls.

To assess if the different drug combinations tested had a synergistic, additive or antagonistic effect, the Combination Index (CI) was calculated according to the Chou-Talalay method (Li et al., 2014). CI values of CI<0.8, 0.8<CI<1.2 and CI>1.2 were considered synergistic, additive and antagonistic effects, respectively. The CI value for the dual and triple drug combinations were calculated according to equations (8) and (9), respectively.

$$\text{CI (dual drug combination)} = \frac{\text{IC50 (Crizotinib+Palbociclib)}}{\text{IC50(Palbociclib)}} \quad (8)$$

$$\text{CI (triple drug combination)} = \frac{\text{IC50 (Crizotinib+Palbociclib+Sildenafil)}}{\text{IC50(Crizotinib+Palbociclib)}} \quad (9)$$

2.2.15. *In vitro* cytotoxicity effect of the loaded micelles

The anti-proliferative effect of all the micellar formulations (C-M, CP-M and CPS-M) was evaluated by the MTS assay (Gaspar et al., 2013). In brief, A549 cells were seeded in 96-well plates at a density of 8 x 10^3 cells/well. After 24 h, cells were incubated with micellar formulations at different concentrations for 48 h. The anti-proliferative effect was then

evaluated by using the MTS assays as above described. Non-incubated cells were used as negative controls (K-) and ethanol treated cells as positive controls (K+).

2.2.16. Statistical analysis

One-way analysis of variance (ANOVA) with the Student–Newman–Keuls test was used to compare the variance between different test groups. A value of $p < 0.05$ was considered statistically significant. Data analysis was performed in GraphPad Prism v.5.0 software (Trial version, GraphPadSoftware, CA, USA).

Chapter 3
Results and Discussion

3. Results and Discussion

3.1. Synthesis of TPGS-PLA diblock copolymer

Amphiphilic block copolymers are highly valuable to formulate drug delivery systems since under specific conditions, they can self-assemble into polymeric micelles. Polymeric micelles have high loading capacity and suitable characteristics for taking advantage of the EPR effect. Moreover, TPGS-PLA micelles are a promising drug delivery system for cancer therapy since they may benefit from TPGS intrinsic characteristics such as anti-tumoral activity, P-gp inhibition and cell cycle arresting capacity (Collnot et al., 2007; Neophytou et al., 2014; Youk et al., 2005).

TPGS-PLA diblock copolymer was synthetized by ROP using $Sn(Oct)_2$ as a catalyst and TPGS hydroxyl terminus (OH-) as initiator. In a typical synthesis procedure, TPGS and L-LA are added to a reaction flask. Then the system is purged with N_2 and dry toluene is added. The N_2 provides an inert atmosphere for the ROP reaction to proceed, since the presence of water and air influence the living character of the polymer. In fact, water presence in both the solvent and in the atmosphere leads to hydrolysis of the LA and PLA chain, thus affecting the PLA polymerization (Auras et al., 2011). Afterwards, the catalyst is added and the reaction takes place at 120 ºC for 4 h. $Sn(Oct)_2$ was chosen as the catalyst since is FDA approved, is soluble in most solvents and allows the production of polymers with high molecular weight (Dechy-Cabaret et al., 2004). The reaction temperature in TPGS-PLA synthesis was kept at 120 ºC, instead of the generally reported 145 ºC, to avoid possible inter and intra-molecular transesterifcation reactions that can increase the polymer polydispersity (PDI) (Albertsson and Varma, 2003).

The TPGS-PLA copolymer was then purified by precipitation and dialysis. First the product was precipitated in MetOH. PLA is insoluble in methanol causing the precipitation of TPGS-PLA diblock copolymer. Moreover, unreacted L-LA monomers and unreacted TPGS are soluble in MetOH and thus are not recovered since they do not precipitate (Ha et al., 2010). Afterwards, the recovered precipitate was still dialyzed to remove traces of other contaminants ($Sn(Oct)_2$ and residues of unreacted LA monomer), further improving the purity of TPGS-PLA diblock copolymer. Finally the recovered dialysis product was freeze dried, yielding the purified TPGS-PLA diblock copolymer that was used from here onwards.

3.2. NMR analysis of TPGS-PLA diblock copolymer

To investigate the successful polymerization of TPGS-PLA and to address the effectiveness of the purification steps, the synthetized product was characterized by NMR analysis. Moreover, the degree of polymerization and the Mn of PLA chain can also be calculated using proton NMR data.

The ^{1}H NMR spectra of TPGS and L-LA are shown in **Figure 13**. As can be seen, the L-LA spectra is characterized by two strong peaks, corresponding to methyne (-CH; δ=5.0 ppm) and methyl ($-CH_3$; δ=1.67 ppm) protons (**Figure 13**; capital letters) (Zhang and Feng, 2006b). In the TPGS spectra a strong peak is present (δ=3.6) corresponding to methylene ($-CH_2$) protons of PEG (**Figure 13**; capital letters). Several other peaks belonging to Vitamin E moieties were assigned in TPGS spectra (**Figure 13**; lowercase a-f) (Yu et al., 2013; Zhang and Feng, 2006b). Looking to TPGS-PLA spectra, both peaks of L-LA and TPGS are present, thus indicating a successful polymerization (**Figure 14**). To further confirm the successful TPGS-PLA polymerization, peak assignment was performed according to literature reports (Yu et al., 2013; Zhang and Feng, 2006b). The δ=5.2 ppm and δ=1.69 ppm signals were assigned to PLA methyne (-CH) and methyl ($-CH_3$) protons (**Figure 14**; capital A and C) (Yu et al., 2013). The δ=3.6 ppm peak was assigned to the methylene groups of PEG ($-CH_2$) (**Figure 14**; capital B) (Yu et al., 2013). Moreover, in TPGS-PLA spectra, smaller peaks were present and those were assigned to vitamin E moieties (**Figure 14**; lowercase a-f) (Yu et al., 2013). The $CDCl_3$ peak is also present in every spectra (δ=7.3 ppm).

The PLA chain length in TPGS-PLA was determined according to a previously established method in the literature (Zhang and Feng, 2006a). The Mn of PLA in the synthetized product was calculated by integrating the TPGS (δ=3.6 ppm) and PLA (δ=5.2 ppm) peak areas according to equation 1. The **Table 3** summarizes the data of TPGS-PLA diblock copolymer characterization.

Table 3 - Degree of Polymerization of PLA, Mn of PLA and Mn of TPGS-PLA diblock copolymer (n=5).

	DP	**Mn PLA**	**Mn TPGS-PLA**
TPGS-PLA	79.3	5710 ± 29.62 Da	7252 ± 29.62 Da

The ^{1}H NMR data confirms the successful polymerization of PLA. Moreover, no additional peaks to those assigned were identified thus indicating a good purity of the synthetized TPGS-PLA diblock copolymer.

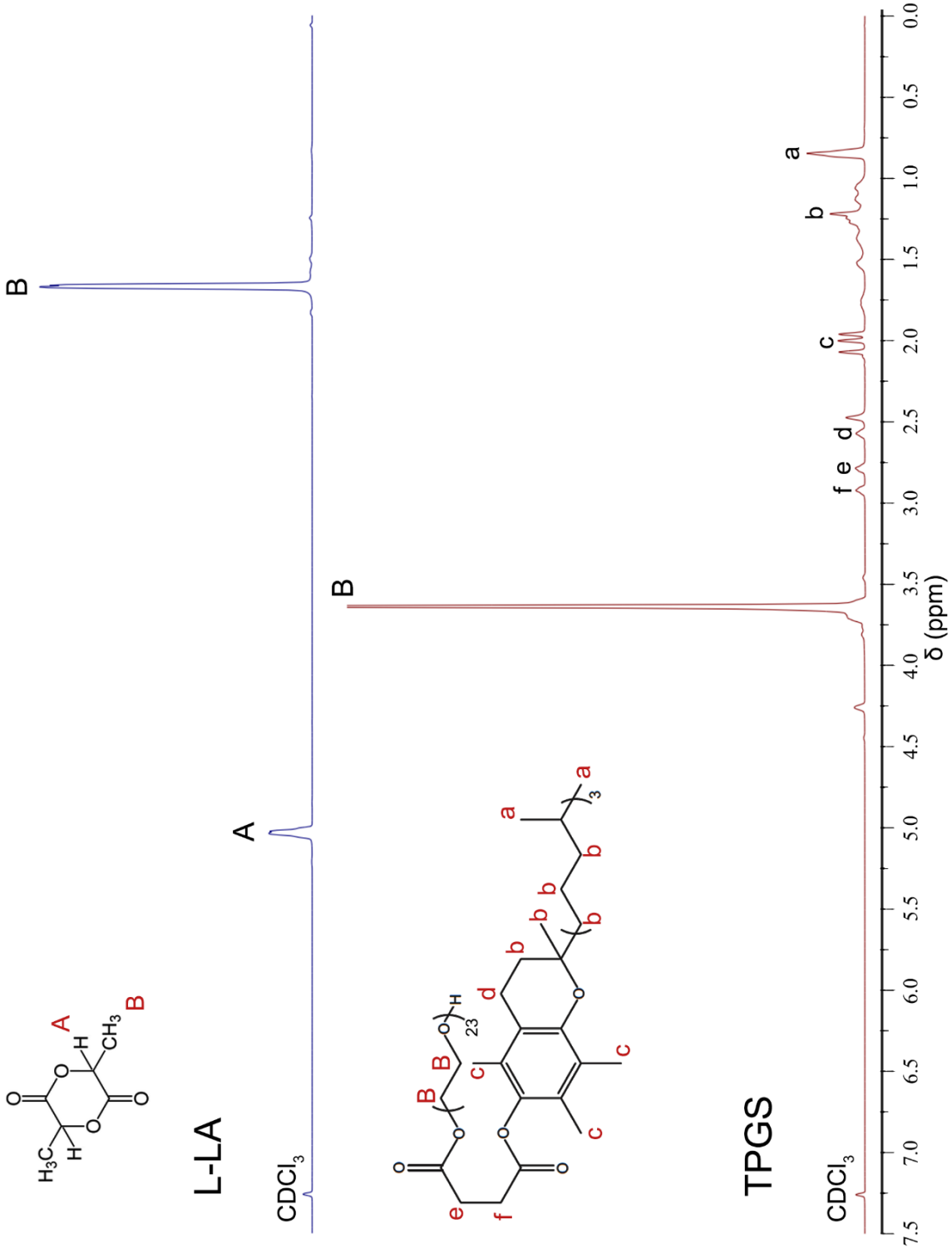

Figure 13 - ^{1}H NMR of L-LA and TPGS raw materials in $CDCl_3$.

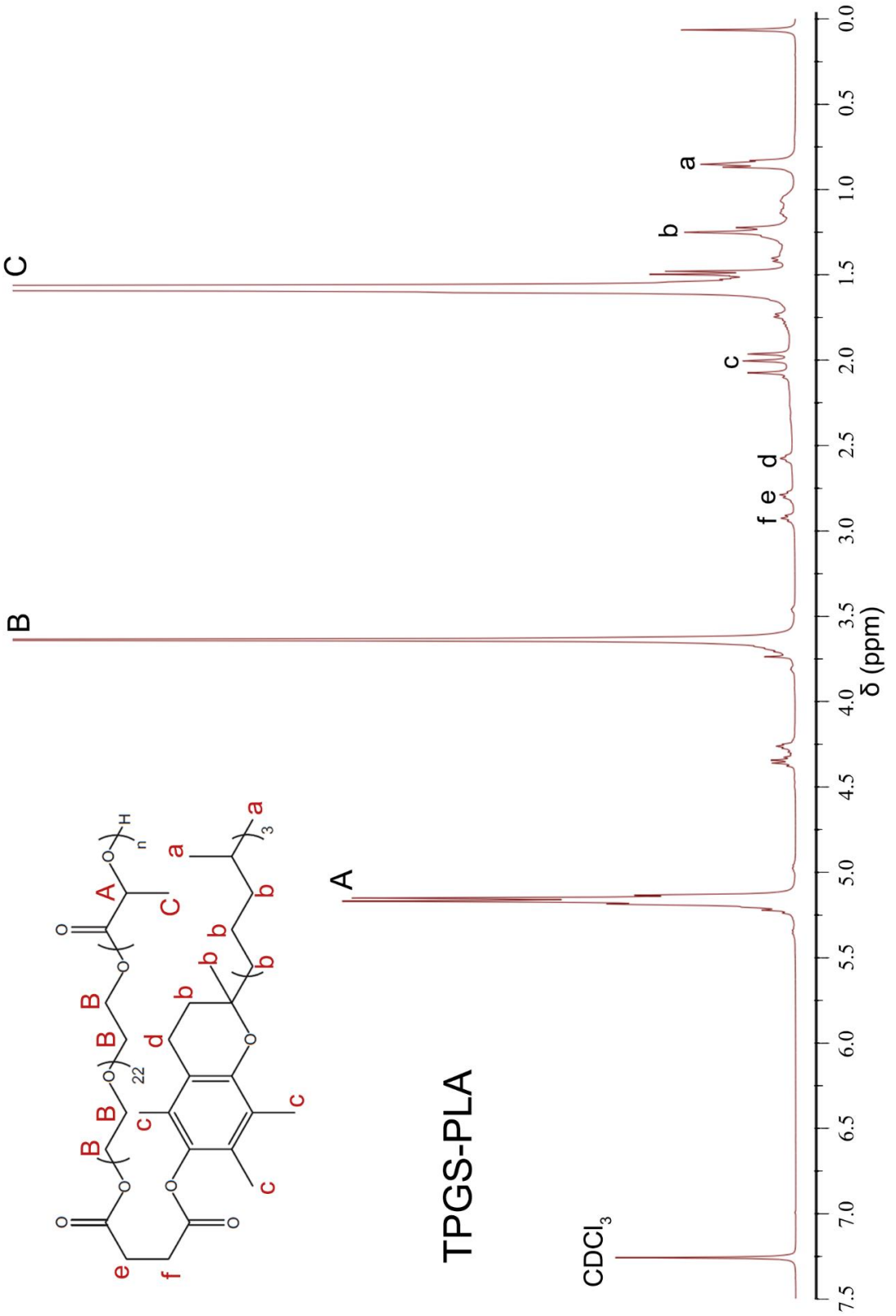

Figure 14 - ^{1}H NMR of the synthetized TPGS-PLA diblock copolymer in $CDCl_3$.

3.3. FTIR analysis of TPGS-PLA diblock copolymer

TPGS-PLA diblock copolymer was also characterized by FTIR. FTIR characterization demonstrates the successful polymerization of TPGS-PLA and is also in accordance to the previous available literature reports (**Figure 15**) (Ha et al., 2010; Zhang and Feng, 2006a). In both spectra C-H stretch band is present, corresponding to methyl group vibrations from L-LA (2932 cm^{-1}), TPGS (2885 cm^{-1}) and TPGS-PLA (2946 cm^{-1}). Carbonyl vibration peak is also present in all spectra. The carbonyl band shift from TPGS to the synthesized diblock copolymer is also visible (TPGS: 1736 cm^{-1}; TPGS-PLA: 1755 cm^{-1}; L-LA: 1753 cm^{-1}). In TPGS and TPGS-PLA the C-O stretch band is also present (1050-1250 cm-1). Finally the 3400-3600 cm-1 band is assigned to the terminal hydroxyl group of the PLA chain.

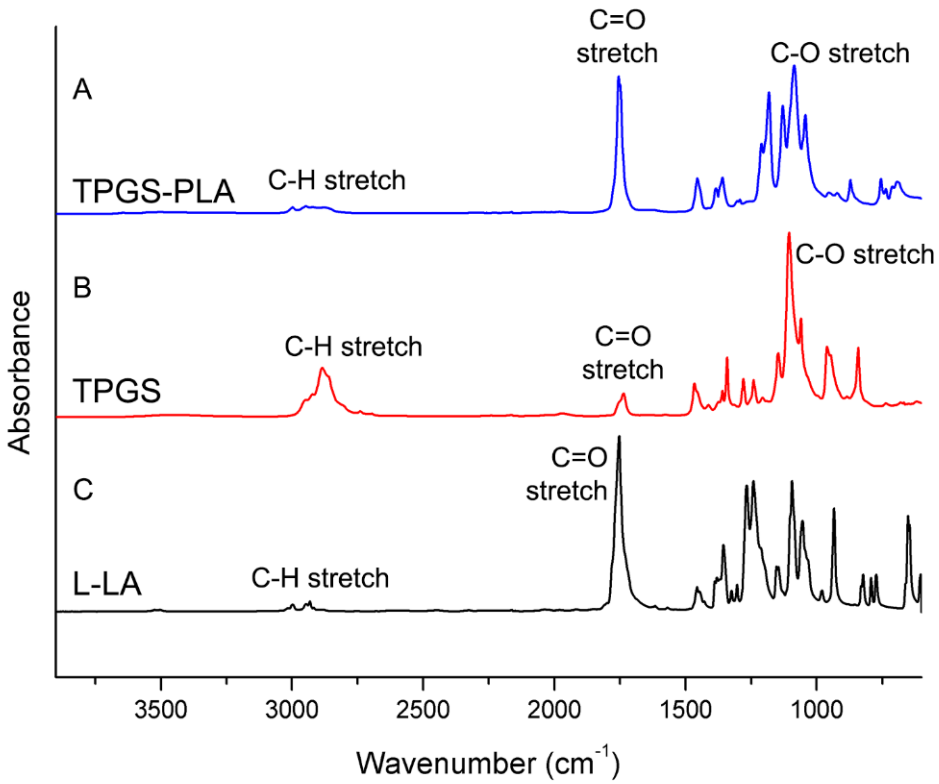

Figure 15 - FTIR spectra of A) TPGS-PLA, B) TPGS and C) L-LA.

3.4. XRD analysis of TPGS-PLA diblock copolymer

The TPGS-PLA diblock copolymer was also characterized by XRD analysis and the results corroborate its successful synthesis (**Figure 16**). The diffraction peaks at 2Θ=18.9° and 23.1° in TPGS spectra and 2Θ=19.1° and 22.45° in TPGS-PLA are PEG characteristic diffraction peaks (Goddeeris et al., 2008; Li, 2003). In TPGS-PLA spectra the L-LA monomer diffraction peak at 2Θ=12.8° is not present, thus indicating a good removal of L-LA traces from the recovered copolymer. The diffraction peak at 2Θ=16.7° is attributed to PLA hydrophobic segment in the TPGS-PLA copolymer (Chen et al., 2007).

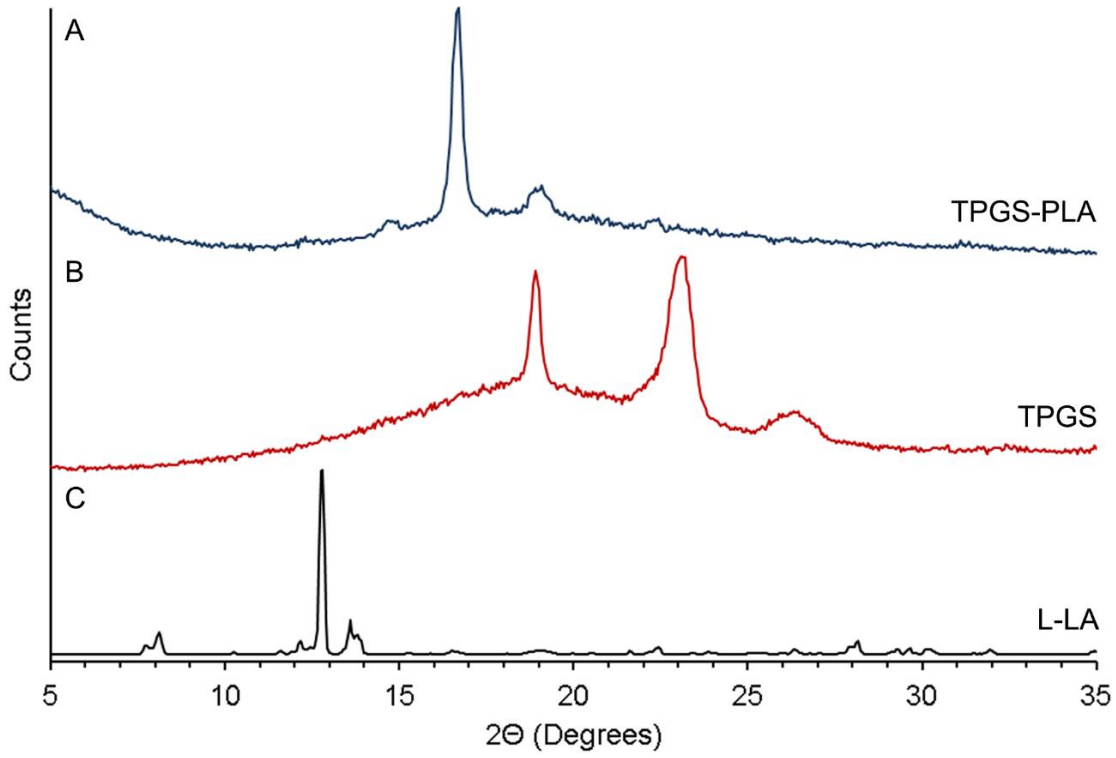

Figure 16 - XRD spectra of A) TPGS-PLA, B) TPGS and C) L-LA.

3.5. TPGS-PLA diblock copolymer CMC determination

Amphiphilic polymers self-assemble into micellar vehicles under specific conditions in aqueous environments. At concentrations above CMC, the amphiphilic polymer chains assemble into micelles, thus reducing the interfacial free energy of the water-polymer system (Owen et al., 2012). However, whenever this concentration is not achieved, the polymer chains are spread in the solution and may act as a surfactant (Owen et al., 2012). Thereby, micelles CMC value greatly affects its stability, since upon dilution the concentration can decrease bellow CMC and micelles can prematurely disassemble and release their cargo without a controlled release profile (Owen et al., 2012).

To investigate if the TPGS-PLA copolymer could self-assemble into micellar carriers its CMC was determined by the pyrene method (Marques et al., 2014b). As can be observed in **Figure 17**, upon reaching a determined polymer concentration, a change in the I_{335}/I_{333} pyrene fluorescence ratio was observed. This change in the intensity ratio is correlated with pyrene entrapment in a hydrophobic core, thus indicating that upon reaching this concentration, the amphiphilic polymers self-assemble into micelles. The determined CMC for the TPGS-PLA micelles was found to be 1.16×10^{-2} mg/ mL and it is lower than that reported by Li and co-workers (2.06×10^{-2} to 7.29×10^{-2} mg/mL), thus indicating that the PLA Mn of the herein formulated TPGS-PLA diblock copolymer allows the formulation of highly stable micelles (Li et al., 2009).

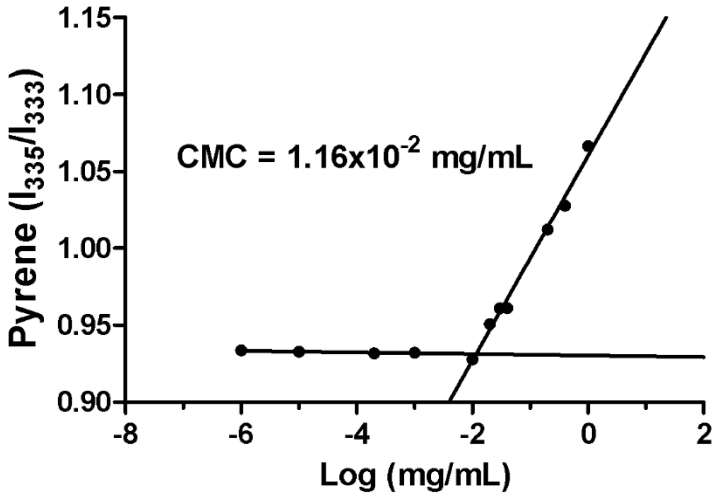

Figure 17 - Determination of TPGS-PLA critical CMC using the pyrene method.

3.6. UPLC method to determine the TPGS-PLA micelles drug loading and release profile

Before optimizing the co-encapsulation of Crizotinib, Palbociclib and Sildenafil in TPGS-PLA micelles for co-delivery purposes, a method for the simultaneous detection of the 3 compounds was initially established by UPLC. Ultraviolet-Visible (UV-VIS) spectroscopy methods are not suitable for the quantification of the 3 drugs, since the spectra of the compounds overlap and no quantification would be possible. Also it is important to emphasize that the common high performance liquid chromatography (HPLC)/UPLC methods employed for the determination of multidrug encapsulation or the drug release from nanosized delivery systems, have a chromatographic run for each analyte, have higher costs and are time consuming (Tan et al., 2014).

To address the ability of TPGS-PLA micelles to simultaneously encapsulate Crizotinib, Palbociclib and Sildenafil a novel UPLC method was established. Our first approach to simultaneously detect the 3 drugs employed a recently published method (Marques et al., 2014b). This UPLC method was optimized for the simultaneously detection of Crizotinib and Sildenafil. During the tests using the previous UPLC method, the 3 drugs and the internal standard (Protriptyline) were detected simultaneously, however, Crizotinib and Palbociclib peaks were not completely resolved. To allow Crizotinib and Palbociclib separation, the run temperature was decreased to 24 ºC and the Acetonitrile/(Na_2HPO_4 + TEA) phase ratio was set to 28:72 (v/v). The temperature was decreased since higher temperatures are usually associated with lower retention of the analytes (McCalley, 2000). Moreover, by reducing the organic solvent in the chromatographic run, the polarity of the mobile phase increases and so the hydrophobic interaction between the analytes and the column are promoted, resulting in longer retention times. These alterations promoted a longer interaction of the analytes with

the chromatographic column, resulting in complete separation of all the analytes peaks (**Figure 18 A**).

The drug loading evaluation process herein employed quantifies both the non-encapsulated drug deposited in the glass apparatus (recovered by methanol wash) and the non-encapsulated drug in the micelles supernatant recovered by centrifugation. Thereby, the UPLC method was optimized to detect the 3 drugs (Crizotinib, Palbociclib and Sildenafil) and the internal standard (Protriptyline) in Methanol and Water - **Figure 18 A**. As seen in the representative chromatogram, Palbociclib was the first compound to elute, followed by Crizotinib and then Protriptyline. Sildenafil was the last peak to elute (**Figure 18 A**).

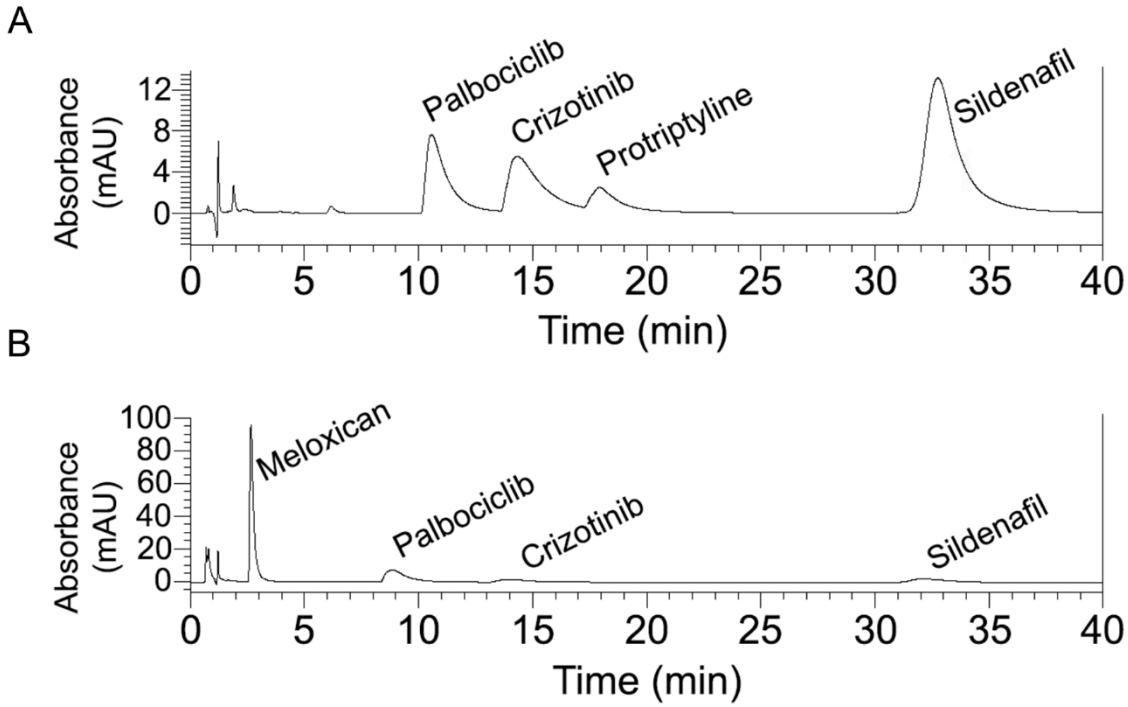

Figure 18 - Representative chromatograms of UPLC separation of Crizotinib, Palbociclib, Sildenafil and the internal standard (Protriptyline (A) and Meloxican (B)) for A) drug loading and B) drug release evaluations.

The established UPLC method was also tested for samples in PBS, so that the release profile of the 3 drugs from TPGS-PLA micelles could be evaluated. However, when performing the calibration curve in PBS medium, Crizotinib and Protriptyline peaks overlapped. So instead of using Protriptyline as internal standard for PBS samples, Meloxican was used and all analytes were therefore eluted with high resolution. In this case Meloxican was the first to elute, followed by the others in the same order as above - **Figure 18 B**.

After all the UPLC optimizations, the UPLC method for the triple drug quantification was comprised by a mobile phase containing Acetonitrile/Na_2HPO_4 (0.015 M, pH 7.4) with 0.01 % (v/v) TEA (28:72) mobile phase. The sample analysis was performed at 24 °C, at constant flow

rate of 1 mL/min in 40 min chromatographic runs. Protriptyline was used as internal standard for water and methanol samples, whereas Meloxican was used for PBS dispersed samples.

3.7. Multiple drug loading in the micellar carriers

To encapsulate the triple drug combination for co-delivery purposes in TPGS-PLA micelles, 3 different methodologies were tested - **Table 4**.

Table 4 - Summary of the triple drug loading optimization parameters.

Methodology	Drug Feed (µg drug/mg polymer)			Sildenafil incubation with TEA
	Crizotinib	Palbociclib	Sildenafil	
Method A	10	10	10	No
Method B	10	10	10	Yes
Method C	30	30	30	Yes

The first approach to simultaneously encapsulate Crizotinib, Palbociclib and Sildenafil used 10 µg of each drug/mg polymer (**Table 4 Method A**). This method resulted in an average encapsulation efficiency of 77% for Crizotinib, 44% for Sildenafil and 63% for Palbociclib (**Figure 19 Method A**). With this methodology Sildenafil citrate was poorly encapsulated and this could have impact on the inhibition effect of efflux transporters. Therefore a different approach was studied (**Table 4 Method B**) based on the formation of the free base of Sildenafil instead of the citrate salt form to favor its encapsulation in the TPGS-PLA micelles hydrophobic core. In this method Sildenafil was mixed with TEA prior to micelle formulation. This strategy proved to be successful, since Sildenafil encapsulation efficiency increased 1.77 fold (**Figure 19 Method B**). Moreover, Palbociclib and Crizotinib encapsulation efficiency was also improved (**Figure 19**). These findings are likely correlated with the establishment of stronger hydrophobic drug-drug and drug-core interactions.

Since the TEA methodology was the one with better encapsulation efficiency, the initial amount of drug inserted in micelles formulation was further increased to 30 µg of each drug/mg polymer (**Table 4 Method C**). Such drug concentration increase did not affect Palbociclib and Sildenafil encapsulation efficiency, while for Crizotinib a slight increase was noticed likely due to stronger hydrophobic interactions (**Figure 19 Method C**). Despite drug encapsulation efficiency of Method B and C being very similar, the Method C has a higher initial drug input and so more drug is encapsulated in TPGS-PLA micelles formulated using this method. Thereby, the micelles formulated with Method C are those with the best anti-tumoral potential. From here on, the

triple drug loaded TPGS micelles formulated with Method C will be referred as CPS-M. CPS-M had a loading capacity of 11.43 ± 1.80% (n=3).

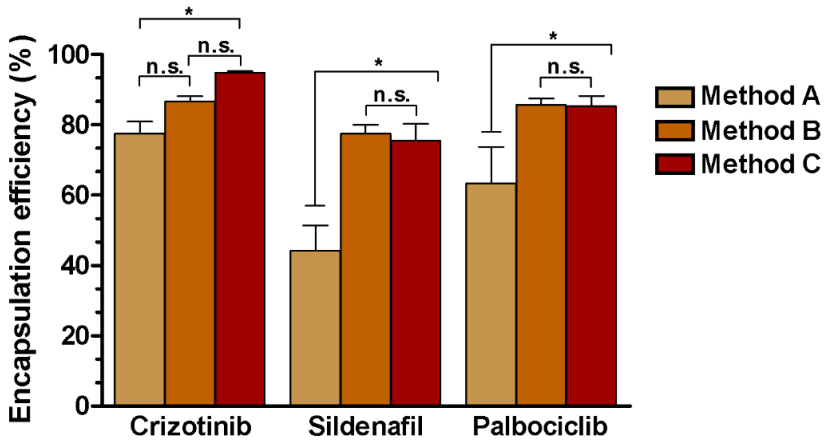

Figure 19 - Optimization of the triple drug loading encapsulation using different methodologies. Data represents mean±SD, n=3, n.s.=non significant, *p<0.05.

3.8. Morphological characterization of TPGS-PLA micelles

The different formulations of TPGS-PLA micelles were characterized by SEM. This analysis is crucial to characterize TPGS-PLA morphology (**Figure 20**). As observed in SEM images the TPGS-PLA blank micelles have spherical morphology (**Figure 20 A**). Moreover, CPS-M morphology is also spherical, suggesting that the drug encapsulation in TPGS-PLA micelles did not affect their morphology **(Figure 20 B).** This spherical morphology is commonly reported in literature for TPGS-PLA nanocarriers (Li et al., 2009; Mi et al., 2013; Yu et al., 2013). Spherical morphology is often related with an increased cellular uptake rate (Florez et al., 2012; Zhang et al., 2008a). Moreover, the spherical morphology has increased *in vivo* tumoral uptake compared to other morphologies (Black et al., 2014).

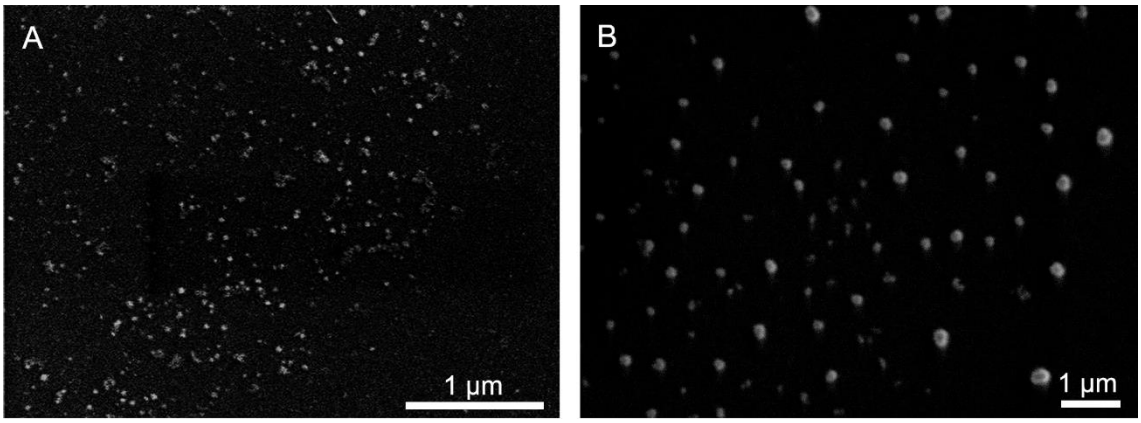

Figure 20 - SEM images of A) blank TPGS-PLA micelles and B) CPS-M.

3.9. TPGS-PLA micelles size and surface charge characterization

TPGS-PLA micelles size, PDI and zeta potential were characterized by DLS. TPGS-PLA blank micelles and CPS-M had an average size of 172.2 and 158.3 nm respectively, thus suggesting that drug loading decreased micelles mean size, most probably due to stronger hydrophobic interactions in the micelles core (**Figure 21**). Regarding the zeta potential analysis, both formulations revealed a negative zeta potential. However, the CPS-M value was slightly lower. Moreover, the PDI value of CPS-M was also bigger than that of blank micelles. Changes in zeta and PDI are likely promoted by drugs inclusion in the micelle core and are also generally reported in the literature (Li et al., 2009; Ma et al., 2010a).

Kulkarni and co-workers studied the effect of TPGS when it was used for coating other nanoparticles (Kulkarni and Feng, 2013). They reported that the TPGS coated nanoparticles with a size of 113-210 nm and a zeta potential ranging from -26.7 to -30.2 mV exhibited the highest cellular uptake. Moreover, the biodistribution studies revealed that TPGS coated particles exhibited lower accumulation in liver and spleen (Kulkarni and Feng, 2013). Zhang *et al.* tested the *in vivo* anti-tumoral efficacy of paclitaxel loaded TPGS-PLA nanoparticles (Zhang et al., 2008b). These TPGS-PLA nanoparticles exhibited a mean size of 343 nm and were capable of retarding the *in vivo* tumor growth. The CPS-M size and surface characteristics are similar or more favorable than those above highlighted reports. Since nanovehicles performance is highly dependent on size and surface characteristics, the CPS-M seem to be suitable for cancer treatment, in what concerns these two physicochemical factors (Feng, 2006).

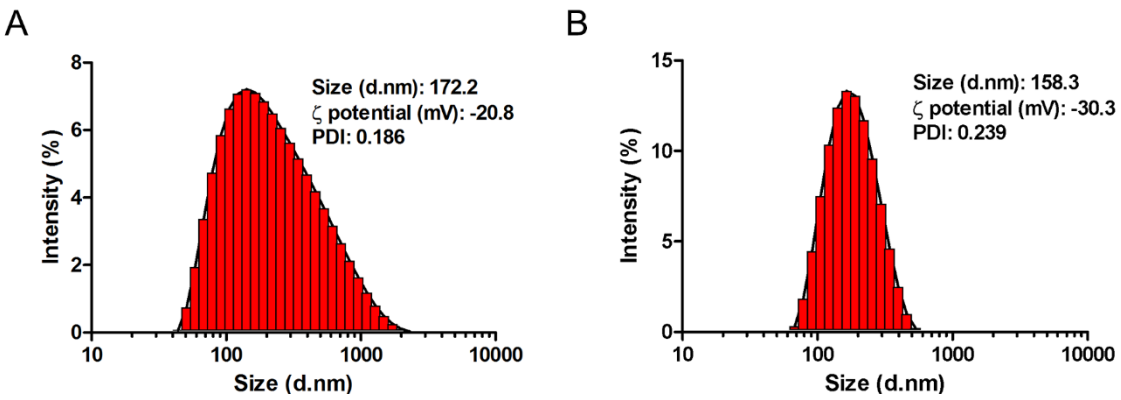

Figure 21 - DLS characterization of A) blank TPGS-PLA micelles and B) CPS-M.

3.10. Evaluation of the drug release profile

To investigate the *in vitro* drug release profile of CPS-M micelles, a release study was performed in PBS in order to simulate the physiological conditions (pH=7.4). The release profile of CPS-M is characterized by 2 main phases: i.) a slightly faster release in the first 12 h and ii.) a slower

and sustained drug release that was incremented along time. Palbociclib exhibited increased release from the micellar carriers in phase I, having 66 % of its content be released after 12 h. Sildenafil and Crizotinib were also released, but in slightly lower amount (**Figure 22**). After this initial drug release, a sustained profile was observed. This release profile is often present in TPGS-PLA nanodevices (Sun and Feng, 2009; Zhang and Feng, 2006a). Zhao and co-workers recently reported for a similar TPGS based system, that the initial burst release might be limited by increasing the PEG chain length of TPGS, although this could also lead to a decrease in cellular uptake and ultimately affect the nanovehicle therapeutic efficacy (Zhao and Feng, 2014).

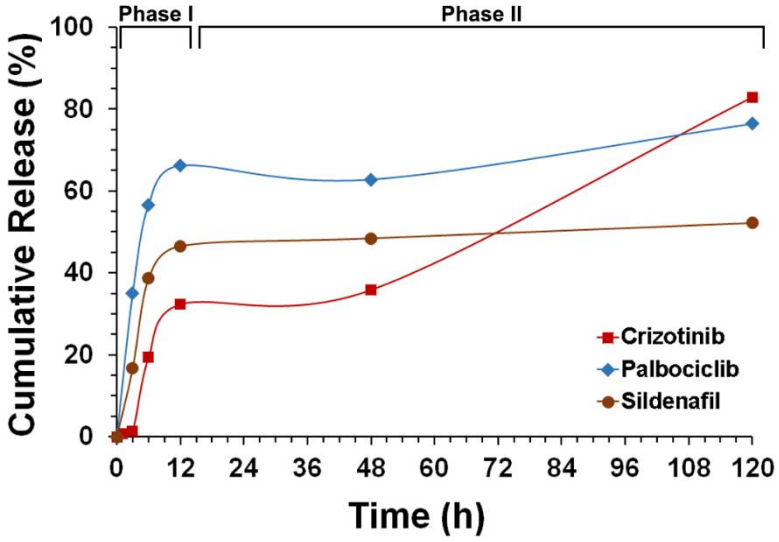

Figure 22 - Cumulative release profile of CPS-M in release buffer (pH=7.4) determined by UPLC.

3.11. Characterization of TPGS-PLA biocompatibility

Blank micelles biocompatibility was evaluated using in A549 and MRC-5 cell lines as model. This assay allowed to assess the influence of micelles formulation conditions and also the effect of TPGS-PLA micelles in cell viability. **Figure 23** shows that all cells incubated with blank TPGS-PLA micelles had a high viability. Taken together, these findings support TPGS-PLA micelles suitability for drug delivery applications reflected by its biosafety. Moreover, the A549 cell viability results are essential to assure that TPGS-PLA micelles will not mask the chemotherapeutic effect of the loaded drugs.

Despite TPGS having intrinsic anti-tumoral activity, its IC50 is quite high (Youk et al., 2005). Moreover it was also reported that the chemical conjugation of TOS with PEG (TPGS) is crucial for its anti-tumoral effect, since TOS and TOS plus PEG combinations presented the same anti-tumoral effect (Youk et al., 2005). Based on the results obtained here, the conjugation of PLA with TPGS might have affected its activity. In fact the herein formulated blank TPGS-PLA micelles did not presented intrinsic anti-tumoral activity as seen in **Figure 23 A**. Tan *et al.*

TPGS-PLA nanoparticles also did not presented intrinsic anti-tumoral activity, even after 72h of incubation (Tan et al., 2014). The same was also reported in TPGS-PLA, TPGS-PLA-PCL and TPGS-PLGA nanoparticles formulated using TPGS as surfactant/emulsifier (Ma et al., 2010a; Ma et al., 2010b; Pan and Feng, 2008; Tao et al., 2013). However micelles formulated only with TPGS or mostly by TPGS present dose dependent cytotoxicity (Mi et al., 2011; Shen et al., 2013). It seems that TPGS mediated anti-tumoral activity in nanodevices is heavily influenced by its concentration and by the degradation rate of the polymers to which it is conjugated.

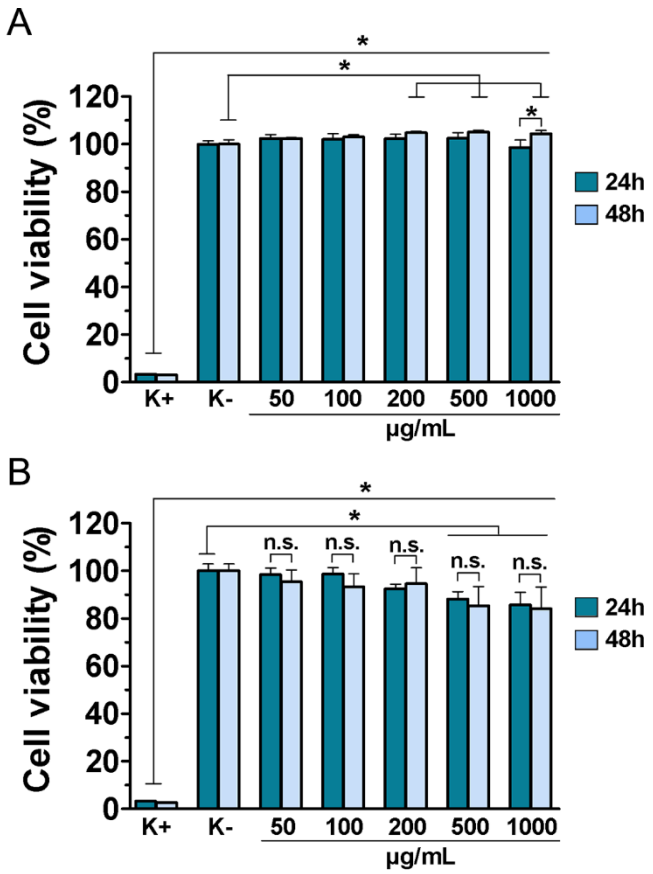

Figure 23 - Evaluation of the cytotoxic profile of blank TPGS-PLA micelles at different concentrations and incubation times using A) A549 cells and B) MRC-5 cells. Data represent mean±SD, n=5, n.s.=non significant, *p<0.05. K+ represent positive control and K- represent negative control.

3.12. TPGS-PLA micelles cellular uptake

TPGS-PLA micelles internalization in A549 lung cancer cells was investigated by CLSM. For this purpose, blank and CPS-M carriers were formulated with RITC (model fluorescent probe). Actin and cell nucleus were also stained for CLSM imaging. As shown in **Figure 24**, TPGS-PLA blank and loaded micelles were extensively localized within cell cytoplasm after 4 h of administration. Despite blank TPGS-PLA micelles and CPS-M having different size and zeta potential, no relevant differences were observed on their uptake.

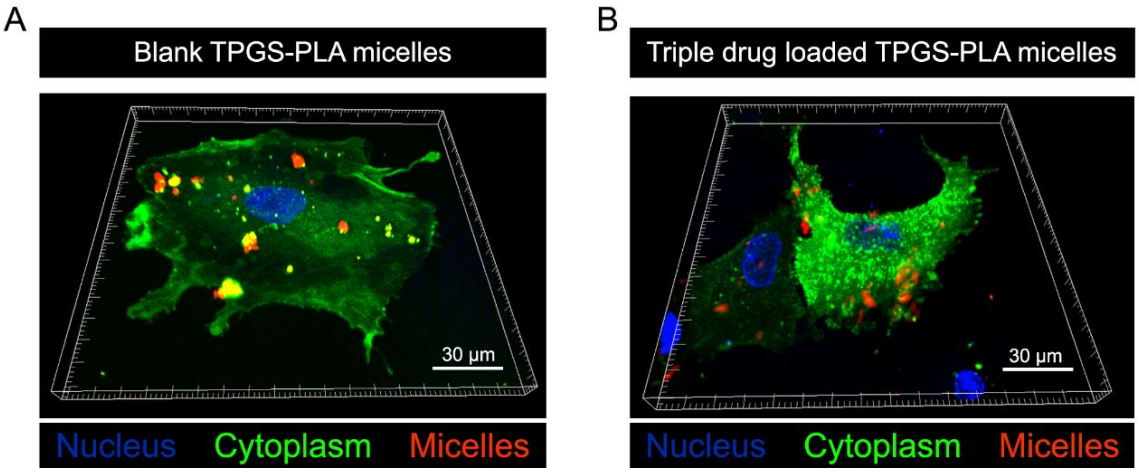

Figure 24 – Representative CLSM images of micelles internalization in A549 cells after 4 h incubation. Internalization of A) blank TPGS-PLA micelles and B) CPS-M. Blue channel: Hoechst 33342® - nucleus. Green channel: Actin-GFP. Red channel: RITC-loaded micelles.

The CPS-M are internalized by A549 lung cancer cells and are not likely absorbed on the cells surface (**Figure 25**; white arrows). Micelles internalization into cancer cells is important for increasing the intracellular concentration of the chemotherapeutic drugs and thus promote a higher interaction with their macromolecular targets. Furthermore, micelles internalization is also crucial for Sildenafil and TPGS to exert their activities.

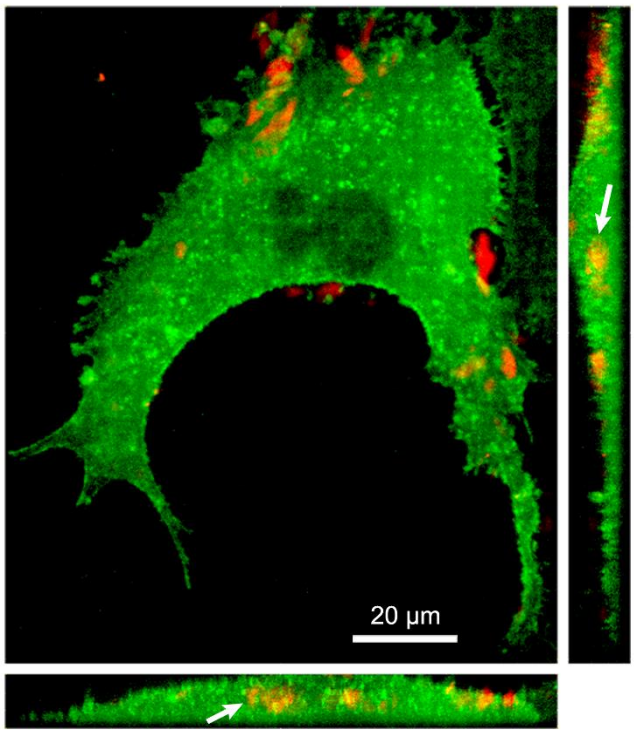

Figure 25 – Maximum intensity projection and orthogonal view of CPS-M uptake. White arrows represent micellar carriers in cell cytoplasm.

3.13. IC50 determination of Crizotinib and Palbociclib in lung cancer cell line

After addressing micelles safety and confirming that they are internalized by cancer cells, the cytotoxic effect of Crizotinib and Palbociclib on A549 NSCLC cell model was studied. Crizotinib is an FDA approved drug for NSCLC, whereas Palbociclib is on clinical trials for breast cancer therapy. The calculated IC50 for Crizotinib and Palbociclib were 26.07 and 17.65 μM, respectively (**Figure 26**). Crizotinib IC50 value is higher than that reported in the literature (2.5-3.5 μM) (Katayama et al., 2011). Palbociclib IC50 value was lower than Crizotinib, thus evidencing the feasibility of its applicability for lung cancer therapy. The IC50 values of Crizotinib and Palbociclib are relatively high compared to those generally reported in the literature for anticancer drugs. This is mostly due to the acquisition of a resistant phenotype by A549 cells during long culture periods. Additionally, Sildenafil did not show cytotoxicity against A549 cells (**Figure 26 C**).

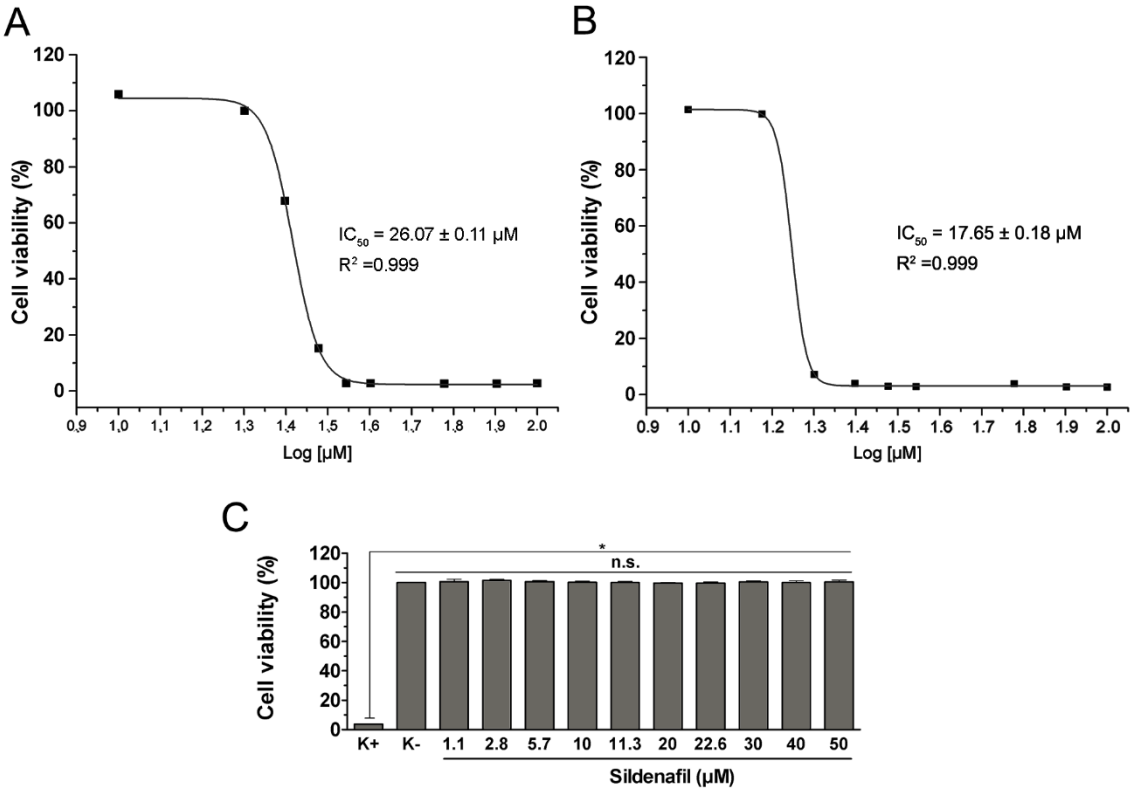

Figure 26 - Evaluation of the IC50 of free administration of A) Crizotinib and B) Palbociclib in A549 cells after 48 h incubation. Data represent mean, n=5. C) Evaluation of Sildenafil cytotoxicity in A549 cells after 48 h incubation. Data represent mean±SD, n=5, n.s.=non significant, *p<0.05. K+ represent positive control and K- represent negative control.

3.14. Evaluation of double and triple drugs combination for lung cancer therapy

Before studying the therapeutic efficacy of CPS-M, first the cytotoxic activity of the different free drug combinations were tested. The cytotoxic activity of Crizotinib/Palbociclib (dual drug combination) and Crizotinib/Palbociclib/Sildenafil (triple drug combinations) were investigated, as well as the nature of its combinatorial effect.

As shown in **Figure 27 A**, the dual drug combination promoted an improved cytotoxic effect (IC50 dual drug combination = 17.63 µM) compared to the single drugs IC50. To unveil the nature of its combinatorial effect, the CI for this combination was calculated using the Chou-Talalay method (Li et al., 2014). The dual drug combination effect was additive (CI=0.99), meaning that the two drugs combined effect is equal to the sum of their individual effects - **Figure 28**. Still, the co-administration of different anti-tumoral drugs is advantageous since it targets different molecular pathways at the same time, thus promoting an improved therapeutic effect. Moreover, when a chemotherapeutic drug is administered, cancer cells can acquire resistance by altering various proliferation pathways, and apoptotic and survival mechanism, thus making the co-delivery of different pharmaceuticals an attractive strategy. Furthermore, potential antagonistic effects of Palbociclib combined with chemotherapeutic drugs have been reported, thus emphasizing the novelty and effectiveness of the tested Crizotinib/Palbociclib drug combination (Dean et al., 2012; Roberts et al., 2012).

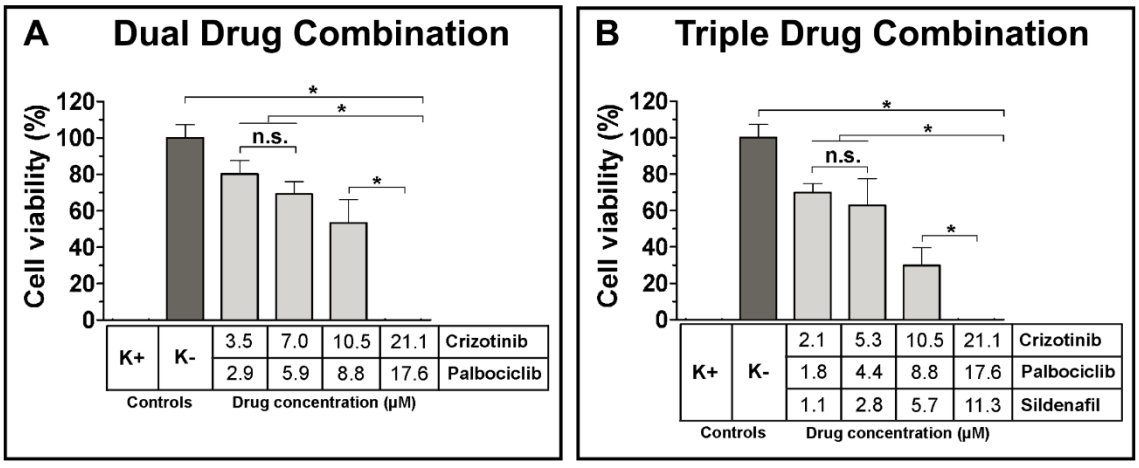

Figure 27 - Evaluation of the cytotoxicity of A) dual drug (Crizotinib plus Palbociclib) and B) triple drug (Crizotinib plus Palbociclib plus Sildenafil) combinations in A549 cells after 48 h incubation. Data represent mean±SD, n=3, n.s.=non significant, *p<0.05. K+ represent positive control and K- represent negative control.

Despite the Crizotinib/Palbociclib combination showed good therapeutic potential, a multidrug therapy with a drug capable of targeting various types of ABC efflux pumps was evaluated. In addition, the effect of Sildenafil in the cytotoxic effect mediated by Crizotinib/Palbociclib was

also investigated. The therapeutic effect was indeed improved (IC50 triple drug combination = 13.26 μM) (**Figure 27 B**). In fact, comparing the cytotoxic effect of Crizotinib plus Palbociclib or the same combination with Sildenafil addition, a significant 1.78 fold decrease in cell viability was observed when Sildenafil was introduced. The triple drug combination exhibited a synergistic effect (CI=0.75) and so it promoted a stronger effect that is greater than that resulting from the sum of the individual drugs (**Figure 28**). It is clear that Sildenafil addition to the previous combination is advantageous in terms of cytotoxicity. Since Sildenafil alone did not affect the A549 cells viability (**Figure 26 C**), the increase in the cytotoxicity when combined with Crizotinib and Palbociclib might be related to the inhibition of the drug efflux pumps associated with cancer resistance. Other reports have also demonstrated the *in vivo* anti-tumoral potential of Sildenafil, where its combination with DOX and Paclitaxel showed improved therapeutic results (Chen et al., 2014; Das et al., 2010)

The triple drug combination synergistic effect and the concerns regarding a free multidrug chemotherapy, corroborates the triple drug co-delivery approach of Crizotinib, Palbociclib and Sildenafil in TPGS-PLA micellar nanocarriers for cancer therapy.

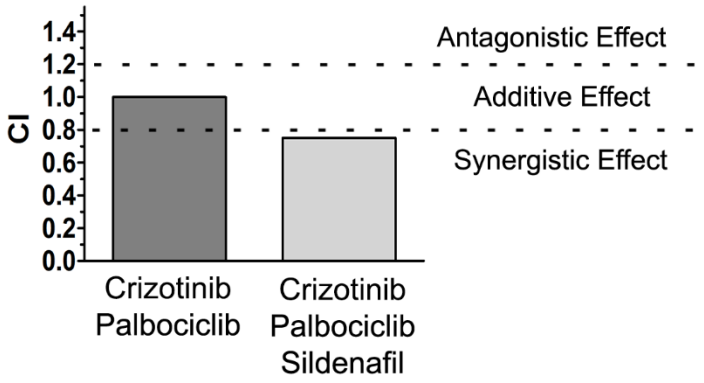

Figure 28 - Chou-Talalay analysis for dual drug and triple drug combinations. CI values of CI<0.8, 0.8<CI<1.2 and CI>1.2 were considered synergistic, additive and antagonistic effects, respectively.

3.15. Evaluation of the cytotoxicity of the different micellar formulations

Chemotherapeutic drugs have some drawbacks such as low solubility and non-specific toxicity that can be greatly circumvented by using nanovehicles for their selective delivery to target cells. In this context this work demonstrates that TPGS-PLA micelles are capable of encapsulating multiple drugs and to be internalized by cancer cells. Moreover, given the superior efficacy of the triple free drug combination (**Figure 27 B**), it was also investigated if triple loaded TPGS-PLA micelles (CPS-M) would have superior efficacy as well. In fact, among the three different TPGS-PLA micelles formulations tested, CPS-M were those that promoted a

higher cytotoxic effect (**Figure 29**). CPS-M achieved a significant efficacy at relatively low micellar concentrations such as 0.2 mg/mL (**Figure 29 C**). For C-M and CP-M a higher concentration was necessary to attain a therapeutic effect (**Figure 29 A and B**). The inclusion of Sildenafil in micelles improved their cytotoxic effect in comparison with dual loaded micelles administration (CP-M), reflecting the dual and triple drug free administration results.

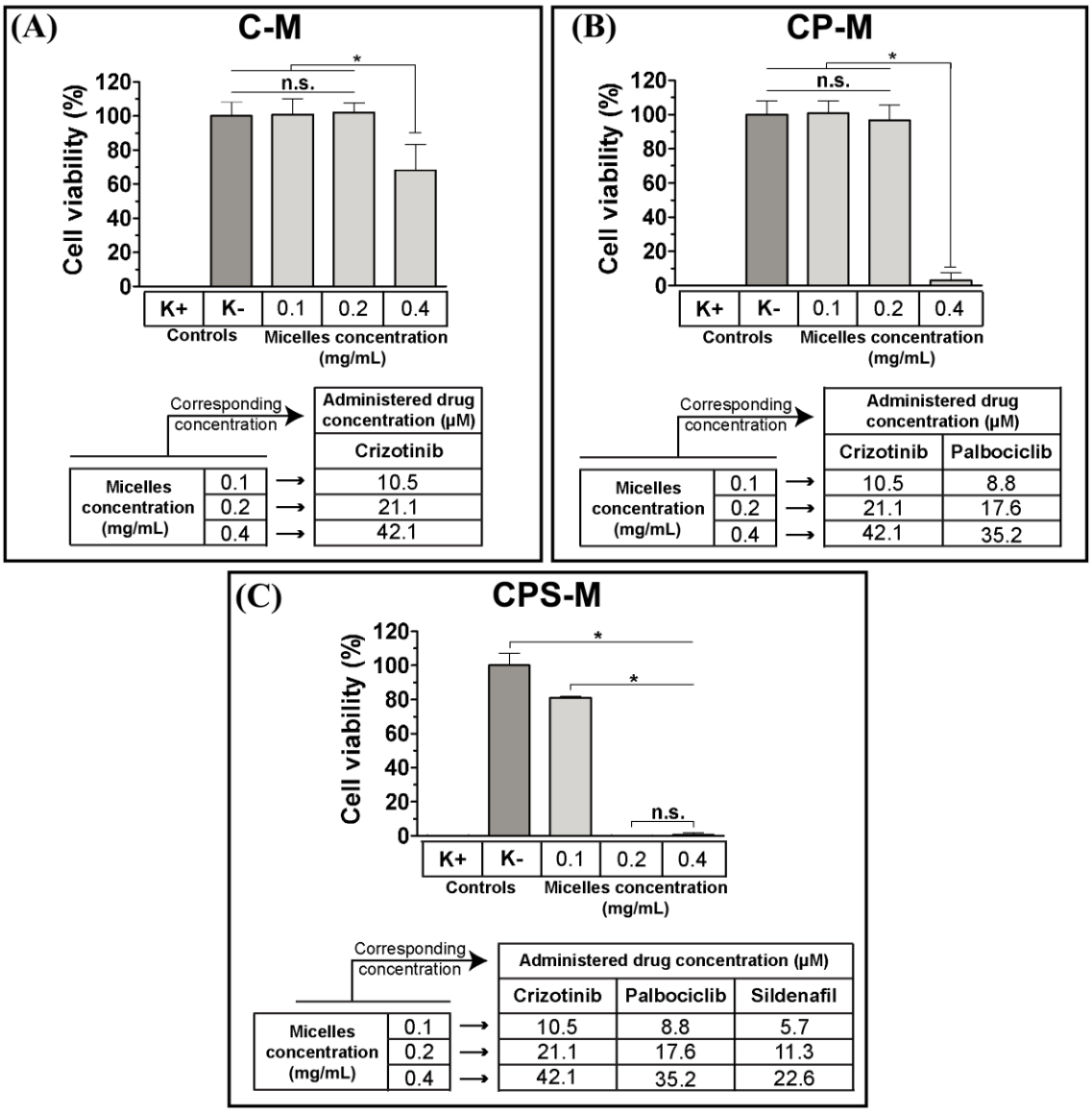

Figure 29 - Evaluation of the cytotoxic activity of A) C-M, B) CP-M and C) CPS-M formulations in A549 cells after 48 h incubation. Data represent mean±SD, n=5, n.s.=non significant, *p<0.05. K+ represent positive control and K- represent negative control.

Comparing the results of the free drug administrations with its respective drug loaded micellar formulation, indicates that micelles exhibited a slightly lower cytotoxic effect using the same concentrations - **Figure 30**. However, it is important to notice that these differences are possibly associated with the release profile of the drugs inside the cells at the time of the

experiment. Nevertheless, the free administration of anti-tumoral drugs is associated with limited bioavailability *in vivo* and non-selective toxicity. In addition, the administration of free drug combinations can lead to drug-drug interactions during circulation and change in pharmacokinetic/pharmacodynamic profile of the original compounds. These issues can be overcome with the delivery in TPGS-PLA nanodevices that are accumulated passively in tumor tissues as demonstrated by Zhang and co-workers (Zhang et al., 2008b). The herein formulated triple drug loaded TPGS-PLA micelles (CPS-M) had greater cytotoxicity than single (C-M) and dual drug loaded micelles (CP-M), at any given concentration of micelles, reflecting the synergistic effect achieved by the triple drug combination administration (**Figure 30**). Overall, these results validate the concept of the co-delivery of Crizotinib, Palbociclib and Sildenafil in TPGS-PLA micelles for lung cancer therapy.

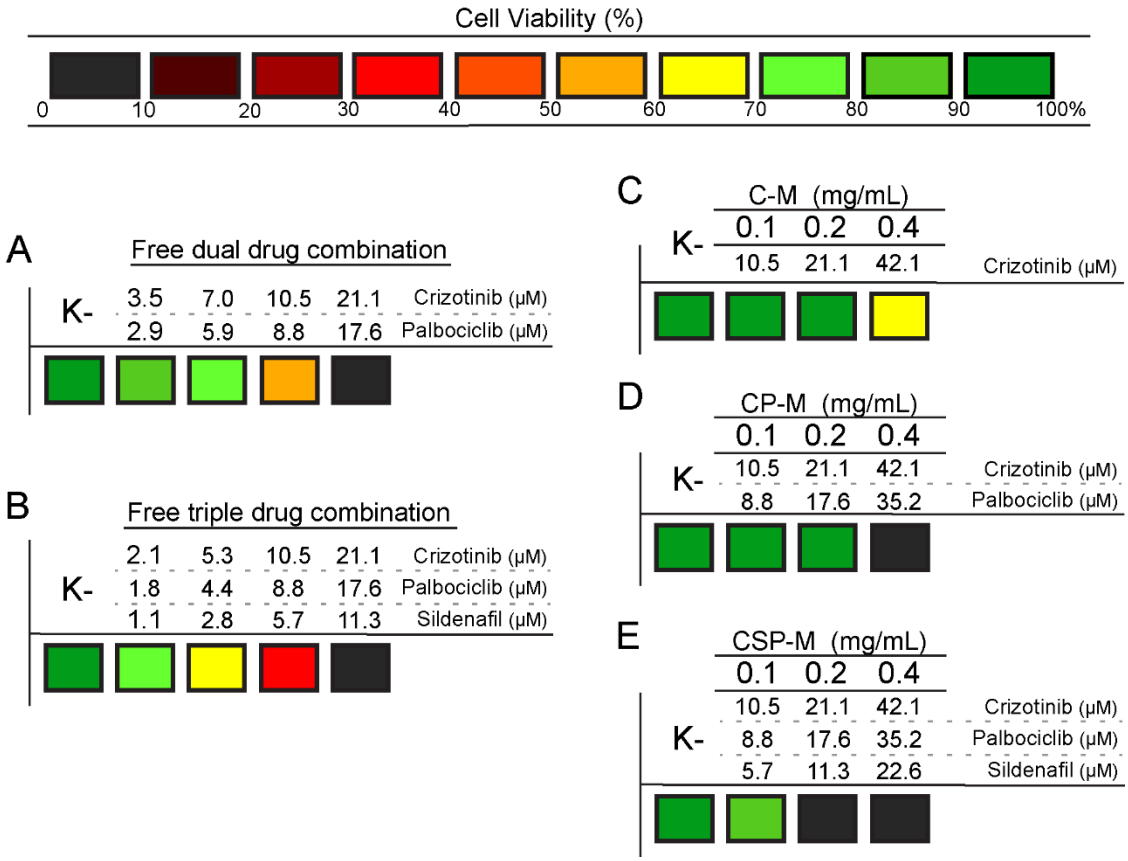

Figure 30 - Heat map global analysis of cytotoxic activity of different free drug combinations and different micelles formulations. Summarizes the data from **Figure 27** and **Figure 29**.

.

Chapter 4

Conclusions and Future Perspectives

4. Conclusions and Future Perspectives

Cancer is a leading cause of death worldwide. Despite the great efforts, to date no fully effective treatment for this disease is available. The efficacy of chemotherapeutic treatments is impaired by factors related with the anti-tumoral drugs themselves, like the poor solubility, non-specific toxicity and undesired pharmacokinetics. Moreover, cell related mechanisms also play an import role mediating chemotherapy inefficacy. Cancer cells can acquire drug resistance mechanisms, whereas the increased drug efflux plays a decisive role. In this context, nanosized delivery systems that mediate multidrug co-delivery to cancer cells are a valuable strategy to improve drugs bioavailability, target cancer hallmarks and overcome cancer drug resistance mechanisms.

In this thesis, the co-delivery of Crizotinib, Palbociclib and Sildenafil in TPGS-PLA micelles were studied for lung cancer therapy. The synthetized TPGS-PLA diblock copolymer assembled under specific conditions into nanosized and stable polymeric micelles, as demonstrated by their low CMC value. Moreover, the TPGS-PLA micelles were capable of encapsulating novel and untested triple drug combination composed by Crizotinib, Palbociclib and Sildenafil. For this purpose a new UPLC method was established. The results revealed that the TPGS-PLA micelles were capable of encapsulating the triple drug combination with high efficiency. This combination is based on the use of an FDA approved drug for NSCLC (Crizotinib), a novel and potent cell cycle arrester under clinical trials (Palbociclib) and potent ABC efflux transporters inhibitor (Sildenafil). Moreover, the micellar system has TPGS in its composition and so it can potentially benefit from TPGS intrinsic properties such MDR1 as inhibiting capacity.

The triple drug combination was tested here for the first time and proved to be advantageous for lung cancer therapy. In fact, the administration of free triple drug exhibited a synergistic effect, whereas, for the dual drug combination (Crizotinib/Palbociclib) only an additive effect was obtained. Among all tested micellar formulations, the triple drug loaded micelles (CPS-M) exhibited the highest cytotoxic effect, thus reflecting the triple free drug combination cytotoxic results. CPS-M results show their potential for being used in lung cancer treatment. Furthermore, CPS-M might also have potential to be effective in multidrug resistant cancers mostly through Sildenafil and TPGS drug efflux pumps inhibiting activities.

Moreover the co-delivery of multiple therapeutic agents by TPGS-PLA micelles formulated in this work is one of the first delivery systems to employ the use of Palbociclib. Additionally, the TPGS and Sildenafil combination with drug efflux inhibition potential is explored here for the first time. The Sildenafil plus TPGS combination has the potential to inhibit several types of the different drug efflux pumps, thus being advantageous compared to the classic employed agents, such as siRNA or Cyclosporin A, that can only inhibit one type of drug efflux pump at a time.

In the future, other chemotherapeutic drugs can be co-encapsulated and tested to take advantage of this simple and versatile MDR inhibiting strategy through TPGS and Sildenafil activities.

Chapter 5
References

5. References

Albertsson, A.C., Varma, I.K., 2003. Recent developments in ring opening polymerization of lactones for biomedical applications. Biomacromolecules 4, 1466-1486.

Albini, A., Sporn, M.B., 2007. The tumour microenvironment as a target for chemoprevention. Nature reviews. Cancer 7, 139-147.

Anderson, J.M., Shive, M.S., 2012. Biodegradation and biocompatibility of PLA and PLGA microspheres. Advanced drug delivery reviews 64, 72-82.

Auras, R.A., Lim, L.-T., Selke, S.E., Tsuji, H., 2011. Poly (lactic acid): synthesis, structures, properties, processing, and applications. John Wiley & Sons.

Black, K.C., Wang, Y., Luehmann, H.P., Cai, X., Xing, W., Pang, B., Zhao, Y., Cutler, C.S., Wang, L.V., Liu, Y., Xia, Y., 2014. Radioactive (198)au-doped nanostructures with different shapes for in vivo analyses of their biodistribution, tumor uptake, and intratumoral distribution. ACS nano 8, 4385-4394.

Boolell, M., Allen, M., Ballard, S., Gepi-Attee, S., Muirhead, G., Naylor, A., Osterloh, I., Gingell, C., 1996. Sildenafil: an orally active type 5 cyclic GMP-specific phosphodiesterase inhibitor for the treatment of penile erectile dysfunction. International journal of impotence research 8, 47-52.

Bouwman, P., Jonkers, J., 2012. The effects of deregulated DNA damage signalling on cancer chemotherapy response and resistance. Nature reviews. Cancer 12, 587-598.

Chen, L., Xie, Z., Hu, J., Chen, X., Jing, X., 2007. Enantiomeric PLA–PEG block copolymers and their stereocomplex micelles used as rifampin delivery. Journal of Nanoparticle Research 9, 777-785.

Chen, Z.S., Shi, Z., Ashby, C.R., 2014. Use of phosphodiesterase inhibitors for treating multidrug resistance. U.S. Patent 8673914 B2.

Chithrani, B.D., Ghazani, A.A., Chan, W.C., 2006. Determining the size and shape dependence of gold nanoparticle uptake into mammalian cells. Nano letters 6, 662-668.

Choi, H.S., Liu, W., Misra, P., Tanaka, E., Zimmer, J.P., Itty Ipe, B., Bawendi, M.G., Frangioni, J.V., 2007. Renal clearance of quantum dots. Nature biotechnology 25, 1165-1170.

Cirri, P., Chiarugi, P., 2012. Cancer-associated-fibroblasts and tumour cells: a diabolic liaison driving cancer progression. Cancer metastasis reviews 31, 195-208.

Collnot, E.M., Baldes, C., Wempe, M.F., Hyatt, J., Navarro, L., Edgar, K.J., Schaefer, U.F., Lehr, C.M., 2006. Influence of vitamin E TPGS poly(ethylene glycol) chain length on apical efflux transporters in Caco-2 cell monolayers. Journal of controlled release 111, 35-40.

Collnot, E.M., Baldes, C., Wempe, M.F., Kappl, R., Huttermann, J., Hyatt, J.A., Edgar, K.J., Schaefer, U.F., Lehr, C.M., 2007. Mechanism of inhibition of P-glycoprotein mediated efflux by vitamin E TPGS: influence on ATPase activity and membrane fluidity. Molecular pharmaceutics 4, 465-474.

Costa, E.C., Gaspar, V.M., Marques, J.G., Coutinho, P., Correia, I.J., 2013. Evaluation of nanoparticle uptake in co-culture cancer models. PloS one 8, e70072.

Czekanska, E.M., 2011. Assessment of cell proliferation with resazurin-based fluorescent dye, Mammalian Cell Viability. Springer, pp. 27-32.

Danhier, F., Feron, O., Preat, V., 2010. To exploit the tumor microenvironment: Passive and active tumor targeting of nanocarriers for anti-cancer drug delivery. Journal of controlled release 148, 135-146.

Das, A., Durrant, D., Mitchell, C., Mayton, E., Hoke, N.N., Salloum, F.N., Park, M.A., Qureshi, I., Lee, R., Dent, P., Kukreja, R.C., 2010. Sildenafil increases chemotherapeutic efficacy of doxorubicin in prostate cancer and ameliorates cardiac dysfunction. Proceedings of the National Academy of Sciences of the United States of America 107, 18202-18207.

Dean, J.L., McClendon, A.K., Knudsen, E.S., 2012. Modification of the DNA damage response by therapeutic CDK4/6 inhibition. The Journal of biological chemistry 287, 29075-29087.

Dechy-Cabaret, O., Martin-Vaca, B., Bourissou, D., 2004. Controlled ring-opening polymerization of lactide and glycolide. Chemical reviews 104, 6147-6176.

Deng, C., Jiang, Y., Cheng, R., Meng, F., Zhong, Z., 2012. Biodegradable polymeric micelles for targeted and controlled anticancer drug delivery: promises, progress and prospects. Nano Today 7, 467-480.

Dijkstra, P.J., Du, H., Feijen, J., 2011. Single site catalysts for stereoselective ring-opening polymerization of lactides. Polymer Chemistry 2, 520-527.

Dong, L.F., Jameson, V.J., Tilly, D., Prochazka, L., Rohlena, J., Valis, K., Truksa, J., Zobalova, R., Mahdavian, E., Kluckova, K., Stantic, M., Stursa, J., Freeman, R., Witting, P.K., Norberg, E., Goodwin, J., Salvatore, B.A., Novotna, J., Turanek, J., Ledvina, M., Hozak, P., Zhivotovsky, B., Coster, M.J., Ralph, S.J., Smith, R.A., Neuzil, J., 2011. Mitochondrial targeting of alpha-tocopheryl succinate enhances its pro-apoptotic efficacy: a new paradigm for effective cancer therapy. Free radical biology & medicine 50, 1546-1555.

Doublier, S., Belisario, D.C., Polimeni, M., Annaratone, L., Riganti, C., Allia, E., Ghigo, D., Bosia, A., Sapino, A., 2012. HIF-1 activation induces doxorubicin resistance in MCF7 3-D spheroids via P-glycoprotein expression: a potential model of the chemo-resistance of invasive micropapillary carcinoma of the breast. BMC cancer 12, 4.

Duhem, N., Danhier, F., Preat, V., 2014. Vitamin E-based nanomedicines for anti-cancer drug delivery. Journal of controlled release 182C, 33-44.

Egeblad, M., Werb, Z., 2002. New functions for the matrix metalloproteinases in cancer progression. Nature reviews. Cancer 2, 161-174.

Elsabahy, M., Wooley, K.L., 2012. Design of polymeric nanoparticles for biomedical delivery applications. Chemical Society reviews 41, 2545-2561.

Ernsting, M.J., Murakami, M., Roy, A., Li, S.D., 2013. Factors controlling the pharmacokinetics, biodistribution and intratumoral penetration of nanoparticles. Journal of controlled release 172, 782-794.

Etheridge, M.L., Campbell, S.A., Erdman, A.G., Haynes, C.L., Wolf, S.M., McCullough, J., 2013. The big picture on nanomedicine: the state of investigational and approved nanomedicine products. Nanomedicine : nanotechnology, biology, and medicine 9, 1-14.

Ettinger, D.S., Akerley, W., Borghaei, H., Chang, A.C., Cheney, R.T., Chirieac, L.R., D'Amico, T.A., Demmy, T.L., Ganti, A.K., Govindan, R., Grannis, F.W., Jr., Horn, L., Jahan, T.M., Jahanzeb, M., Kessinger, A., Komaki, R., Kong, F.M., Kris, M.G., Krug, L.M., Lennes, I.T., Loo, B.W., Jr., Martins, R., O'Malley, J., Osarogiagbon, R.U., Otterson, G.A., Patel, J.D., Pinder-Schenck, M.C., Pisters, K.M., Reckamp, K., Riely, G.J., Rohren, E., Swanson, S.J., Wood, D.E., Yang, S.C., Hughes, M., Gregory, K.M., Nccn, 2012. Non-small cell lung cancer. Journal of the National Comprehensive Cancer Network 10, 1236-1271.

Falasca, M., Linton, K.J., 2012. Investigational ABC transporter inhibitors. Expert opinion on investigational drugs 21, 657-666.

Feng, S.S., 2006. New-concept chemotherapy by nanoparticles of biodegradable polymers: where are we now? Nanomedicine (Lond) 1, 297-309.

Fletcher, J.I., Haber, M., Henderson, M.J., Norris, M.D., 2010. ABC transporters in cancer: more than just drug efflux pumps. Nature reviews. Cancer 10, 147-156.

Florez, L., Herrmann, C., Cramer, J.M., Hauser, C.P., Koynov, K., Landfester, K., Crespy, D., Mailander, V., 2012. How shape influences uptake: interactions of anisotropic polymer nanoparticles and human mesenchymal stem cells. Small 8, 2222-2230.

Fry, D.W., Harvey, P.J., Keller, P.R., Elliott, W.L., Meade, M., Trachet, E., Albassam, M., Zheng, X., Leopold, W.R., Pryer, N.K., Toogood, P.L., 2004. Specific inhibition of cyclin-dependent kinase 4/6 by PD 0332991 and associated antitumor activity in human tumor xenografts. Molecular cancer therapeutics 3, 1427-1438.

Gaspar, V.M., Marques, J.G., Sousa, F., Louro, R.O., Queiroz, J.A., Correia, I.J., 2013. Biofunctionalized nanoparticles with pH-responsive and cell penetrating blocks for gene delivery. Nanotechnology 24, 275101.

Gherardi, E., Birchmeier, W., Birchmeier, C., Vande Woude, G., 2012. Targeting MET in cancer: rationale and progress. Nature reviews. Cancer 12, 89-103.

Goddeeris, C., Willems, T., Van den Mooter, G., 2008. Formulation of fast disintegrating tablets of ternary solid dispersions consisting of TPGS 1000 and HPMC 2910 or PVPVA 64 to improve the dissolution of the anti-HIV drug UC 781. European journal of pharmaceutical sciences 34, 293-302.

Gong, J., Chen, M., Zheng, Y., Wang, S., Wang, Y., 2012. Polymeric micelles drug delivery system in oncology. Journal of controlled release 159, 312-323.

Gottesman, M.M., 2002. Mechanisms of cancer drug resistance. Annual review of medicine 53, 615-627.

Gottesman, M.M., Fojo, T., Bates, S.E., 2002. Multidrug resistance in cancer: role of ATP-dependent transporters. Nature reviews. Cancer 2, 48-58.

Gou, M., Men, K., Shi, H., Xiang, M., Zhang, J., Song, J., Long, J., Wan, Y., Luo, F., Zhao, X., Qian, Z., 2011. Curcumin-loaded biodegradable polymeric micelles for colon cancer therapy in vitro and in vivo. Nanoscale 3, 1558-1567.

Gratton, S.E., Ropp, P.A., Pohlhaus, P.D., Luft, J.C., Madden, V.J., Napier, M.E., DeSimone, J.M., 2008. The effect of particle design on cellular internalization pathways. Proceedings of the National Academy of Sciences of the United States of America 105, 11613-11618.

Ha, P.T., Tran, T.M.N., Pham, H.D., Nguyen, Q.H., Nguyen, X.P., 2010. The synthesis of poly (lactide)-vitamin E TPGS (PLA-TPGS) copolymer and its utilization to formulate a curcumin nanocarrier. Advances in Natural Sciences: Nanoscience and Nanotechnology 1, 015012.

Hallberg, B., Palmer, R.H., 2013. Mechanistic insight into ALK receptor tyrosine kinase in human cancer biology. Nature reviews. Cancer 13, 685-700.

Hanahan, D., Coussens, L.M., 2012. Accessories to the crime: functions of cells recruited to the tumor microenvironment. Cancer cell 21, 309-322.

Hanahan, D., Weinberg, R.A., 2000. The hallmarks of cancer. Cell 100, 57-70.

Hanahan, D., Weinberg, R.A., 2011. Hallmarks of cancer: the next generation. Cell 144, 646-674.

Heldin, C.H., Rubin, K., Pietras, K., Ostman, A., 2004. High interstitial fluid pressure - an obstacle in cancer therapy. Nature reviews. Cancer 4, 806-813.

Herbst, R.S., Heymach, J.V., Lippman, S.M., 2008. Lung cancer. The New England journal of medicine 359, 1367-1380.

Holohan, C., Van Schaeybroeck, S., Longley, D.B., Johnston, P.G., 2013. Cancer drug resistance: an evolving paradigm. Nature reviews. Cancer 13, 714-726.

Jain, R.K., Stylianopoulos, T., 2010. Delivering nanomedicine to solid tumors. Nature reviews. Clinical oncology 7, 653-664.

Jemal, A., Bray, F., Center, M.M., Ferlay, J., Ward, E., Forman, D., 2011. Global cancer statistics. CA: a cancer journal for clinicians 61, 69-90.

Jokerst, J.V., Lobovkina, T., Zare, R.N., Gambhir, S.S., 2011. Nanoparticle PEGylation for imaging and therapy. Nanomedicine (Lond) 6, 715-728.

Kadara, H., Kabbout, M., Wistuba, II, 2012. Pulmonary adenocarcinoma: a renewed entity in 2011. Respirology 17, 50-65.

Kalemkerian, G.P., Akerley, W., Bogner, P., Borghaei, H., Chow, L., Downey, R.J., Gandhi, L., Ganti, A.K., Govindan, R., Grecula, J.C., Hayman, J., Heist, R.S., Horn, L., Jahan, T.M., Koczywas, M., Moran, C.A., Niell, H.B., O'Malley, J., Patel, J.D., Ready, N., Rudin, C.M., Williams, C.C., Jr., National Comprehensive Cancer, N., 2011. Small cell lung cancer. Journal of the National Comprehensive Cancer Network 9, 1086-1113.

Katayama, R., Khan, T.M., Benes, C., Lifshits, E., Ebi, H., Rivera, V.M., Shakespeare, W.C., Iafrate, A.J., Engelman, J.A., Shaw, A.T., 2011. Therapeutic strategies to overcome crizotinib resistance in non-small cell lung cancers harboring the fusion oncogene EML4-ALK. Proceedings of the National Academy of Sciences of the United States of America 108, 7535-7540.

Katayama, R., Shaw, A.T., Khan, T.M., Mino-Kenudson, M., Solomon, B.J., Halmos, B., Jessop, N.A., Wain, J.C., Yeo, A.T., Benes, C., Drew, L., Saeh, J.C., Crosby, K., Sequist, L.V., Iafrate, A.J., Engelman, J.A., 2012. Mechanisms of acquired crizotinib resistance in ALK-rearranged lung Cancers. Science translational medicine 4, 120ra117.

Knop, K., Hoogenboom, R., Fischer, D., Schubert, U.S., 2010. Poly(ethylene glycol) in drug delivery: pros and cons as well as potential alternatives. Angewandte Chemie 49, 6288-6308.

Kulkarni, S.A., Feng, S.S., 2013. Effects of particle size and surface modification on cellular uptake and biodistribution of polymeric nanoparticles for drug delivery. Pharmaceutical research 30, 2512-2522.

Kumari, A., Yadav, S.K., Yadav, S.C., 2010. Biodegradable polymeric nanoparticles based drug delivery systems. Colloids and surfaces. B, Biointerfaces 75, 1-18.

Lee, H., Hoang, B., Fonge, H., Reilly, R.M., Allen, C., 2010. In vivo distribution of polymeric nanoparticles at the whole-body, tumor, and cellular levels. Pharmaceutical research 27, 2343-2355.

Li, P., Lai, P., Lin, C., 2009. Reversal of multidrug resistance using poly (L-lactide)-Vitamin E TPGS micelles in breast cancer cell, Biomedical and Pharmaceutical Engineering, 2009. ICBPE'09. International Conference on. IEEE, pp. 1-5.

Li, S., 2003. Bioresorbable Hydrogels Prepared Through Stereocomplexation between Poly (L-lactide) and Poly (D-lactide) Blocks Attached to Poly (ethylene glycol). Macromolecular bioscience 3, 657-661.

Li, X., Tong, L.J., Ding, J., Meng, L.H., 2014. Systematic combination screening reveals synergism between rapamycin and sunitinib against human lung cancer. Cancer letters 342, 159-166.

Lin, F., Hoogendijk, L., Buil, L., Beijnen, J.H., van Tellingen, O., 2013. Sildenafil is not a useful modulator of ABCB1 and ABCG2 mediated drug resistance in vivo. European Journal of Cancer 49, 2059-2064.

Lozano, R., Naghavi, M., Foreman, K., Lim, S., Shibuya, K., Aboyans, V., Abraham, J., Adair, T., Aggarwal, R., Ahn, S.Y., AlMazroa, M.A., Alvarado, M., Anderson, H.R., Anderson, L.M., Andrews, K.G., Atkinson, C., Baddour, L.M., Barker-Collo, S., Bartels, D.H., Bell, M.L., Benjamin, E.J., Bennett, D., Bhalla, K., Bikbov, B., Abdulhak, A.B., Birbeck, G., Blyth, F., Bolliger, I., Boufous, S., Bucello, C., Burch, M., Burney, P., Carapetis, J., Chen, H., Chou, D., Chugh, S.S., Coffeng, L.E., Colan, S.D., Colquhoun, S., Colson, K.E., Condon, J., Connor, M.D., Cooper, L.T., Corriere, M., Cortinovis, M., de Vaccaro, K.C., Couser, W., Cowie, B.C., Criqui, M.H., Cross, M., Dabhadkar, K.C., Dahodwala, N., De Leo, D., Degenhardt, L., Delossantos, A., Denenberg, J., Des Jarlais, D.C., Dharmaratne, S.D., Dorsey, E.R., Driscoll, T., Duber, H., Ebel, B., Erwin, P.J., Espindola, P., Ezzati, M., Feigin, V., Flaxman, A.D., Forouzanfar, M.H., Fowkes, F.G.R., Franklin, R., Fransen, M., Freeman, M.K., Gabriel, S.E., Gakidou, E., Gaspari, F., Gillum, R.F., Gonzalez-Medina, D., Halasa, Y.A., Haring, D., Harrison, J.E., Havmoeller, R., Hay, R.J., Hoen, B., Hotez, P.J., Hoy, D., Jacobsen, K.H., James, S.L., Jasrasaria, R., Jayaraman, S., Johns, N., Karthikeyan, G., Kassebaum, N., Keren, A., Khoo, J.-P., Knowlton, L.M., Kobusingye, O., Koranteng, A., Krishnamurthi, R., Lipnick, M., Lipshultz, S.E., Ohno, S.L., Mabweijano, J., MacIntyre, M.F., Mallinger, L., March, L., Marks, G.B., Marks, R., Matsumori, A., Matzopoulos, R., Mayosi, B.M., McAnulty, J.H., McDermott, M.M., McGrath, J., Memish, Z.A., Mensah, G.A., Merriman, T.R., Michaud, C., Miller, M., Miller, T.R., Mock, C., Mocumbi, A.O., Mokdad, A.A., Moran, A., Mulholland, K., Nair, M.N., Naldi, L., Narayan, K.M.V., Nasseri, K., Norman, P., O'Donnell, M., Omer, S.B., Ortblad, K., Osborne, R., Ozgediz, D., Pahari, B., Pandian, J.D., Rivero, A.P., Padilla, R.P., Perez-Ruiz, F., Perico, N., Phillips, D., Pierce, K., Pope Iii, C.A., Porrini, E., Pourmalek, F., Raju, M., Ranganathan, D., Rehm, J.T., Rein, D.B., Remuzzi, G., Rivara, F.P., Roberts, T., De León, F.R., Rosenfeld, L.C., Rushton, L., Sacco, R.L., Salomon, J.A., Sampson, U., Sanman, E., Schwebel, D.C., Segui-Gomez, M., Shepard, D.S., Singh, D., Singleton, J., Sliwa, K., Smith, E., Steer, A., Taylor, J.A., Thomas, B., Tleyjeh, I.M., Towbin, J.A., Truelsen, T., Undurraga, E.A., Venketasubramanian, N., Vijayakumar, L., Vos, T., Wagner, G.R., Wang, M., Wang, W., Watt, K., Weinstock, M.A., Weintraub, R., Wilkinson, J.D., Woolf, A.D., Wulf, S., Yeh, P.-H., Yip, P., Zabetian, A., Zheng, Z.-J., Lopez, A.D., Murray, C.J.L., 2012. Global and regional mortality from 235 causes of death for 20 age groups in 1990 and 2010: a systematic analysis for the Global Burden of Disease Study 2010. The Lancet 380, 2095-2128.

Ma, Y., Huang, L., Song, C., Zeng, X., Liu, G., Mei, L., 2010a. Nanoparticle formulation of poly(ε-caprolactone-co-lactide)-d-α-tocopheryl polyethylene glycol 1000 succinate random copolymer for cervical cancer treatment. Polymer 51, 5952-5959.

Ma, Y., Zheng, Y., Liu, K., Tian, G., Tian, Y., Xu, L., Yan, F., Huang, L., Mei, L., 2010b. Nanoparticles of Poly(Lactide-Co-Glycolide)-d-a-Tocopheryl Polyethylene Glycol 1000 Succinate Random Copolymer for Cancer Treatment. Nanoscale research letters 5, 1161-1169.

Madhavan Nampoothiri, K., Nair, N.R., John, R.P., 2010. An overview of the recent developments in polylactide (PLA) research. Bioresource technology 101, 8493-8501.

Mantovani, A., Schioppa, T., Porta, C., Allavena, P., Sica, A., 2006. Role of tumor-associated macrophages in tumor progression and invasion. Cancer metastasis reviews 25, 315-322.

Marques, J.G., Gaspar, V.M., Costa, E., Paquete, C.M., Correia, I.J., 2014a. Synthesis and characterization of micelles as carriers of non-steroidal anti-inflammatory drugs (NSAID) for application in breast cancer therapy. Colloids and surfaces. B, Biointerfaces 113, 375-383.

Marques, J.G., Gaspar, V.M., Markl, D., Costa, E.C., Gallardo, E., Correia, I.J., 2014b. Co-delivery of Sildenafil (Viagra®) and Crizotinib for Synergistic and Improved Anti-tumoral Therapy. Pharmaceutical research, 1-13.

McCalley, D.V., 2000. Effect of temperature and flow-rate on analysis of basic compounds in high-performance liquid chromatography using a reversed-phase column. Journal of Chromatography A 902, 311-321.

Mei, L., Zhang, Z., Zhao, L., Huang, L., Yang, X.L., Tang, J., Feng, S.S., 2013. Pharmaceutical nanotechnology for oral delivery of anticancer drugs. Advanced drug delivery reviews 65, 880-890.

Mi, Y., Liu, Y., Feng, S.S., 2011. Formulation of Docetaxel by folic acid-conjugated d-alpha-tocopheryl polyethylene glycol succinate 2000 (Vitamin E TPGS(2k)) micelles for targeted and synergistic chemotherapy. Biomaterials 32, 4058-4066.

Mi, Y., Zhao, J., Feng, S.S., 2013. Targeted co-delivery of docetaxel, cisplatin and herceptin by vitamin E TPGS-cisplatin prodrug nanoparticles for multimodality treatment of cancer. Journal of controlled release 169, 185-192.

Nasongkla, N., Bey, E., Ren, J., Ai, H., Khemtong, C., Guthi, J.S., Chin, S.F., Sherry, A.D., Boothman, D.A., Gao, J., 2006. Multifunctional polymeric micelles as cancer-targeted, MRI-ultrasensitive drug delivery systems. Nano letters 6, 2427-2430.

Nazir, S., Hussain, T., Ayub, A., Rashid, U., MacRobert, A.J., 2014. Nanomaterials in combating cancer: therapeutic applications and developments. Nanomedicine : nanotechnology, biology, and medicine 10, 19-34.

Neophytou, C.M., Constantinou, C., Papageorgis, P., Constantinou, A.I., 2014. d-alpha-tocopheryl polyethylene glycol succinate (TPGS) induces cell cycle arrest and apoptosis selectively in Survivin-overexpressing breast cancer cells. Biochemical pharmacology 89, 31-42.

O'Bryant, C.L., Wenger, S.D., Kim, M., Thompson, L.A., 2013. Crizotinib: a new treatment option for ALK-positive non-small cell lung cancer. The Annals of pharmacotherapy 47, 189-197.

Okamoto, W., Okamoto, I., Arao, T., Kuwata, K., Hatashita, E., Yamaguchi, H., Sakai, K., Yanagihara, K., Nishio, K., Nakagawa, K., 2012. Antitumor action of the MET tyrosine kinase inhibitor crizotinib (PF-02341066) in gastric cancer positive for MET amplification. Molecular cancer therapeutics 11, 1557-1564.

Owen, S.C., Chan, D.P., Shoichet, M.S., 2012. Polymeric micelle stability. Nano Today 7, 53-65.

Ozben, T., 2006. Mechanisms and strategies to overcome multiple drug resistance in cancer. FEBS letters 580, 2903-2909.

Pan, J., Feng, S.S., 2008. Targeted delivery of paclitaxel using folate-decorated poly(lactide)-vitamin E TPGS nanoparticles. Biomaterials 29, 2663-2672.

Panyam, J., Labhasetwar, V., 2003. Biodegradable nanoparticles for drug and gene delivery to cells and tissue. Advanced drug delivery reviews 55, 329-347.

Parhi, P., Mohanty, C., Sahoo, S.K., 2012. Nanotechnology-based combinational drug delivery: an emerging approach for cancer therapy. Drug discovery today 17, 1044-1052.

Park, K., 2014. The Controlled Drug Delivery Systems: Past Forward and Future Back. Journal of Controlled Release. In Press.

Parveen, S., Misra, R., Sahoo, S.K., 2012. Nanoparticles: a boon to drug delivery, therapeutics, diagnostics and imaging. Nanomedicine : nanotechnology, biology, and medicine 8, 147-166.

Peer, D., Karp, J.M., Hong, S., Farokhzad, O.C., Margalit, R., Langer, R., 2007. Nanocarriers as an emerging platform for cancer therapy. Nature nanotechnology 2, 751-760.

Peters, S., Adjei, A.A., 2012. MET: a promising anticancer therapeutic target. Nature reviews. Clinical oncology 9, 314-326.

Prabhakar, U., Maeda, H., Jain, R.K., Sevick-Muraca, E.M., Zamboni, W., Farokhzad, O.C., Barry, S.T., Gabizon, A., Grodzinski, P., Blakey, D.C., 2013. Challenges and key considerations of the enhanced permeability and retention effect for nanomedicine drug delivery in oncology. Cancer research 73, 2412-2417.

Quail, D.F., Joyce, J.A., 2013. Microenvironmental regulation of tumor progression and metastasis. Nature medicine 19, 1423-1437.

Raaschou-Nielsen, O., Andersen, Z.J., Beelen, R., Samoli, E., Stafoggia, M., Weinmayr, G., Hoffmann, B., Fischer, P., Nieuwenhuijsen, M.J., Brunekreef, B., Xun, W.W., Katsouyanni, K., Dimakopoulou, K., Sommar, J., Forsberg, B., Modig, L., Oudin, A., Oftedal, B., Schwarze, P.E., Nafstad, P., De Faire, U., Pedersen, N.L., Ostenson, C.G., Fratiglioni, L., Penell, J., Korek, M., Pershagen, G., Eriksen, K.T., Sorensen, M., Tjonneland, A., Ellermann, T., Eeftens, M., Peeters, P.H., Meliefste, K., Wang, M., Bueno-de-Mesquita, B., Key, T.J., de Hoogh, K., Concin, H., Nagel, G., Vilier, A., Grioni, S., Krogh, V., Tsai, M.Y., Ricceri, F., Sacerdote, C., Galassi, C., Migliore, E., Ranzi, A., Cesaroni, G., Badaloni, C., Forastiere, F., Tamayo, I., Amiano, P., Dorronsoro, M., Trichopoulou, A., Bamia, C., Vineis, P., Hoek, G., 2013. Air pollution and lung cancer incidence in 17 European cohorts: prospective analyses from the European Study of Cohorts for Air Pollution Effects (ESCAPE). The lancet oncology 14, 813-822.

Roberts, P.J., Bisi, J.E., Strum, J.C., Combest, A.J., Darr, D.B., Usary, J.E., Zamboni, W.C., Wong, K.K., Perou, C.M., Sharpless, N.E., 2012. Multiple roles of cyclin-dependent kinase 4/6 inhibitors in cancer therapy. Journal of the National Cancer Institute 104, 476-487.

Rocca, A., Farolfi, A., Bravaccini, S., Schirone, A., Amadori, D., 2014. Palbociclib (PD 0332991) : targeting the cell cycle machinery in breast cancer. Expert opinion on pharmacotherapy 15, 407-420.

Sandler, A., Gray, R., Perry, M.C., Brahmer, J., Schiller, J.H., Dowlati, A., Lilenbaum, R., Johnson, D.H., 2006. Paclitaxel-carboplatin alone or with bevacizumab for non-small-cell lung cancer. The New England journal of medicine 355, 2542-2550.

Sartore-Bianchi, A., Martini, M., Molinari, F., Veronese, S., Nichelatti, M., Artale, S., Di Nicolantonio, F., Saletti, P., De Dosso, S., Mazzucchelli, L., Frattini, M., Siena, S., Bardelli, A., 2009. PIK3CA mutations in colorectal cancer are associated with clinical resistance to EGFR-targeted monoclonal antibodies. Cancer research 69, 1851-1857.

Schroeder, A., Heller, D.A., Winslow, M.M., Dahlman, J.E., Pratt, G.W., Langer, R., Jacks, T., Anderson, D.G., 2012. Treating metastatic cancer with nanotechnology. Nature reviews. Cancer 12, 39-50.

Shanker, M., Willcutts, D., Roth, J.A., Ramesh, R., 2010. Drug resistance in lung cancer. Lung Cancer: Targets and Therapy 1, 23-26.

Shaw, A.T., Kim, D.W., Mehra, R., Tan, D.S., Felip, E., Chow, L.Q., Camidge, D.R., Vansteenkiste, J., Sharma, S., De Pas, T., Riely, G.J., Solomon, B.J., Wolf, J., Thomas, M., Schuler, M., Liu, G., Santoro, A., Lau, Y.Y., Goldwasser, M., Boral, A.L., Engelman, J.A., 2014. Ceritinib in ALK-rearranged non-small-cell lung cancer. The New England journal of medicine 370, 1189-1197.

Shen, J., Meng, Q., Sui, H., Yin, Q., Zhang, Z., Yu, H., Li, Y., 2013. iRGD Conjugated TPGS Mediates Codelivery of Paclitaxel and Survivin shRNA for the Reversal of Lung Cancer Resistance. Molecular pharmaceutics.

Shi, Z., Tiwari, A.K., Patel, A.S., Fu, L.W., Chen, Z.S., 2011a. Roles of sildenafil in enhancing drug sensitivity in cancer. Cancer research 71, 3735-3738.

Shi, Z., Tiwari, A.K., Shukla, S., Robey, R.W., Singh, S., Kim, I.W., Bates, S.E., Peng, X., Abraham, I., Ambudkar, S.V., Talele, T.T., Fu, L.W., Chen, Z.S., 2011b. Sildenafil reverses ABCB1- and ABCG2-mediated chemotherapeutic drug resistance. Cancer research 71, 3029-3041.

Shieh, M.J., Hsu, C.Y., Huang, L.Y., Chen, H.Y., Huang, F.H., Lai, P.S., 2011. Reversal of doxorubicin-resistance by multifunctional nanoparticles in MCF-7/ADR cells. Journal of controlled release 152, 418-425.

Shim, M.S., Kwon, Y.J., 2010. Efficient and targeted delivery of siRNA in vivo. The FEBS journal 277, 4814-4827.

Siegel, R., Ma, J., Zou, Z., Jemal, A., 2014. Cancer statistics, 2014. CA: a cancer journal for clinicians 64, 9-29.

Sittampalam, G.S., Gal-Edd, N., Arkin, M., Auld, D., Austin, C., Bejcek, B., Glicksman, M., Inglese, J., Lemmon, V., Li, Z., 2013. Cell Viability Assays.

Soma, C.E., Dubernet, C., Bentolila, D., Benita, S., Couvreur, P., 2000. Reversion of multidrug resistance by co-encapsulation of doxorubicin and cyclosporin A in polyalkylcyanoacrylate nanoparticles. Biomaterials 21, 1-7.

Sos, M.L., Koker, M., Weir, B.A., Heynck, S., Rabinovsky, R., Zander, T., Seeger, J.M., Weiss, J., Fischer, F., Frommolt, P., Michel, K., Peifer, M., Mermel, C., Girard, L., Peyton, M., Gazdar, A.F., Minna, J.D., Garraway, L.A., Kashkar, H., Pao, W., Meyerson, M., Thomas, R.K., 2009. PTEN loss contributes to erlotinib resistance in EGFR-mutant lung cancer by activation of Akt and EGFR. Cancer research 69, 3256-3261.

Stanford, M.J., Dove, A.P., 2010. Stereocontrolled ring-opening polymerisation of lactide. Chemical Society reviews 39, 486-494.

Stordal, B., Hamon, M., McEneaney, V., Roche, S., Gillet, J.P., O'Leary, J.J., Gottesman, M., Clynes, M., 2012. Resistance to paclitaxel in a cisplatin-resistant ovarian cancer cell line is mediated by P-glycoprotein. PloS one 7, e40717.

Sun, B., Feng, S.-S., 2009. Trastuzumab-functionalized nanoparticles of biodegradable copolymers for targeted delivery of docetaxel. Nanomedicine : nanotechnology, biology, and medicine 4, 431-445.

Swartz, M.A., Iida, N., Roberts, E.W., Sangaletti, S., Wong, M.H., Yull, F.E., Coussens, L.M., DeClerck, Y.A., 2012. Tumor microenvironment complexity: emerging roles in cancer therapy. Cancer research 72, 2473-2480.

Tan, G.R., Feng, S.S., Leong, D.T., 2014. The reduction of anti-cancer drug antagonism by the spatial protection of drugs with PLA-TPGS nanoparticles. Biomaterials 35, 3044-3051.

Tao, W., Zeng, X., Liu, T., Wang, Z., Xiong, Q., Ouyang, C., Huang, L., Mei, L., 2013. Docetaxel-loaded nanoparticles based on star-shaped mannitol-core PLGA-TPGS diblock copolymer for breast cancer therapy. Acta biomaterialia 9, 8910-8920.

Thomas, C.M., 2010. Stereocontrolled ring-opening polymerization of cyclic esters: synthesis of new polyester microstructures. Chemical Society reviews 39, 165-173.

van Meerbeeck, J.P., Fennell, D.A., De Ruysscher, D.K., 2011. Small-cell lung cancer. Lancet 378, 1741-1755.

Walkey, C.D., Olsen, J.B., Guo, H., Emili, A., Chan, W.C., 2012. Nanoparticle size and surface chemistry determine serum protein adsorption and macrophage uptake. Journal of the American Chemical Society 134, 2139-2147.

Wang, B.L., Shen, Y.M., Zhang, Q.W., Li, Y.L., Luo, M., Liu, Z., Li, Y., Qian, Z.Y., Gao, X., Shi, H.S., 2013. Codelivery of curcumin and doxorubicin by MPEG-PCL results in improved efficacy of systemically administered chemotherapy in mice with lung cancer. International journal of nanomedicine 8, 3521-3531.

Williams, C.K., 2007. Synthesis of functionalized biodegradable polyesters. Chemical Society reviews 36, 1573-1580.

Win, K.Y., Feng, S.S., 2006. In vitro and in vivo studies on vitamin E TPGS-emulsified poly(D,L-lactic-co-glycolic acid) nanoparticles for paclitaxel formulation. Biomaterials 27, 2285-2291.

Wong, R.S.Y., Radhakrishnan, A.K., 2012. Tocotrienol research: past into present. Nutr Rev 70, 483-490.

Wu, C., Ying, A., Ren, S., 2013. Fabrication of polymeric micelles with core–shell–corona structure for applications in controlled drug release. Colloid and Polymer Science 291, 827-834.

Xing, F., Saidou, J., Watabe, K., 2010. Cancer associated fibroblasts (CAFs) in tumor microenvironment. Frontiers in bioscience 15, 166-179.

Xiong, X.B., Lavasanifar, A., 2011. Traceable multifunctional micellar nanocarriers for cancer-targeted co-delivery of MDR-1 siRNA and doxorubicin. ACS nano 5, 5202-5213.

Yang, Q., Jones, S.W., Parker, C.L., Zamboni, W.C., Bear, J.E., Lai, S.K., 2014. Evading Immune Cell Uptake and Clearance Requires PEG Grafting at Densities Substantially Exceeding the Minimum for Brush Conformation. Molecular pharmaceutics.

Yezhelyev, M., Yacoub, R., O'Regan, R., 2009. Inorganic nanoparticles for predictive oncology of breast cancer. Nanomedicine (Lond) 4, 83-103.

Youk, H.J., Lee, E., Choi, M.K., Lee, Y.J., Chung, J.H., Kim, S.H., Lee, C.H., Lim, S.J., 2005. Enhanced anticancer efficacy of alpha-tocopheryl succinate by conjugation with polyethylene glycol. Journal of controlled release 107, 43-52.

Yu, Y., Tan, S., Zhao, S., Zhuang, X., Song, Q., Wang, Y., Zhou, Q., Zhang, Z., 2013. Antitumor activity of docetaxel-loaded polymeric nanoparticles fabricated by Shirasu porous glass membrane-emulsification technique. International journal of nanomedicine 8, 2641-2652.

Yuan, F., Dellian, M., Fukumura, D., Leunig, M., Berk, D.A., Torchilin, V.P., Jain, R.K., 1995. Vascular permeability in a human tumor xenograft: molecular size dependence and cutoff size. Cancer research 55, 3752-3756.

Zamboni, W.C., Torchilin, V., Patri, A.K., Hrkach, J., Stern, S., Lee, R., Nel, A., Panaro, N.J., Grodzinski, P., 2012. Best practices in cancer nanotechnology: perspective from NCI nanotechnology alliance. Clinical cancer research 18, 3229-3241.

Zhang, K., Fang, H., Chen, Z., Taylor, J.S., Wooley, K.L., 2008a. Shape effects of nanoparticles conjugated with cell-penetrating peptides (HIV Tat PTD) on CHO cell uptake. Bioconjugate chemistry 19, 1880-1887.

Zhang, Z., Feng, S.S., 2006a. The drug encapsulation efficiency, in vitro drug release, cellular uptake and cytotoxicity of paclitaxel-loaded poly(lactide)-tocopheryl polyethylene glycol succinate nanoparticles. Biomaterials 27, 4025-4033.

Zhang, Z., Feng, S.S., 2006b. Nanoparticles of poly(lactide)/vitamin E TPGS copolymer for cancer chemotherapy: synthesis, formulation, characterization and in vitro drug release. Biomaterials 27, 262-270.

Zhang, Z., Lee, S.H., Gan, C.W., Feng, S.S., 2008b. In vitro and in vivo investigation on PLA-TPGS nanoparticles for controlled and sustained small molecule chemotherapy. Pharmaceutical research 25, 1925-1935.

Zhang, Z., Tan, S., Feng, S.-S., 2012. Vitamin E TPGS as a molecular biomaterial for drug delivery. Biomaterials 33, 4889-4906.

Zhao, J., Feng, S.S., 2014. Effects of PEG tethering chain length of vitamin E TPGS with a Herceptin-functionalized nanoparticle formulation for targeted delivery of anticancer drugs. Biomaterials 35, 3340-3347.

Zhou, W.J., Zhang, X., Cheng, C., Wang, F., Wang, X.K., Liang, Y.J., To, K.K., Zhou, W., Huang, H.B., Fu, L.W., 2012. Crizotinib (PF-02341066) reverses multidrug resistance in cancer cells by inhibiting the function of P-glycoprotein. British journal of pharmacology 166, 1669-1683.

Zhu, H., Chen, H., Zeng, X., Wang, Z., Zhang, X., Wu, Y., Gao, Y., Zhang, J., Liu, K., Liu, R., Cai, L., Mei, L., Feng, S.S., 2014. Co-delivery of chemotherapeutic drugs with vitamin E TPGS by porous PLGA nanoparticles for enhanced chemotherapy against multi-drug resistance. Biomaterials 35, 2391-2400.